Биофотоника:
проблемы и инновационные подходы к их решению в области биомедицинской визуализации и фототерапии

Валерий Викторович Тучин

Кафедра оптики и биофотоники, научный медицинский центр, СГУ им. Н.Г. Чернышевского, Саратов

Лаборатория проблем лазерной диагностики технических и живых систем, ФИЦ «Саратовский научный центр РАН», Саратов

Лаборатория биофотоники, Томский государственный университет, Томск

tuchinvv@mail.ru

Saratov State University & Saratov State Medical University

- Tissue optics
- Basics of tissue optical clearing
- OCAs
- Creation of UV-THz windows
- Spectrophotometry
- Monitoring of tissue cancer
- Diabetes mellitus, glycation
- Fluorescence measurements
- Fluorescence/MRT
- Multiphoton imaging
- Raman spectroscopy of tissues
- OCT imaging
- Stokes imaging
- Photoacoustics
- Phantoms
- Metabolic OCAs
- Drug delivery
- Practical examples
- Summary
- Conclusion

Typical structures and sizes of biological tissue components

$$\mu_s' = \mu_s(1-g) \sim (2a)^2 \rho (2a/\lambda)^{0.37} (m-1)^2$$

$$m \equiv n_s/n_0$$

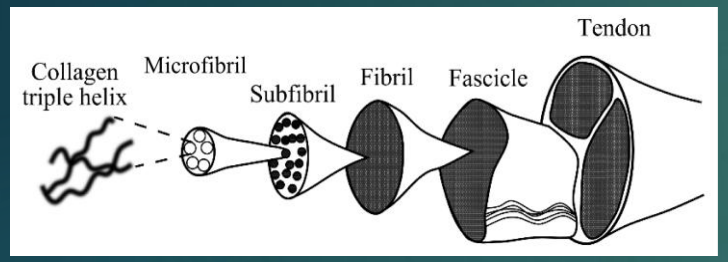

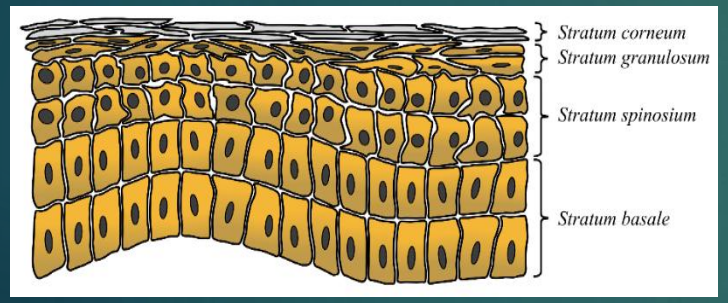

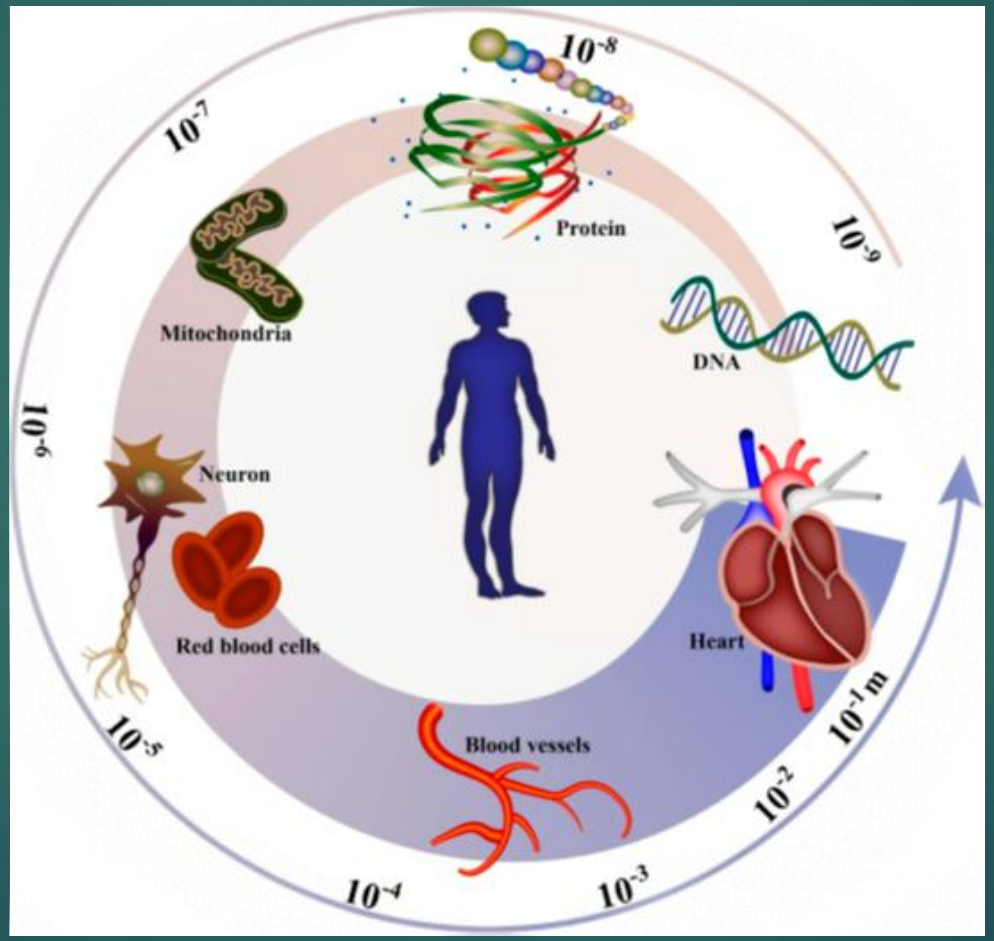

From Rayleigh to Mie scattering

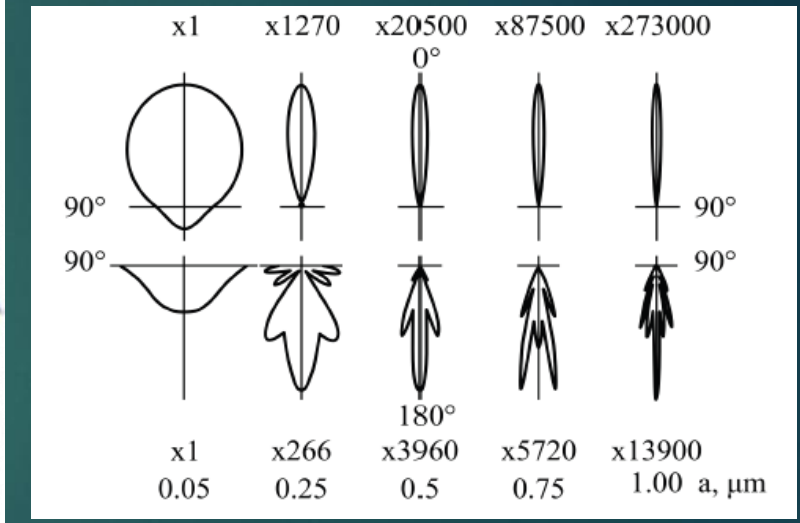

V.V. Tuchin, Tissue Optics, 3rd edition, SPIE Press, PM 254, 2015

X. Yang et al., Observing single cells in whole organs with optical imaging, *J. Innov. Opt. Health Sci.* **16** (1) 2330002-1-26 (2023)

ОПТИКА БИОТКАНЕЙ ОТ УФ ДО ТГЦ: ПОГЛОЩЕНИЕ И РАССЕЯНИЕ

Закон Бугера-Бера-Ламберта:

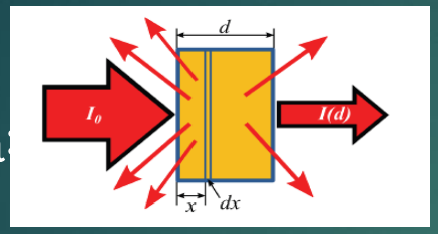

$$I = I_0 \exp[-\mu_t d]$$
$$\mu_t = \mu_a + \mu_s$$

Модификация закона при многократном рассеянии:

$$I = b_s I_0 \exp[-\mu_{eff} d]$$
$$\mu_{eff} = 1/\delta$$
$$\delta = 1/\sqrt{3\mu_a(\mu_a + \mu_s')}$$

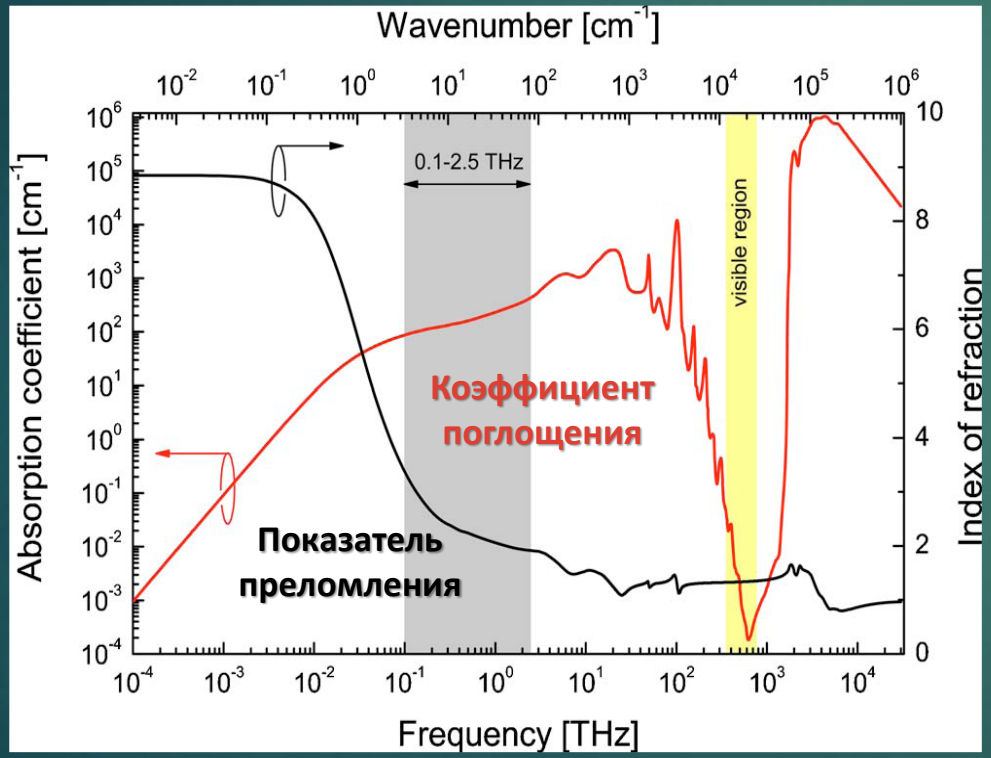

Поглощение и показатель преломления воды
Møller et al., J. Opt. Soc. Am. B, 26 (9), 2009

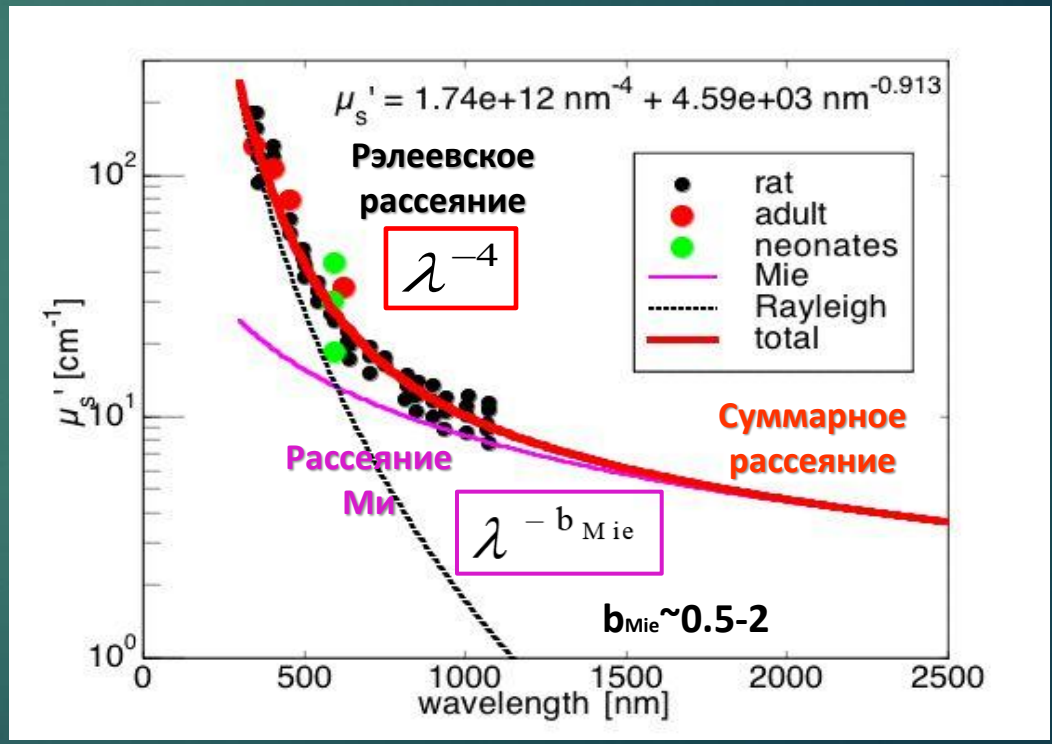

Приведенный коэффициент рассеяния кожи
Steven L. Jacques, Ulm, LALS-2014

Light propagation in biological tissue

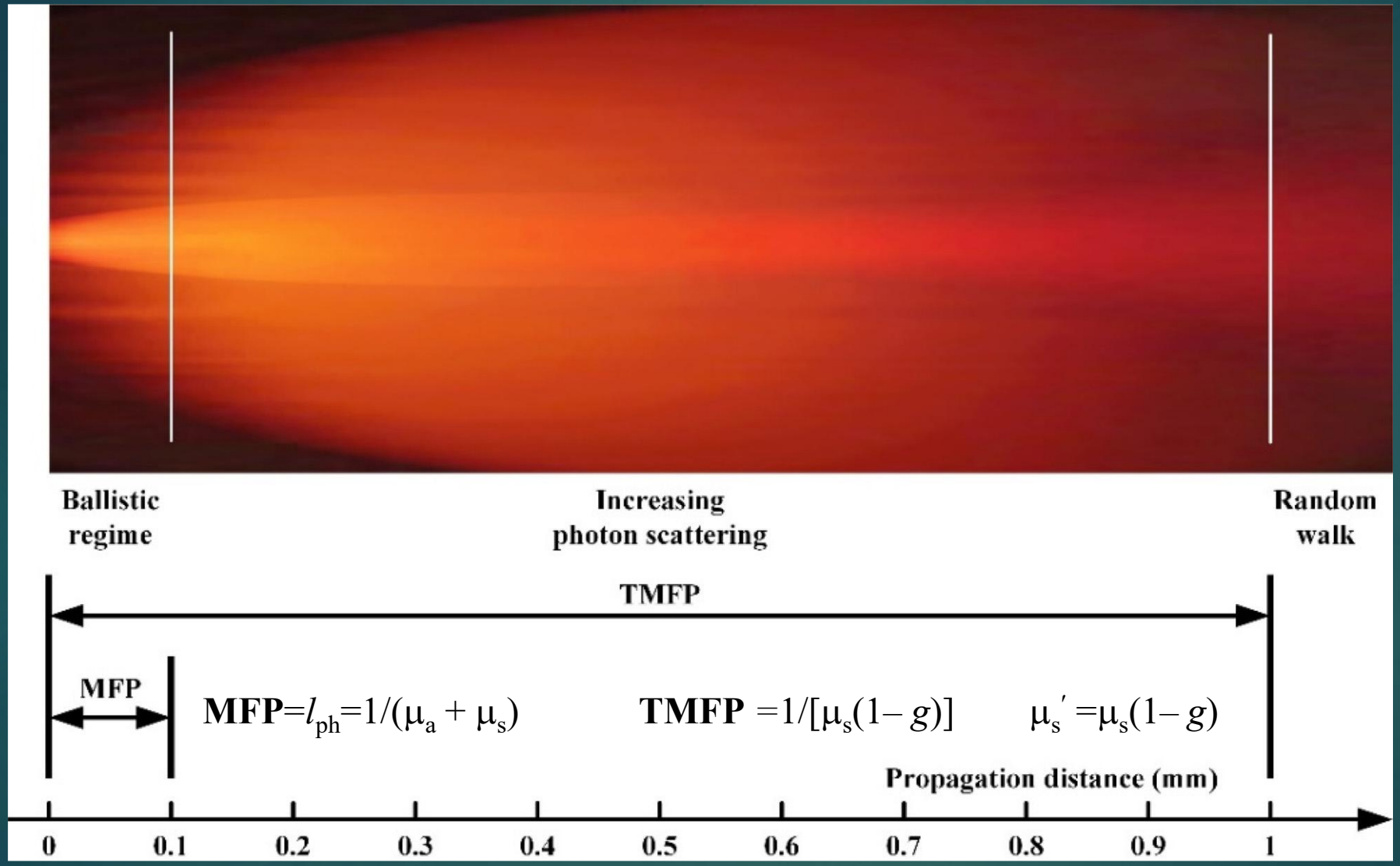

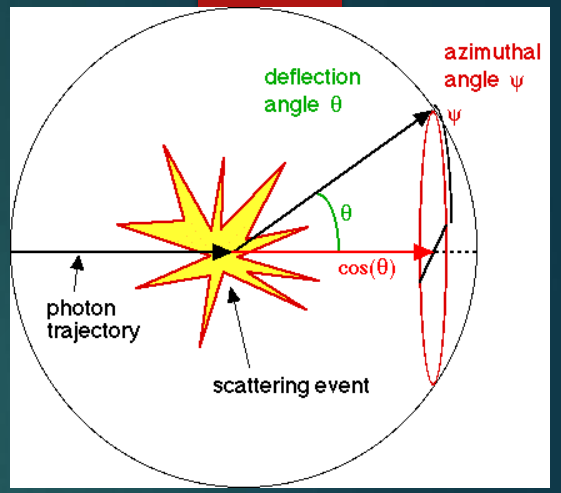

g – factor of scattering anisotropy (mean Cos of the scattering angle)

$g \rightarrow 0 - 1$

$\delta = 1/\mu_{eff}$

$$\mu_{eff} = \sqrt{3\mu_a(\mu_a + \mu_s')}$$

X. Yang et al., Observing single cells in whole organs with optical imaging, *J. Innovat. Opt. Health Sci.* **16** (1) 2330002-1-26 (2023)

ОПТИЧЕСКИЕ МЕТОДЫ ИССЛЕДОВАНИЯ БИОТКАНЕЙ

Спектрофотометрия

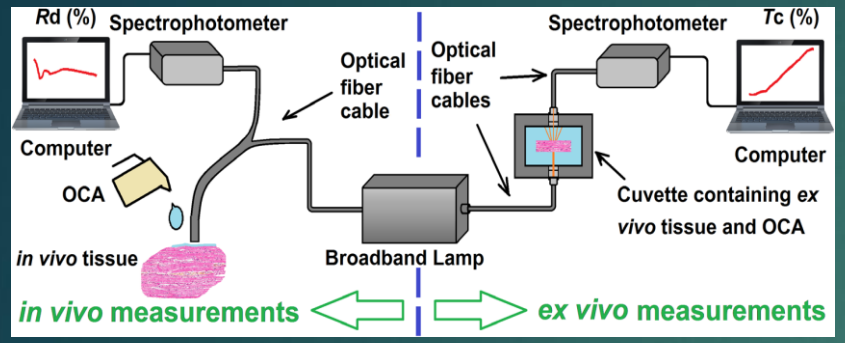

ОКТ

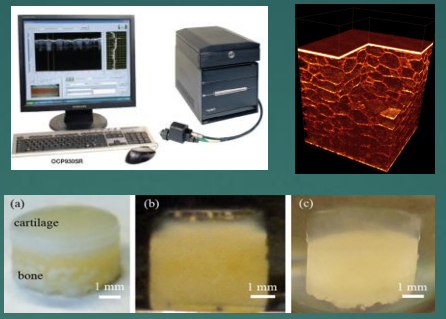

Спекл-визуализация

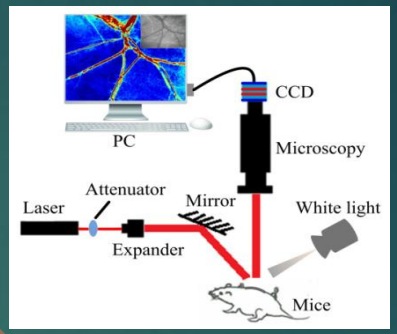

Спектроскопия КР

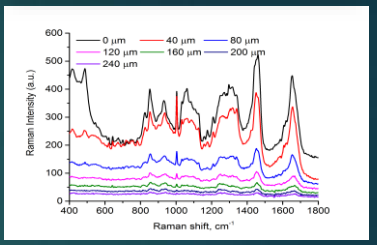

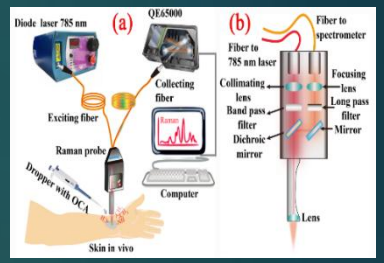

Флуоресцентное картирование

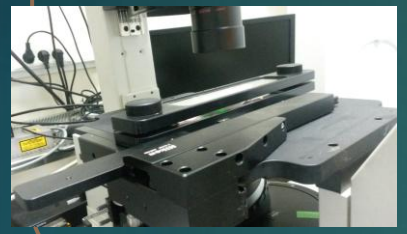

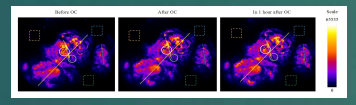

Многофотонная томография

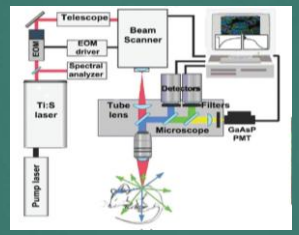

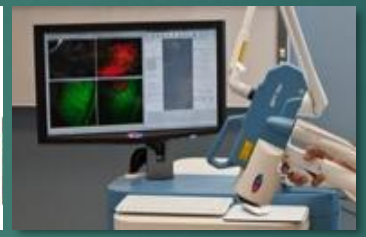

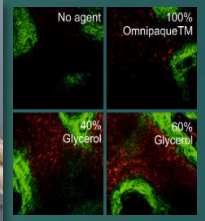

Фотоакустическая визуализация

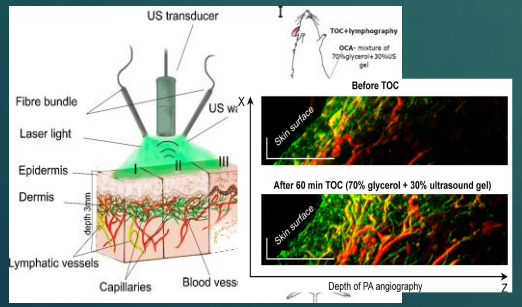

Терагерцовая визуализация

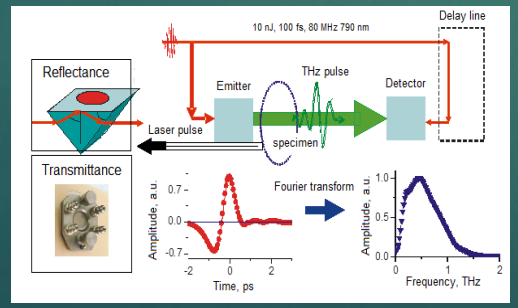

ЛИП (LIBS) картирование

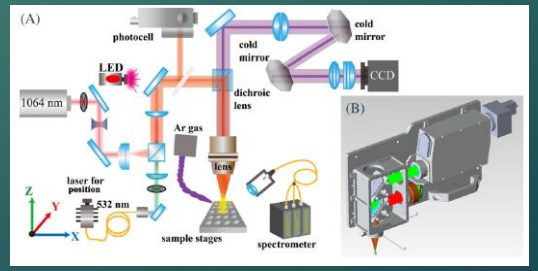

Микроскопия светового листа

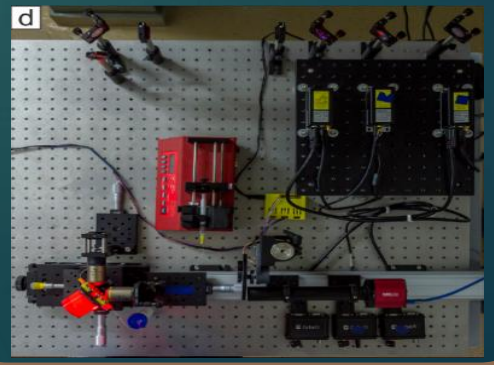

ТРАДИЦИОННЫЕ ОКНА ПРОЗРАЧНОСТИ БИОЛОГИЧЕСКИХ ТКАНЕЙ

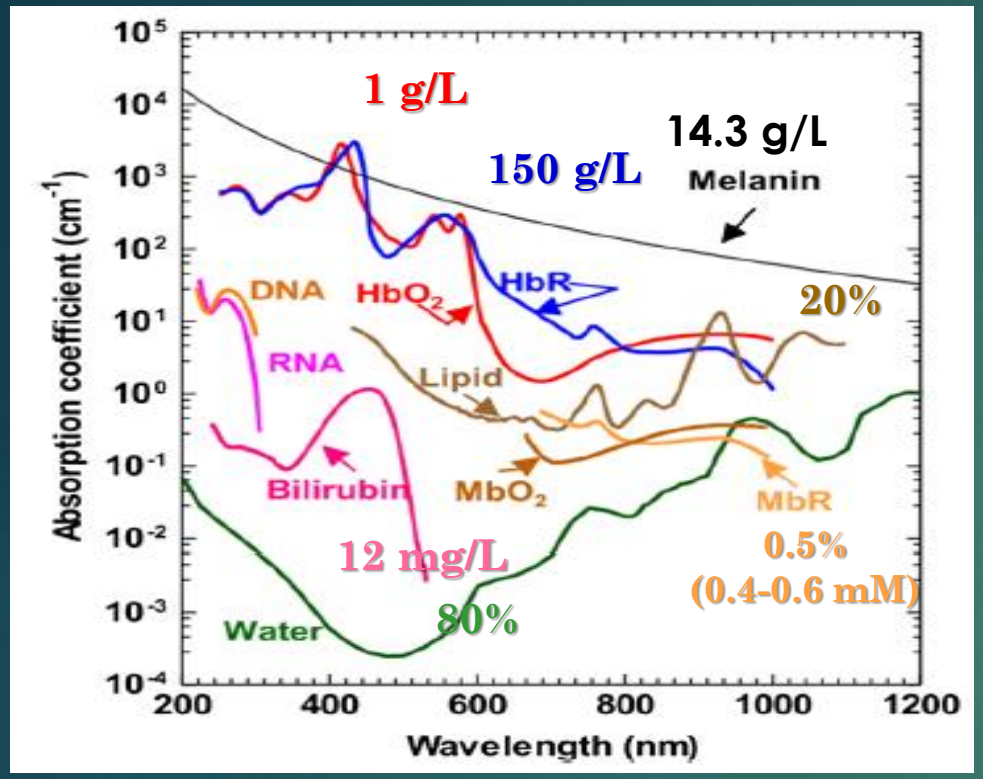

Y. Zhou, et al. J. Biomed. Opt. 21(6), 061007 (2016)

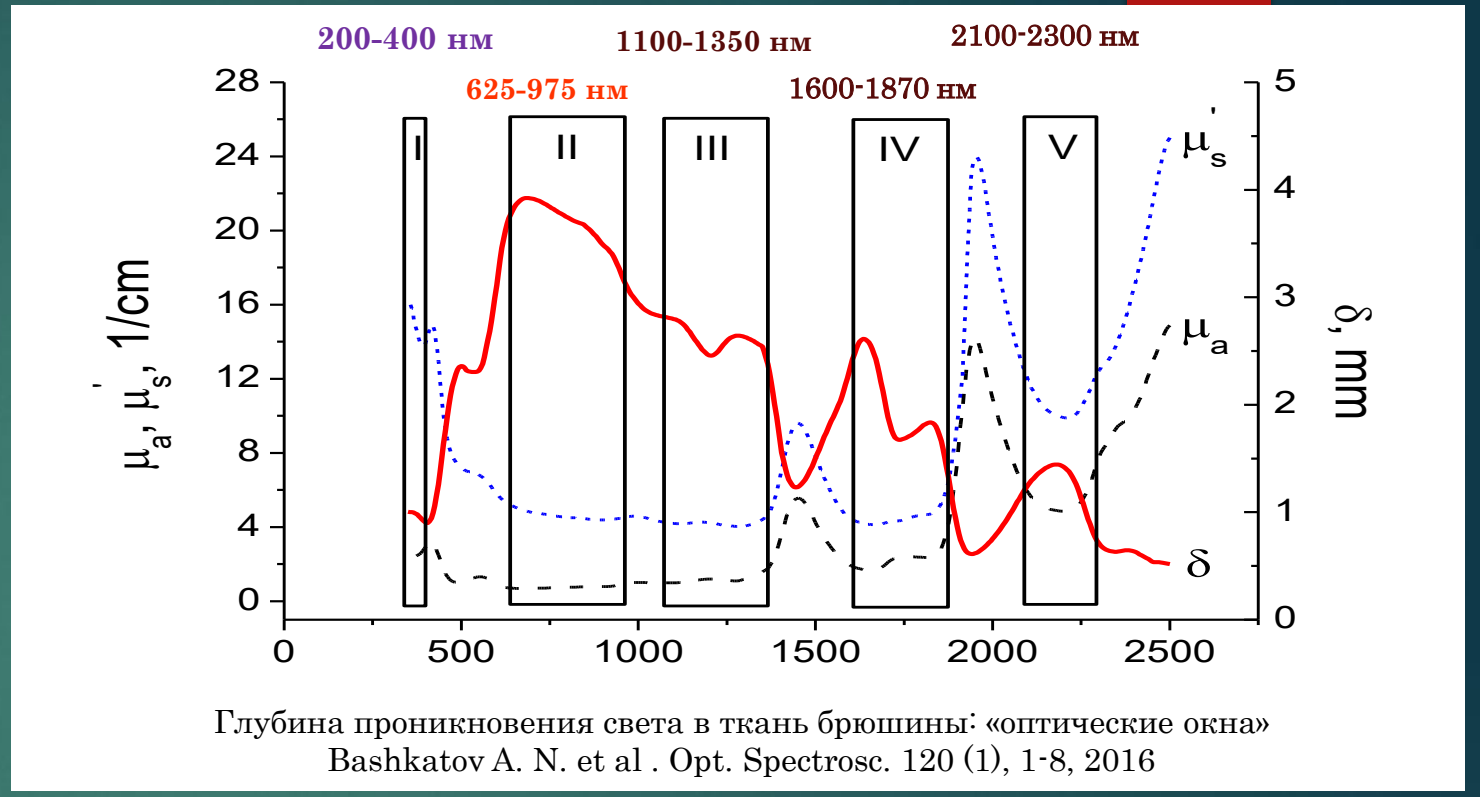

Глубина проникновения света в ткань брюшины: «оптические окна»
Bashkatov A. N. et al . Opt. Spectrosc. 120 (1), 1-8, 2016

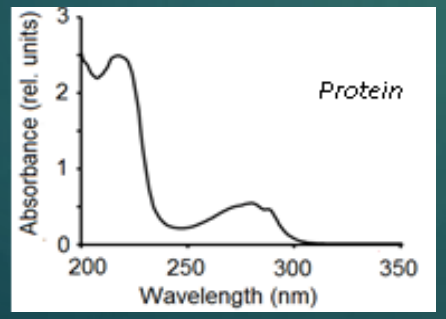

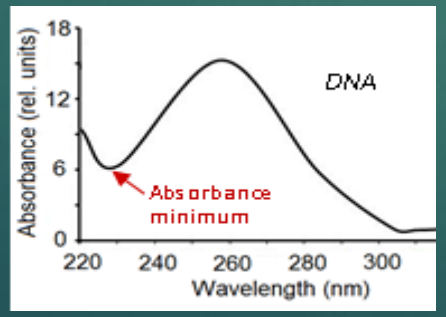

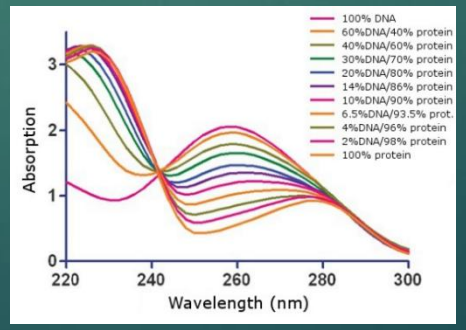

$$\delta = 1/\sqrt{3\mu_a\left(\mu_a + \mu_s'\right)}$$

http://elte.prompt.hu/sites/default/files/tananyagok/IntroductionToPracticalBiochemistry/ch04s06.html

Motivation: Challenges of Optical Imaging and Treatment

Soft limit $\sim \delta$

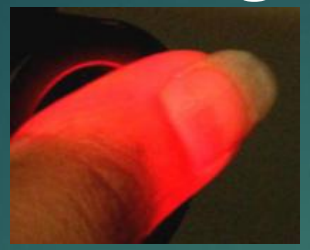

1 – 2 mm

$$\delta = 1/\sqrt{3\mu_a(\mu_a + \mu_s')}$$

Hard limit ~10 δ

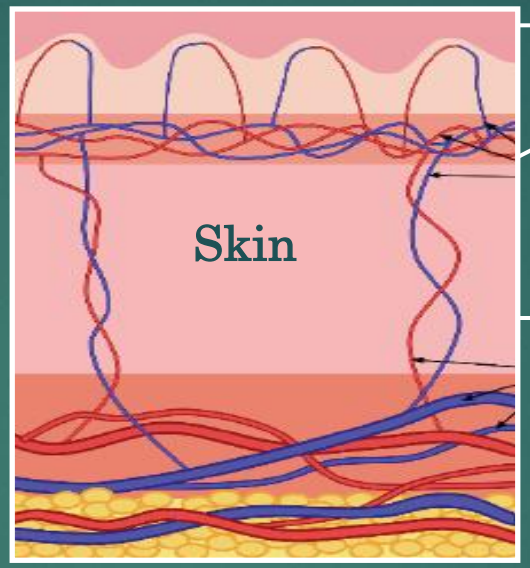

OM, SNOM

CFM, 2PM, SHM, etc.

OCT

DOT,
UOT, PAT

Ballistic photons:
Bouguer-Beer-Lambert law:
$I = I_0 \exp[-(\mu_a + \mu_s)d]$

$\text{MFP} = l_{ph} = 1/(\mu_a + \mu_s)$

OM: Optical microscopy
SNOM: Scanning near-field optical microscopy
CFM: Confocal microscopy
2PM: Two-photon microscopy
SHM: Second harmonic microscopy
OCT: Optical coherence tomography
DOT: Diffuse optical tomography
UOT: Ultrasound-modulated optical tomography
PAT: Photoacoustic tomography

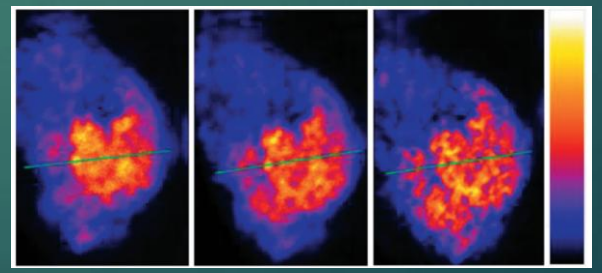

Fluorescence
cancer cell imaging

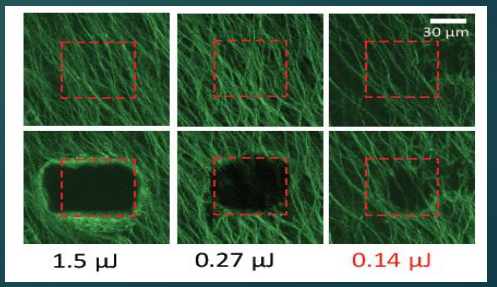

Femtosecond Laser
Treatment

Immersion Optical Clearing (OC) Method

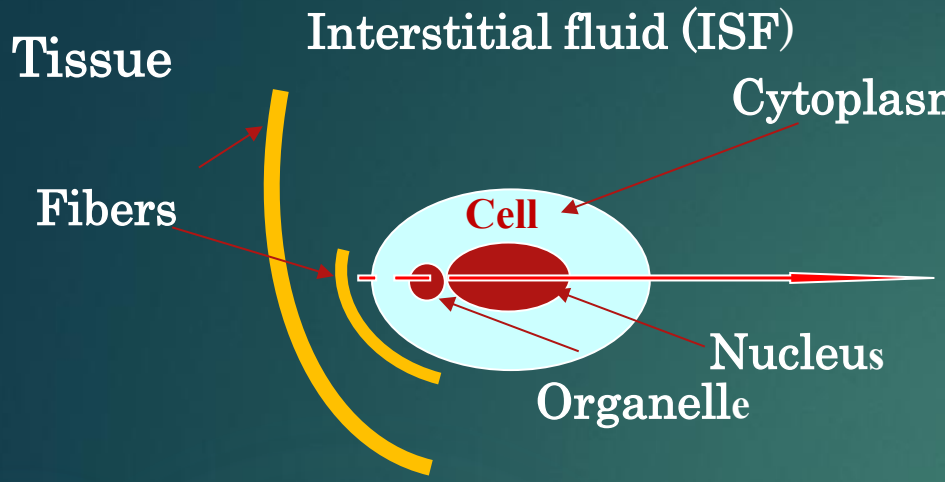

$$m \equiv n_s/n_0$$

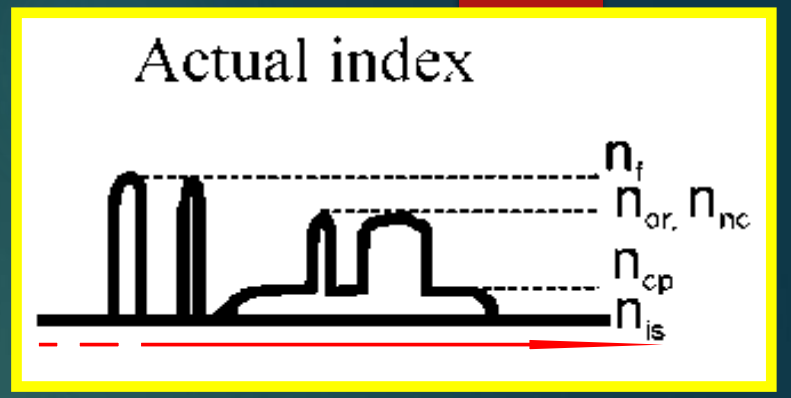

$$\mu_s' = \mu_s(1-g) \sim d^2\rho(d/\lambda)^{0.37}(m-1)^2$$

1) OCA diffusion into tissue/cell leads to replacement tissue/cell water by an OCA
2) Tissue/cell temporal/reversible dehydration caused by osmotic action of an OCA is followed by tissue/cell shrinkage: less thickness and better ordering of collagen fibers or cell skeleton with volume fraction $f_c(t)$

$$\mu_s' = \mu_s(1-g) \sim [1-f_c(t)]^3/[1+f_c(t)]$$

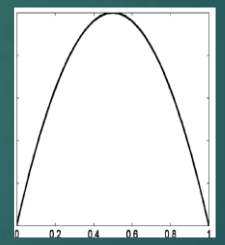

OCT

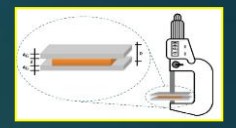

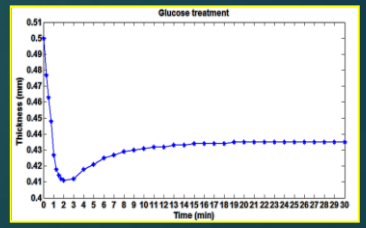

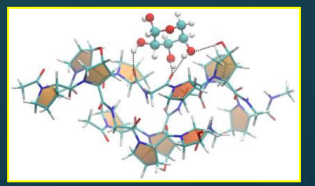

The main mechanisms of OC:

1 - **Refractive index matching** of tissue/cell components and ISF/cytoplasm
2 - Cell temporal/reversible **dehydration**
3 - Collagen molecules reversible **dissociation**

V.V. Tuchin, *Tissue Optics*, 3rd edition, SPIE Press, **PM 254**, 2015

ПРОСТРАНСТВЕННАЯ КОРРЕЛЯЦИЯ КОЛЛАГЕНОВЫХ ВОЛОКОН

Диаметр 30.8±0.8 нм, расстояние 55.3±4.0 нм, m=1.47/1.35

СЭМ : Роговица

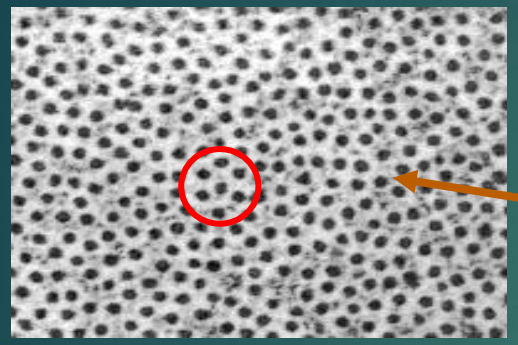

Диаметр 25-230 нм, средний 100 нм, m=1.47/1.35

Склера

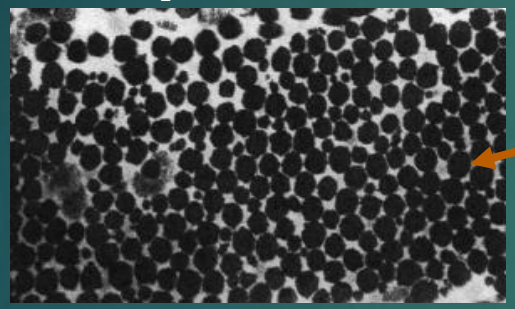

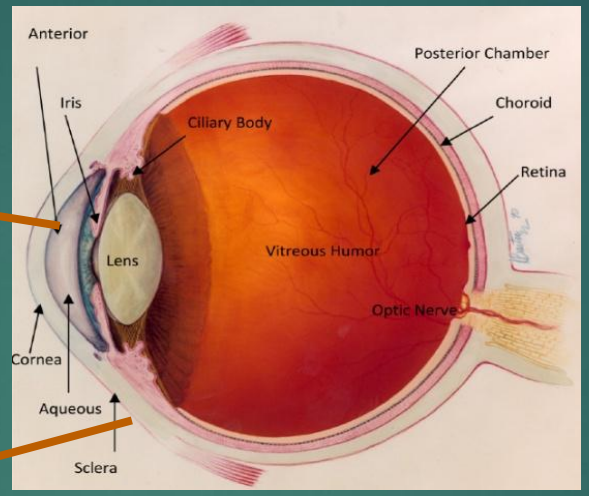

From Oliveira et al., SFM, 2020

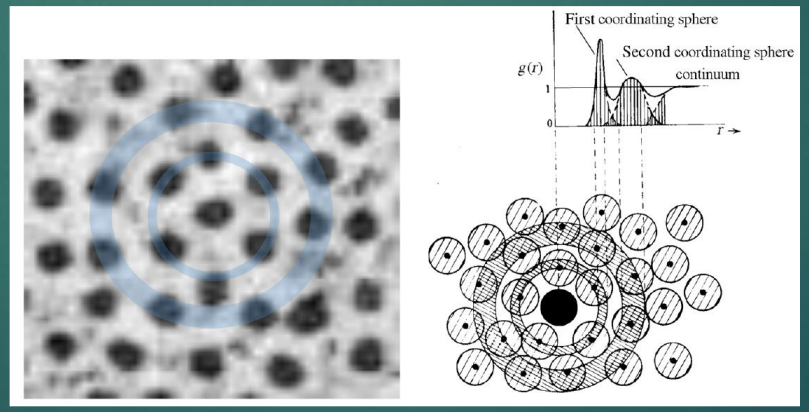

V.V. Tuchin, Polarized light interaction with tissues (tutorial), JBO 21(7), 071114 (2016)

ОКТ :
Примеры прозрачных и мутных (рассеивающих) тканей

ОКТ изображения и А-сканы

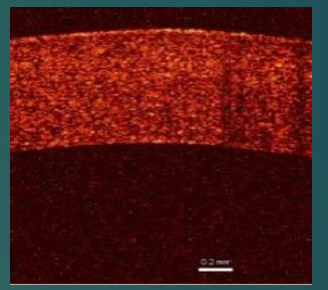

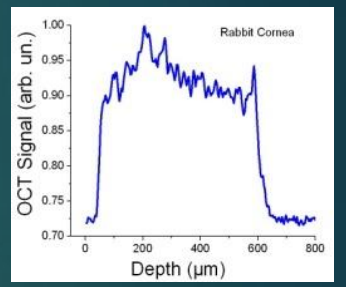

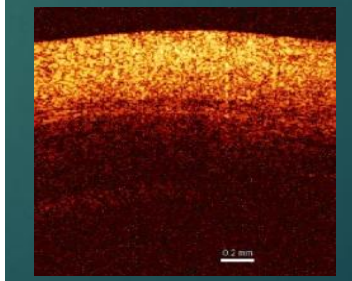

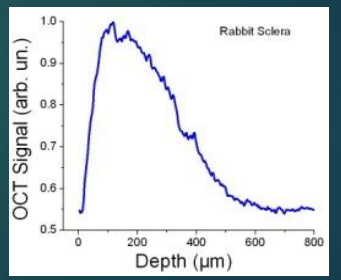

M.G. Ghosn, V. V Tuchin, K. V. Larin, IOVS, 2007

Optical clearing method helps to reduce scattering of tissues

$$\mu_s' = \mu_s(1-g) \sim d^2\rho(d/\lambda)^{0.37}(m-1)^2$$

$$m \equiv n_s/n_0$$

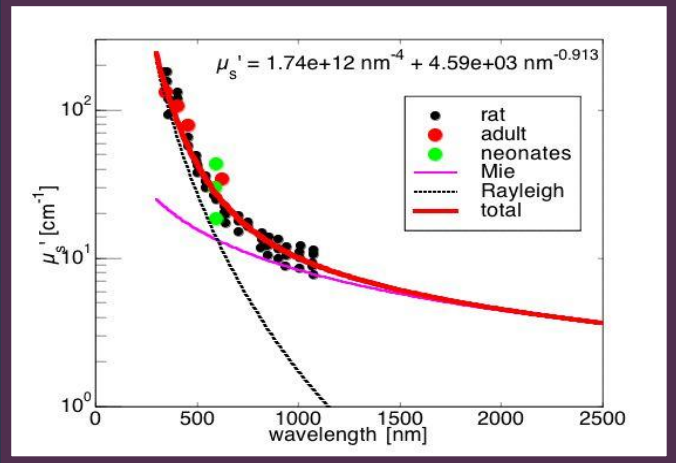

Refractive index matching mechanism

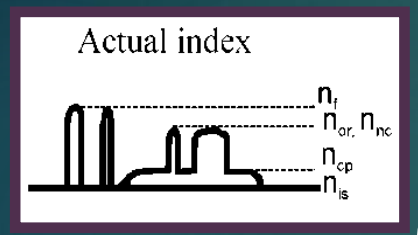

The Invisible Man
Herbert G. Wells, 1897

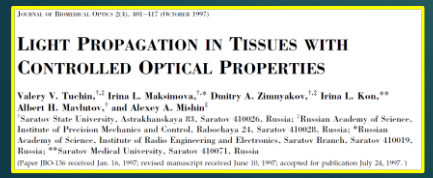

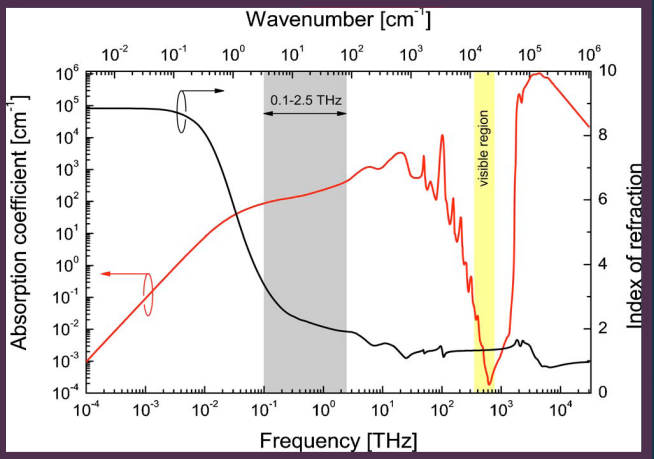

Dehydration mechanism

Rat skin *in vivo*

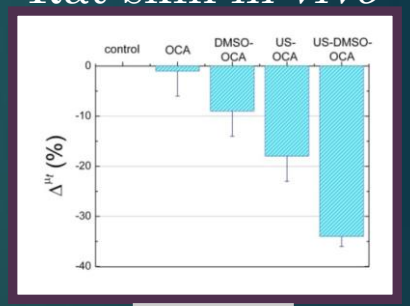

Optical clearing agents

Hyperosmotic agents:

- Glucose
- Sorbitol
- Glycerol
- Polyethylene glycol
- Propylene glycol
- Dimethyl sulfoxide

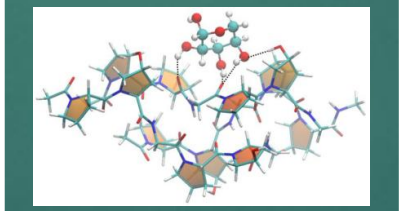

Isosmotic solutions:

- X-ray contrast agents: iohexol, iodixanol
- MRI contrast agents: gadobutrol, etc.

From Dan Zhu, HUST

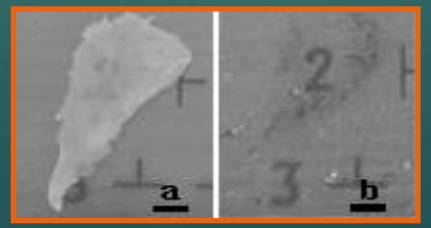

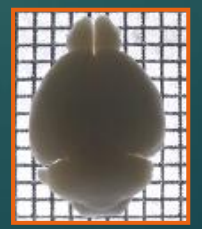

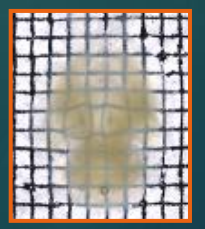

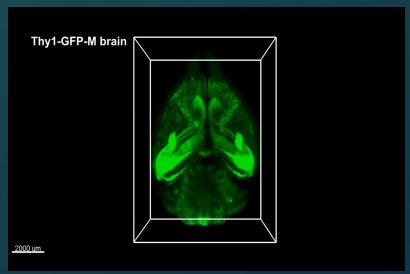

Thy1-GFP-M brain

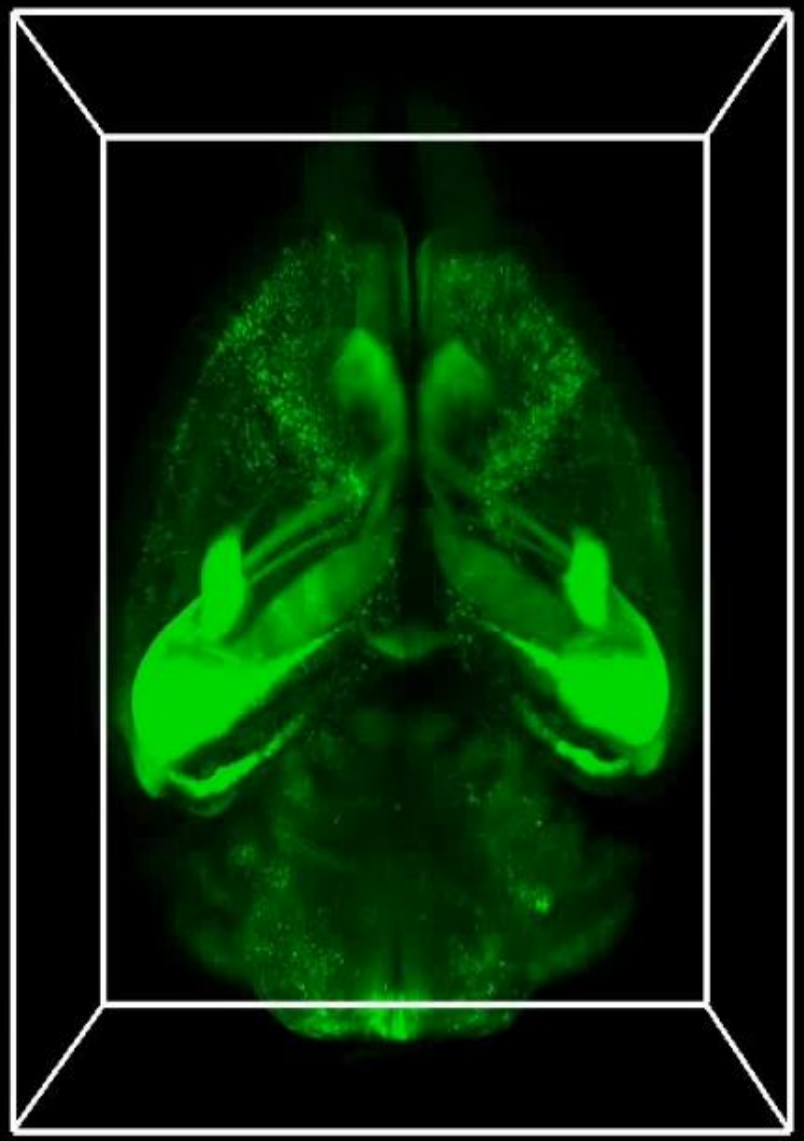

2000 um

Enhancers for *in vivo* delivery of OCAs through biological membranes

E.V. Lengert, E. E. Talnikova, V. V. Tuchin, Yu. I. Svenskaya, Prospective strategies for enhanced intra- and transdermal delivery of antifungal drugs, *Skin Pharmacology and Physiology* **33**, 261–269 (2020)

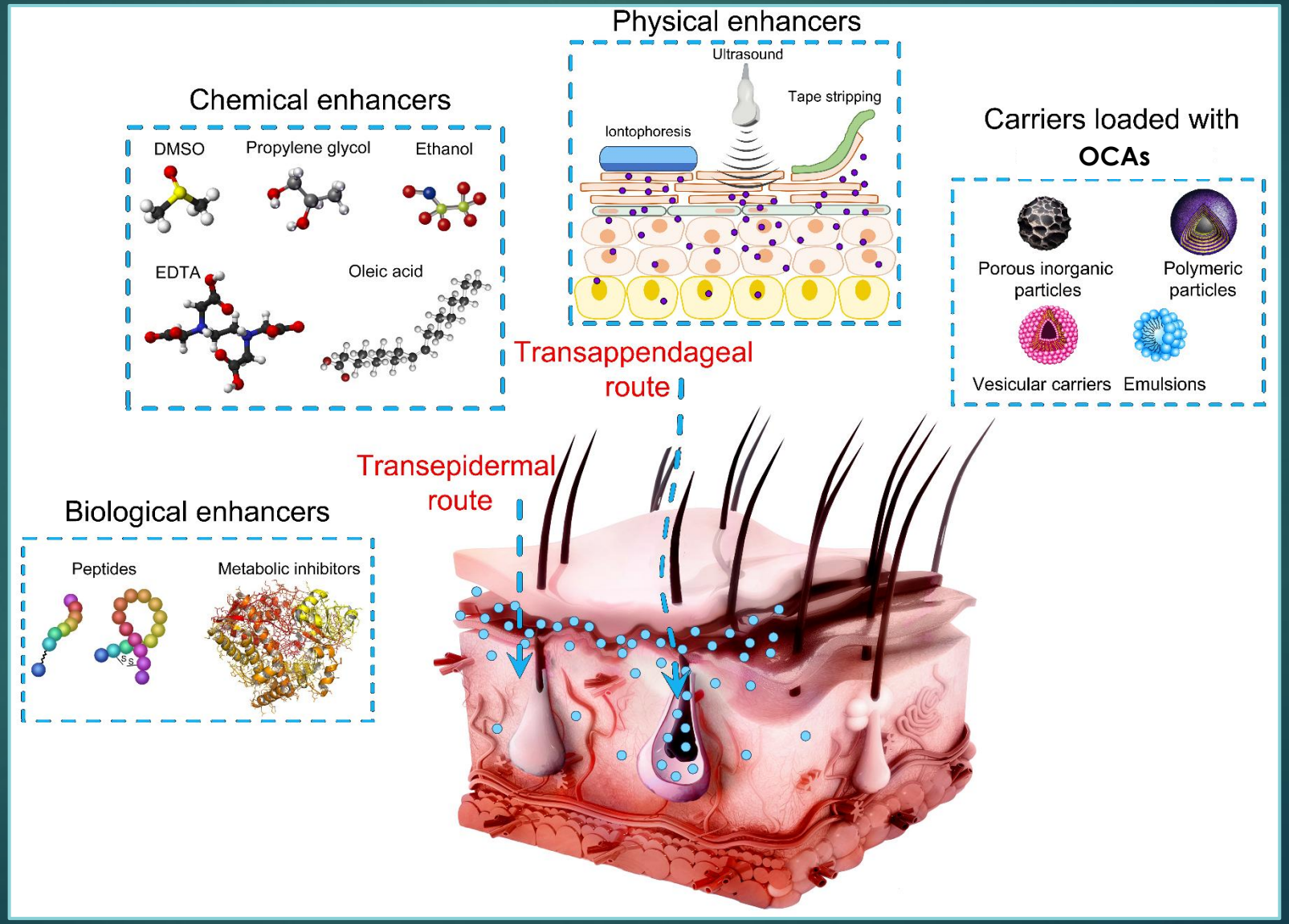

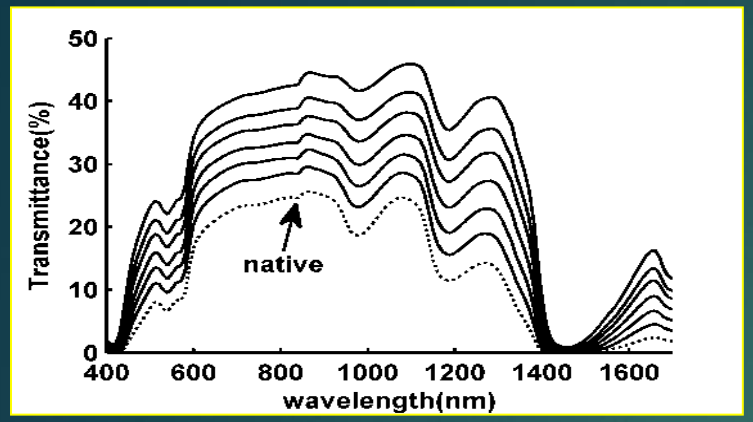

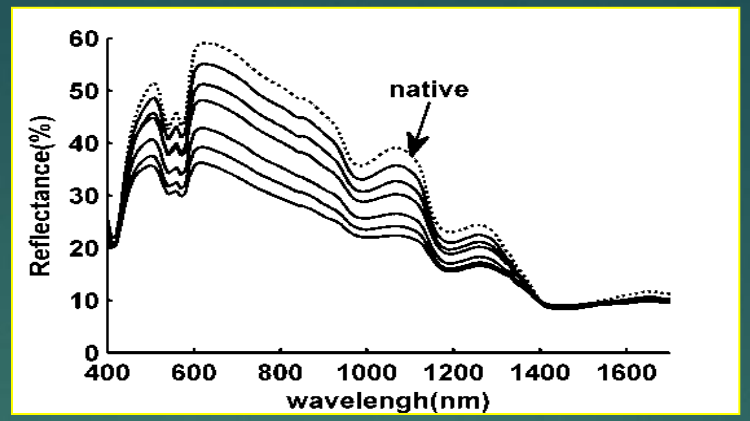

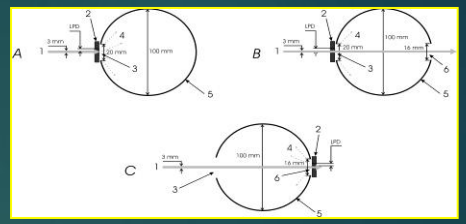

T. Yu, X. Wen, V.V .Tuchin, Q. Luo, D. Zhu, *J. Biomed. Opt.* 16 (2011)

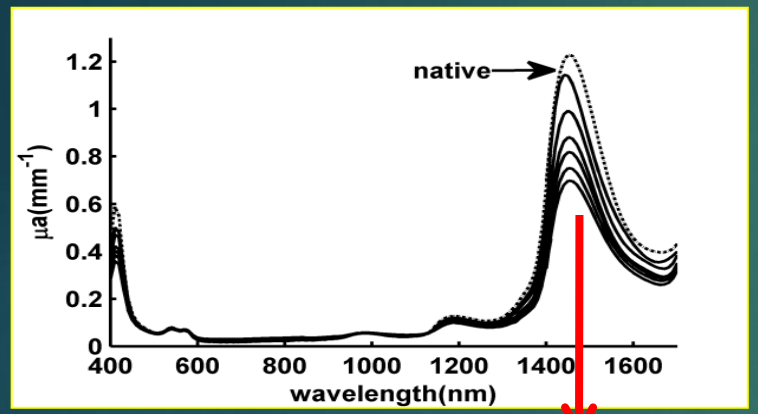

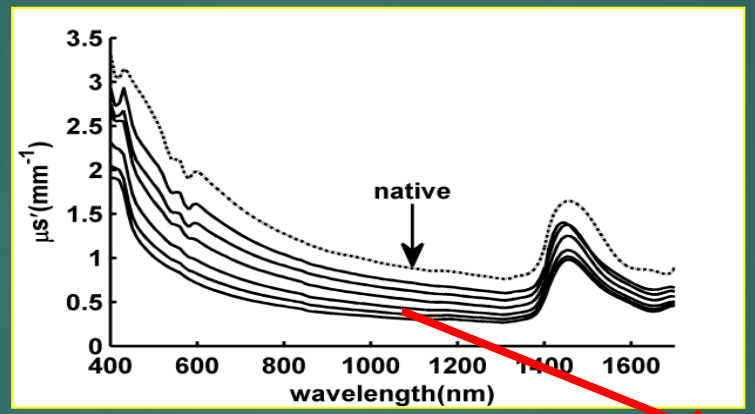

Pig skin sample before and after treatment by Propylene glycol 1,2-PG at time intervals of 0 (native), 10, 20, 30, 40, 50 and 60 min

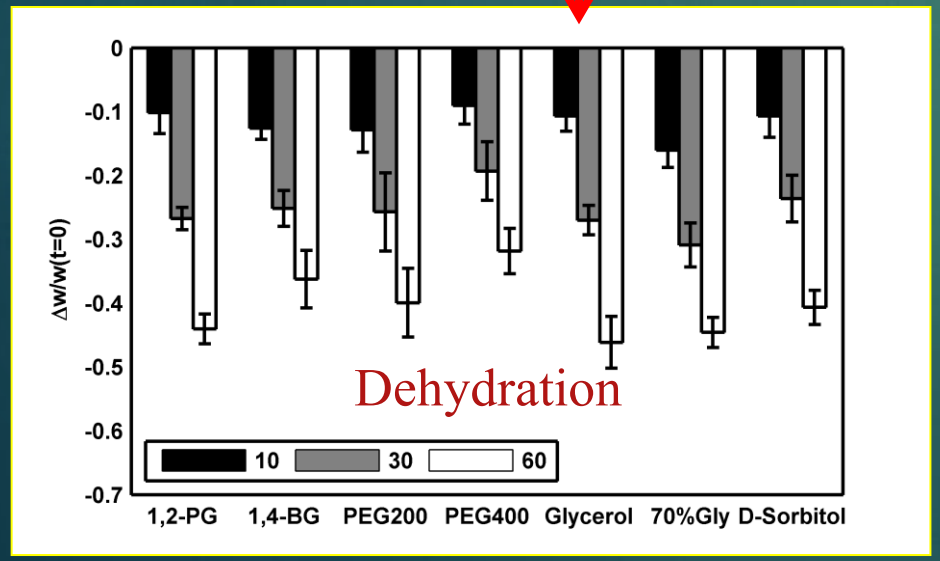

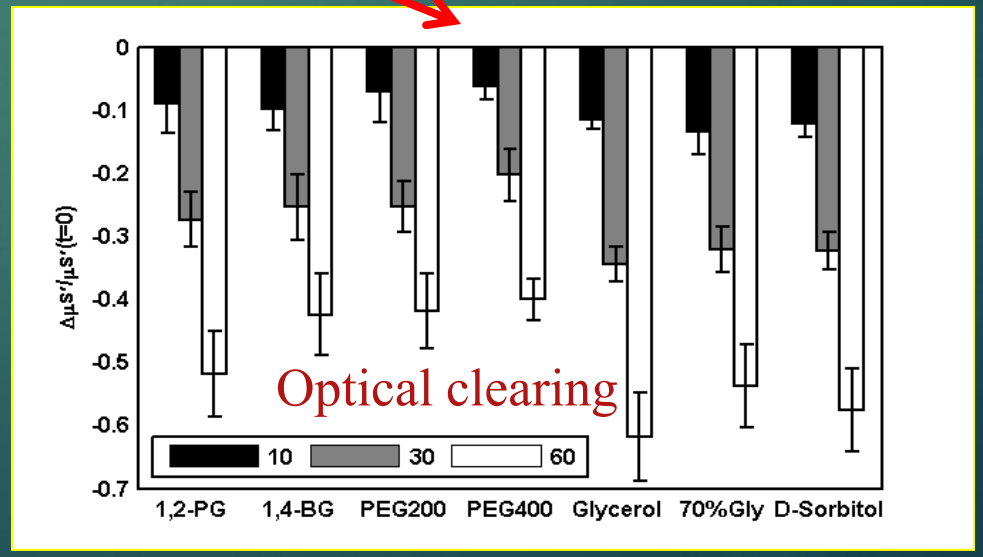

Optical clearing in THz range

Enhancement of the probing depth in tissues using optical clearing techniques

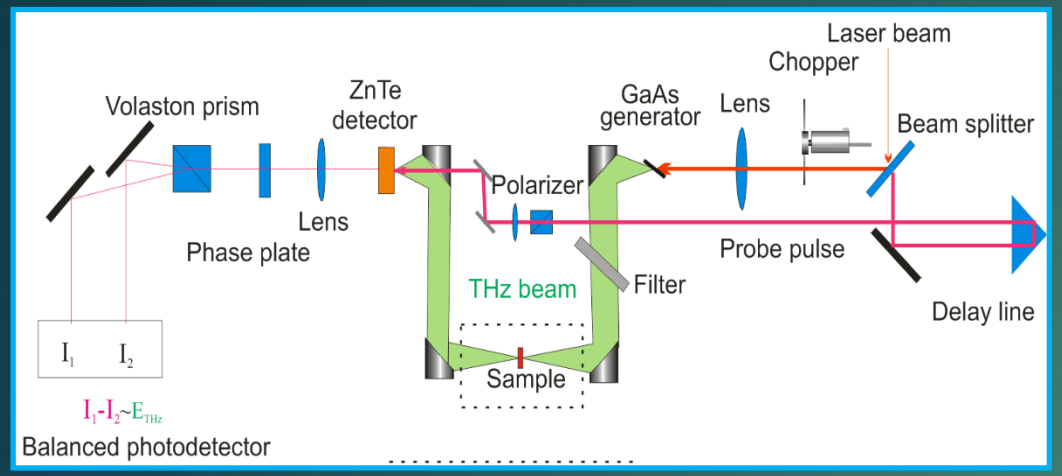

THz Time-Domain Spectrometer

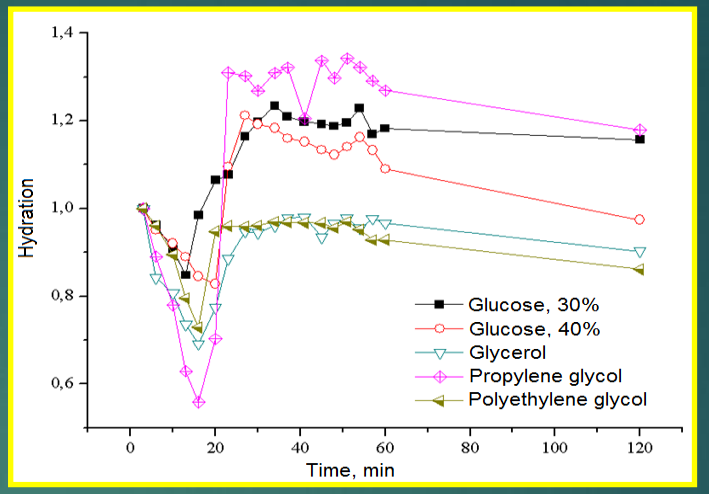

Human skin *in vivo* dehydration by different OCAs: alternative measurements

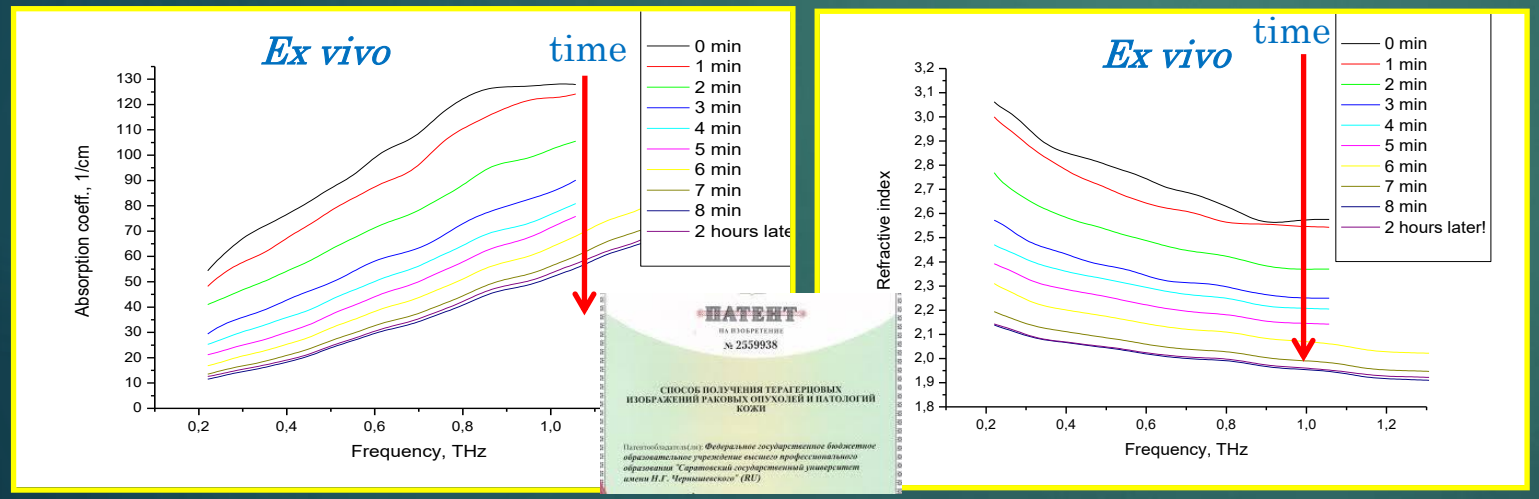

Bovine muscle tissue dehydration by glycerol measured using THz spectrometer in transmittance mode

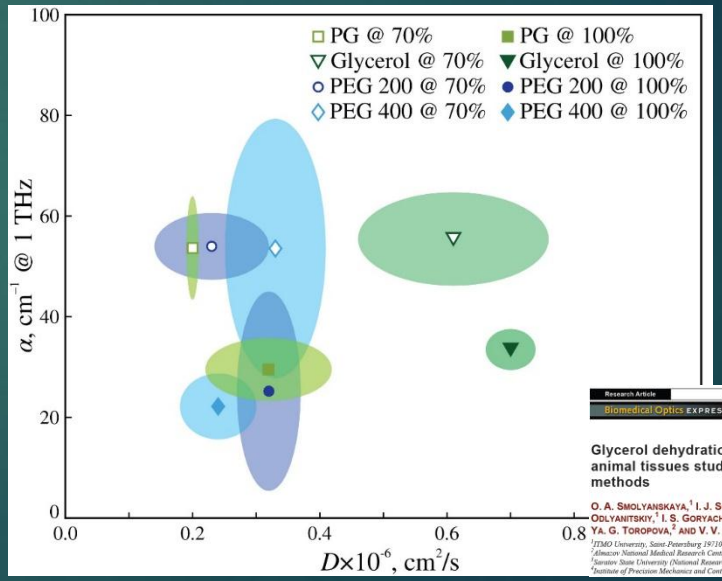

G.R. Musina et al., *J. Biophotonics* **13**, e202000297 (2020)

Time dependence for collimated transmittance for the rat muscle treatment with glucose (L.Oliveira, et al. *JIOHS*, Vol. 6, No. 2, 1350012, 2013; JBO, 2015)

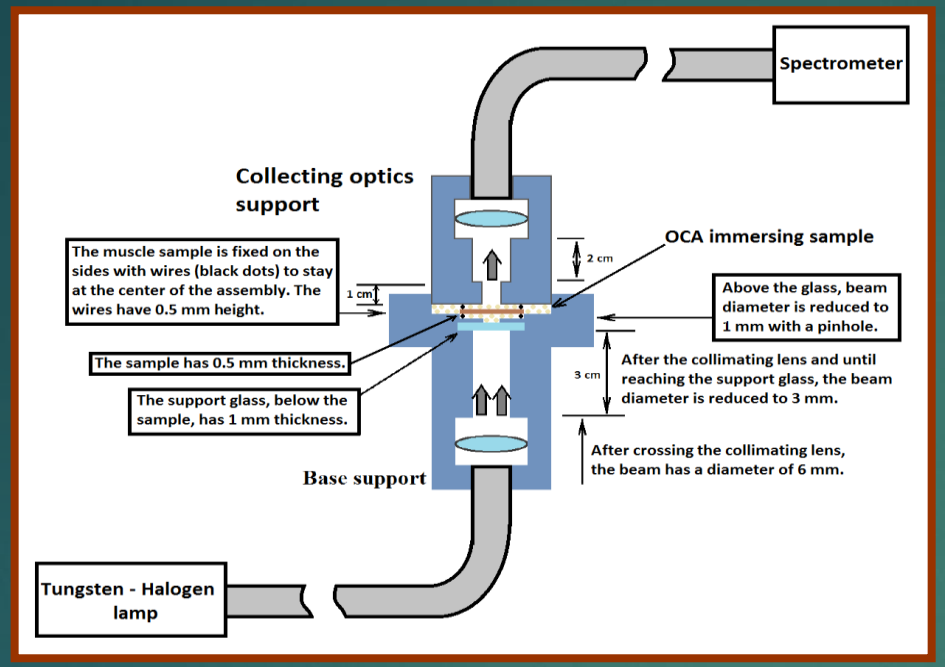

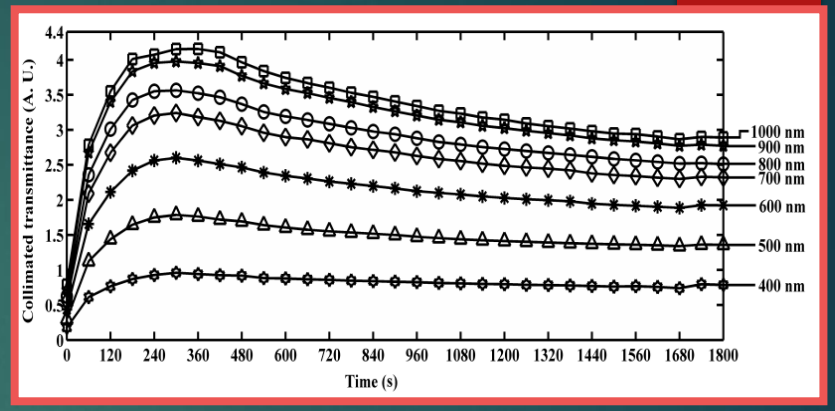

Glucose 20%

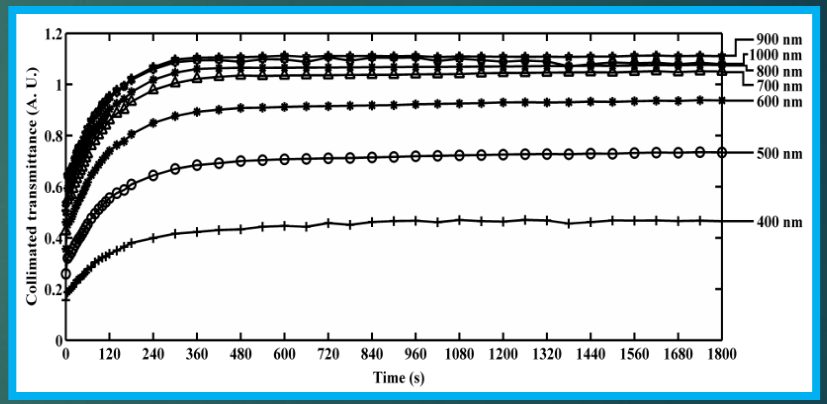

Glucose 50%

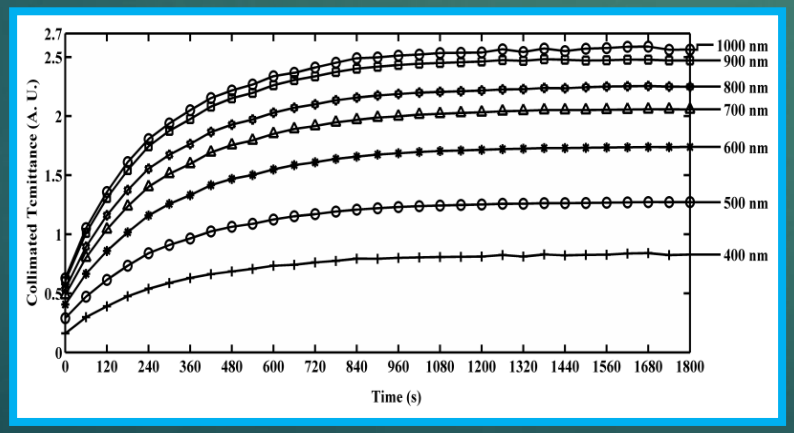

Glucose 40%

$$T_c(\lambda) \propto 1 - \exp\left(-\frac{t}{\tau}\right)$$

Diffusion time of Glucose and Ethylene Glycol in rat muscle

(L.Oliveira, M.I. Carvalho, E. Nogueira, V. V. Tuchin, *Laser Physics*, 2013, JBO, 2015)

$$\tau = \frac{l^2}{\pi^2 D_a}$$

$$D_a = 8.4 \times 10^{-7}\ cm^2 / s$$

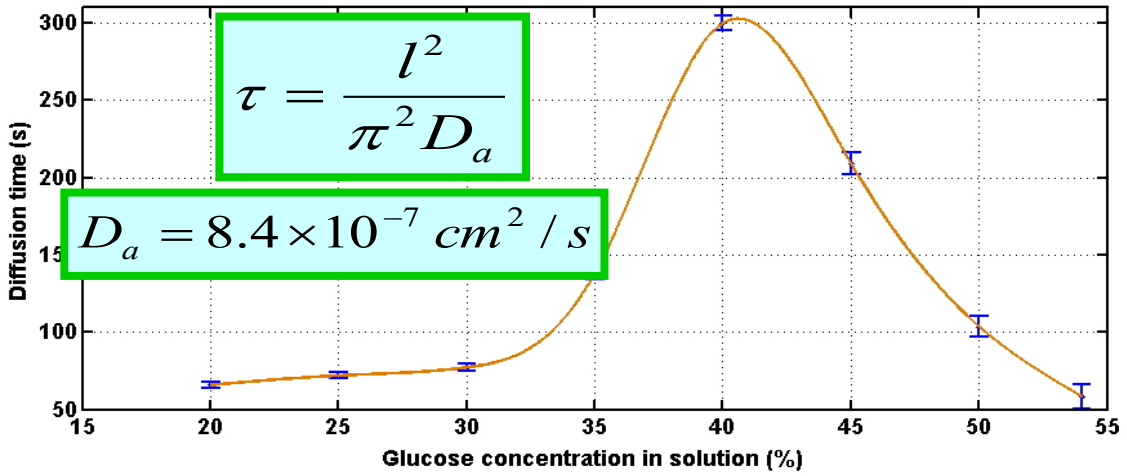

$$D_{EG} = 5.7 \times 10^{-7}\ cm^2 / s$$

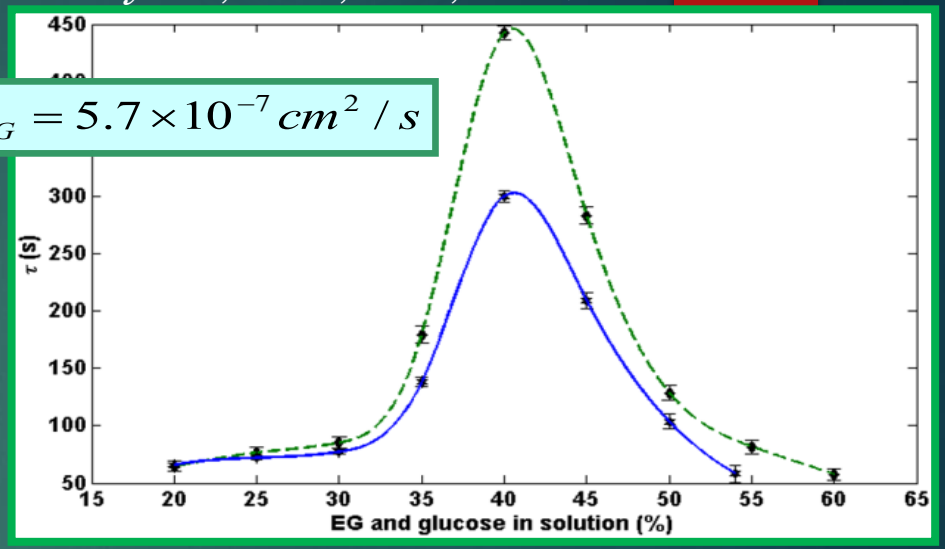

$$f_{water\ natural} = f_{bound\ water} + f_{free\ water} = 0.161 + 0.595 = 0.756$$

$$f_{solid\ part} = 0.244$$

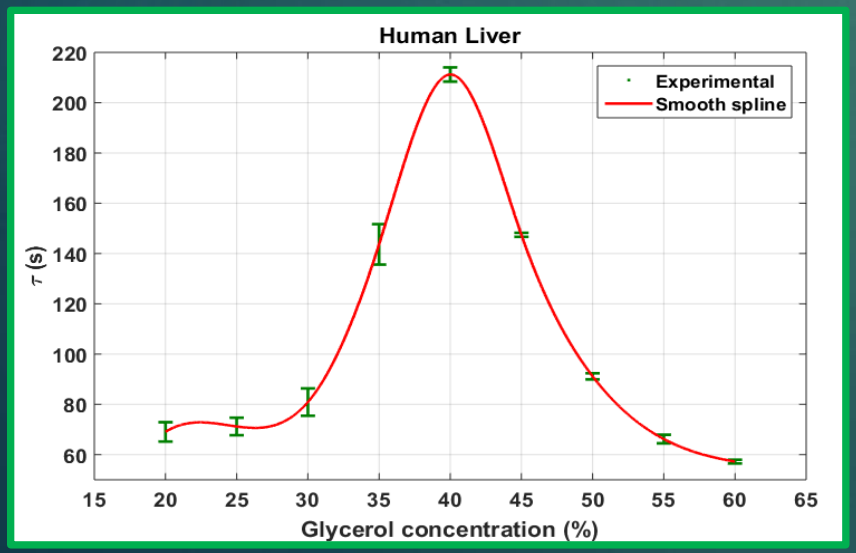

Evaluation of Water Content in **Human Liver**

I. Carneiro , S. Carvalho , R. Henrique , L. Oliveira , V. V. Tuchin, Simple multimodal optical technique for evaluation of free/bound water and dispersion of human liver tissue *J. Biomed. Opt.* 22(12), 125002 (2017)

Glycerol-Water Solution

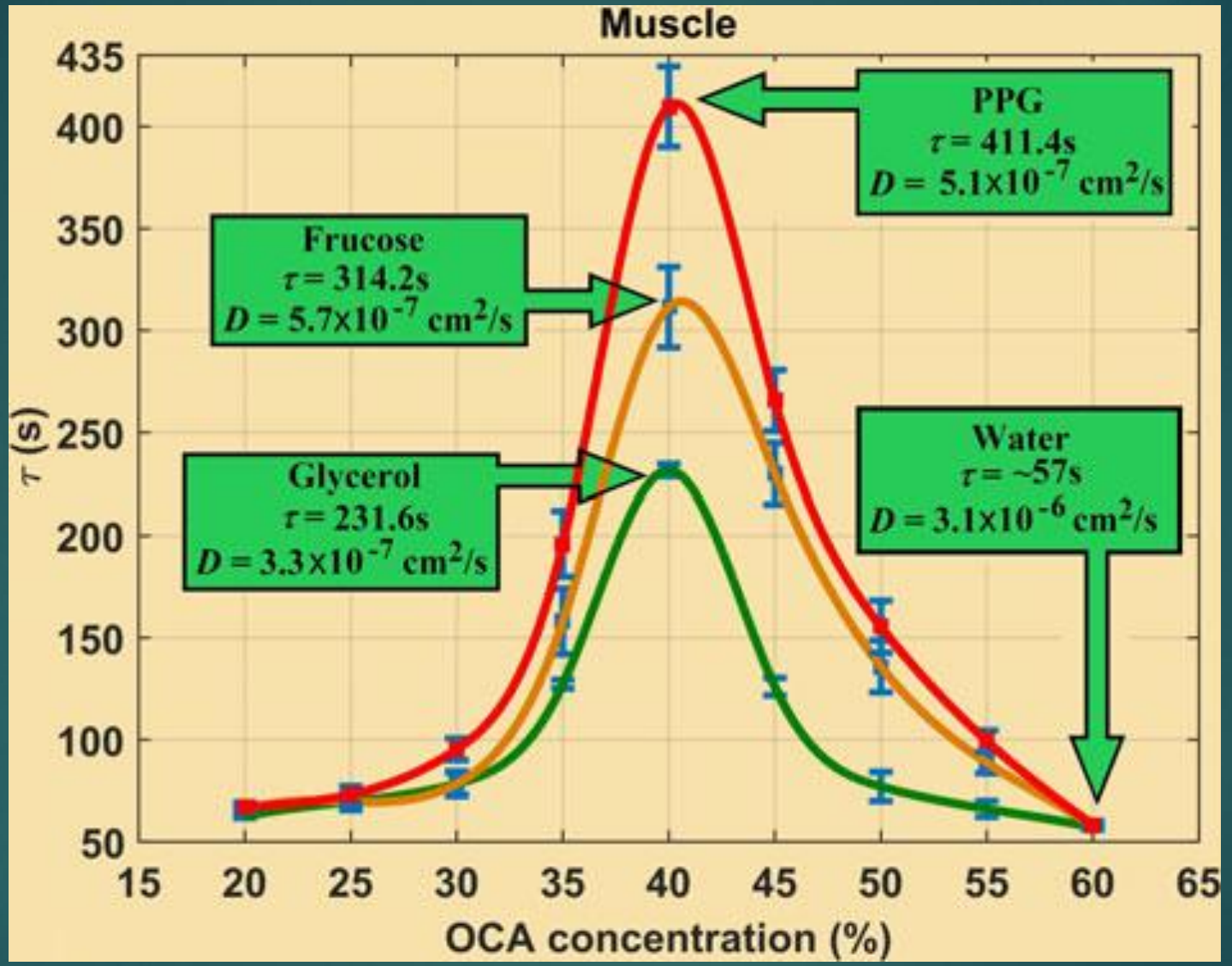

I. Carneiro, S. Carvalho, R. Henrique, L. M. Oliveira, V. V. Tuchin, A robust *ex vivo* method to evaluate the diffusion properties of agents in biological tissues, *J. Biophotonics* **12**(4), e201800333 (2019)

Diffusion time for healthy colon mucosa and tumor

Tissue type	Healphy mucosa									
OCA concentration	10%	15%	20%	25%	30%	35%	40%	45%	50%	54%
Diffusion time , s			65.1	69.4	81.1	138.4	299.2	211.5	104.3	55.7
SD			0.2	3.2	6.1	5.9	4.7	6.1	1.3	5.9
Tissue type	Tumor									
Diffusion time , s	62.9	68.6	71.1	73.9	136.1	320.6	234.9	139.0	82.7	58.4
SD	0.5	0.2	0.5	1.5	1.1	10.6	4.1	14.0	2.0	1.7

(L. Oliveira *et al*, Glucose diffusion in colon mucosa – a comparative study between healthy and cancerous tissue, J. Biomed. Opt. 22(9), 091506 (2017))

Tumor has ~5% more free-water content than healthy mucosa
Glucose takes more time to diffuse in tumor than in healthy mucosa

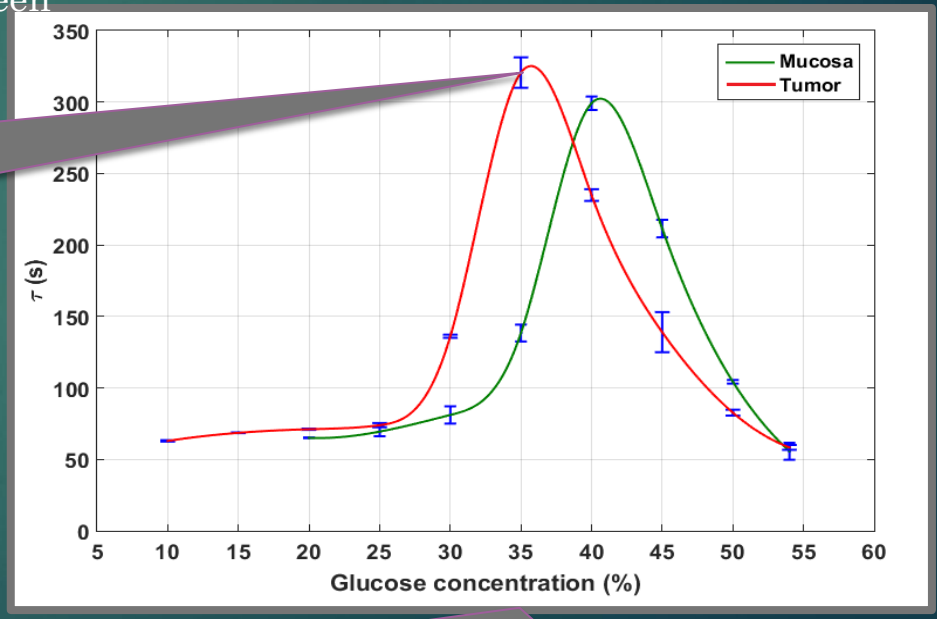

Software : P. Peixoto, L. Oliveira, M. I. Carvalho, E. Nogueira, and V.V. Tuchin, Software development for estimation of optical clearing agent's diffusion coefficients in biological tissues, *J. Biomed. Photonics & Eng* 1(4) 255, 2016

Normal mucosa shows similar results to muscle tissue (Oliveira *et al*, 2013)

Creation of UV window

I. Carneiro, S. Carvalho, R. Henrique, L. M. Oliveira, V. V. Tuchin, Moving tissue spectral window to the deep-ultraviolet via optical clearing, *J. Biophotonics*. 2019; e201900181.

Collimated transmittance spectra of 0.5 mm-thick tissue samples immersed in the glycerol solution were measured (200-1000 nm) during 30 min treatment with a 5 s - time resolution

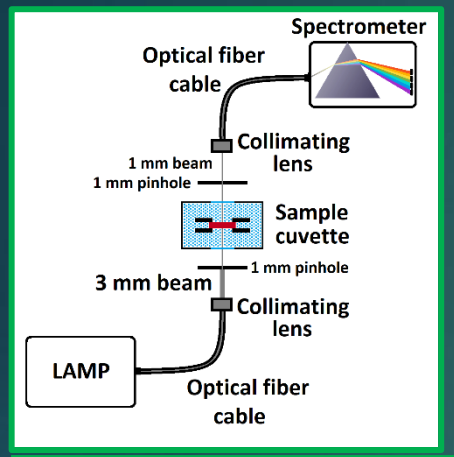

Surgical colorectal human specimen

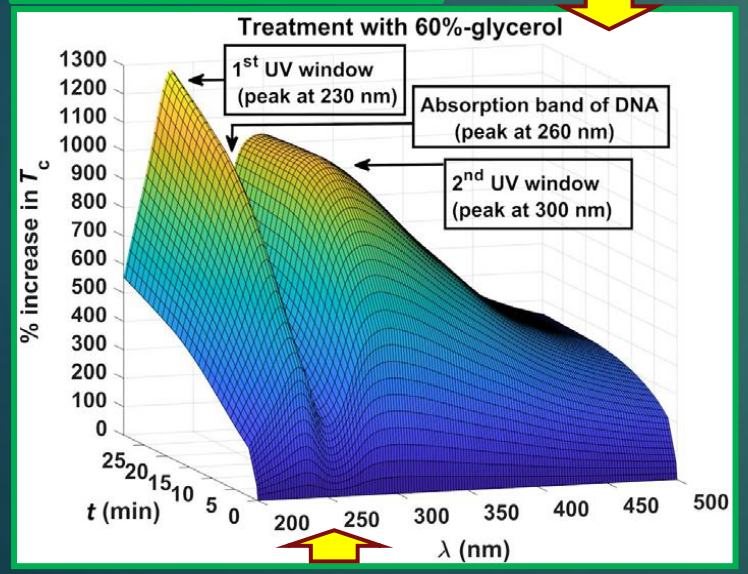

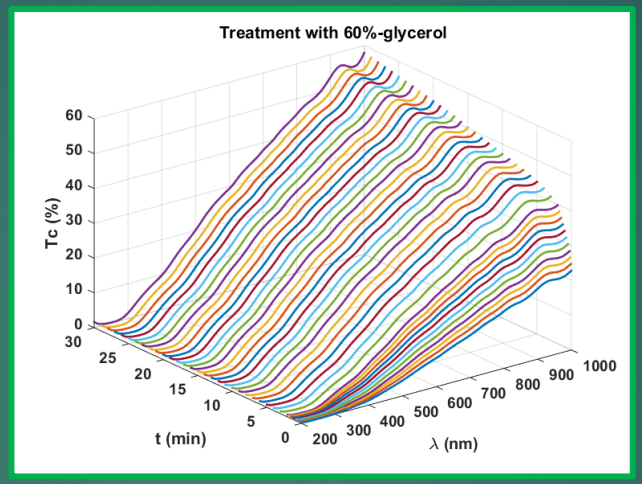

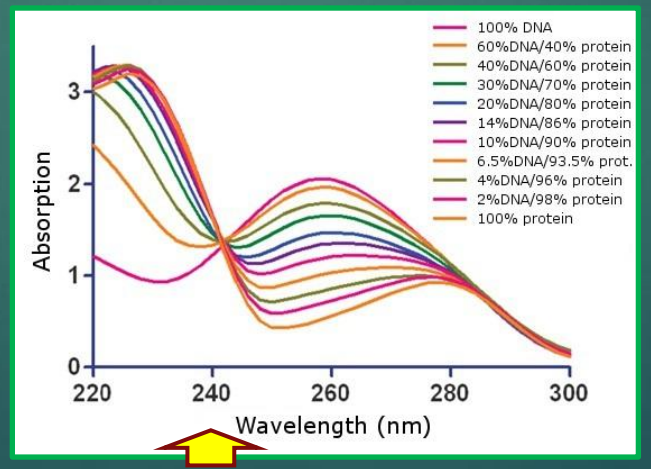

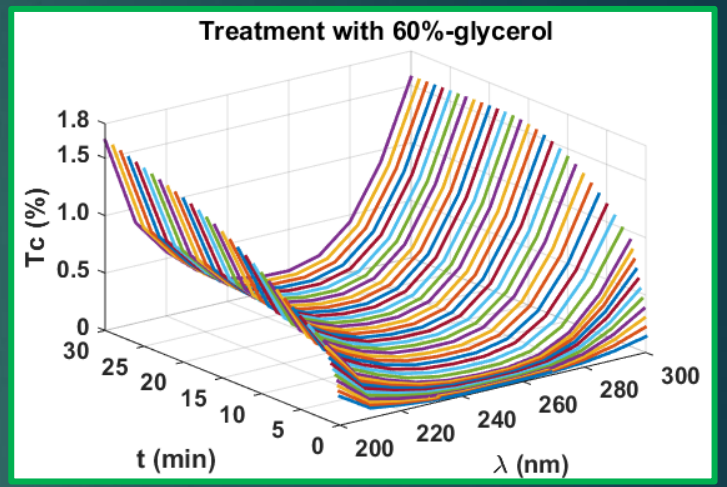

The OC effect in UV improves with the increase of glycerol concentration in the solution

$$T_c(\lambda) \propto 1 - \exp\left(-\frac{t}{\tau}\right)$$

$$\tau = \frac{l^2}{\pi^2 D_a}$$

$$\%\ \textbf{increase in}\ T_c = \frac{T_c(\lambda, t) - T_c(\lambda, t=0)}{T_c(\lambda, t=0)} \times 100\%$$

Why is Glycerol good for use as a deep UV OCA?

M. N. Polyanskiy. Refractiveindex.info database of optical constants. *Sci. Data* **11**, 94 (2024) https://doi.org/10.1038/s41597-023-02898-2

Optical constants of $C_3H_5(OH)_3$ (Glycerol)

Birkhoff et al. 1978: n,k 0.0512–0.620 µm

Wavelength: 0.2 µm (0.05123–0.61992) line select unit converter

Complex refractive index (*n+ik*) [i]

Refractive index [i]

$n = 1.6747$

Extinction coefficient [i]

$k = 0.0000$

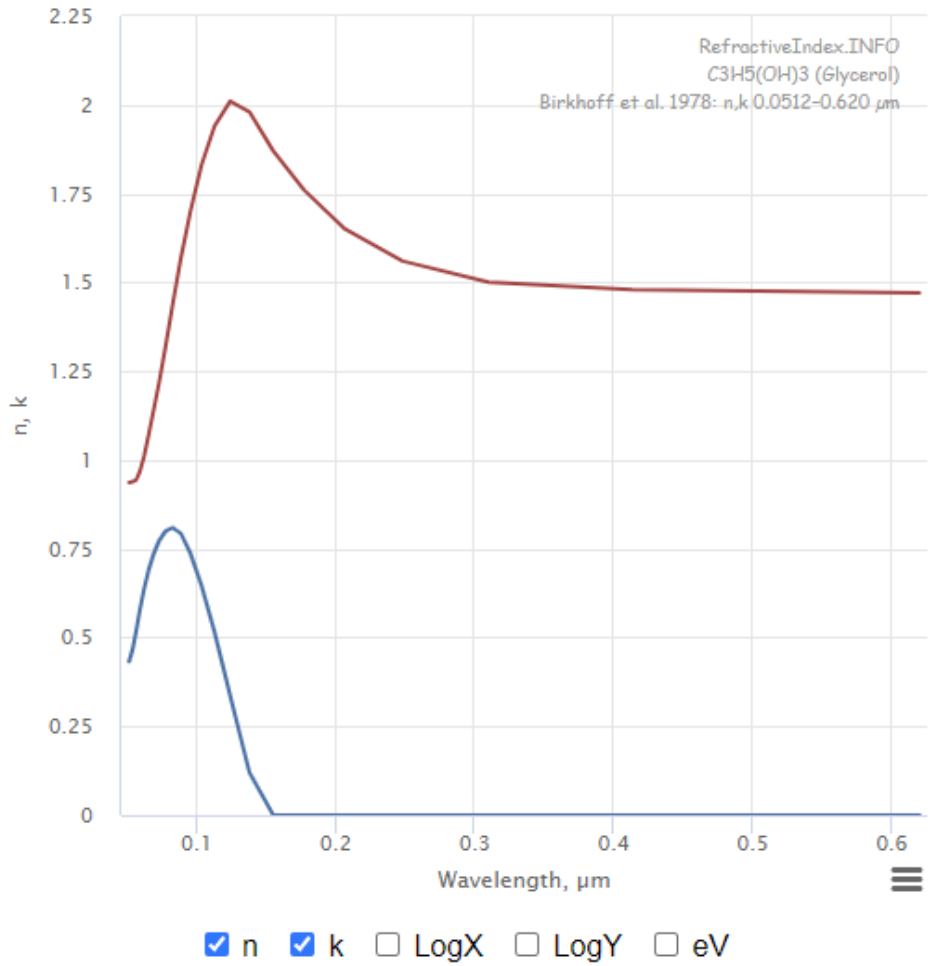

Transmittance [i]

$T = 1.0000$

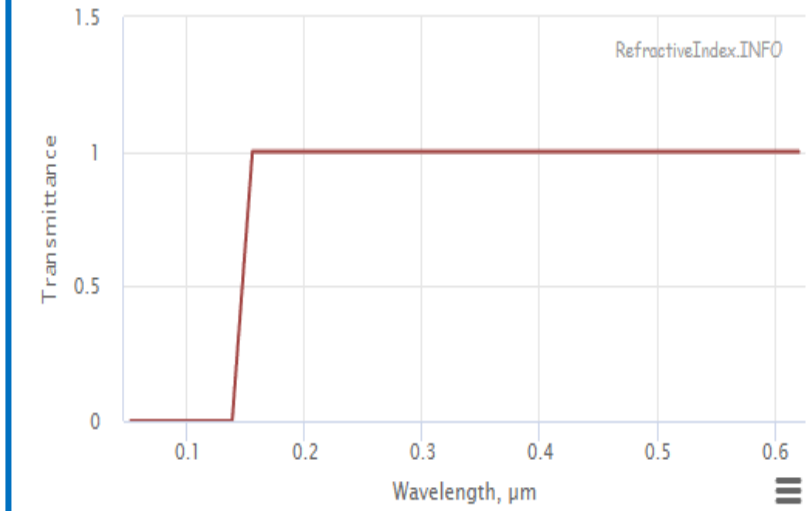

The effectiveness of human gingival tissue OC and therapy

A.A. Selifonov and V.V. Tuchin, Control of the optical properties of gums and dentin tissue of a human tooth at laser spectral lines in the range of 200 – 800 nm, Quantum Electronics, 50 (1), 47-54 (2020)
I. Carneiro, S. Carvalho, R. Henrique, A. Selifonov, L. Oliveira, V.V. Tuchin, Enhanced ultraviolet spectroscopy by optical clearing for biomedical applications, *IEEE Journal of Selected Topics in Quantum Electronics* **27** (4), 7200108-1-8 (2021)

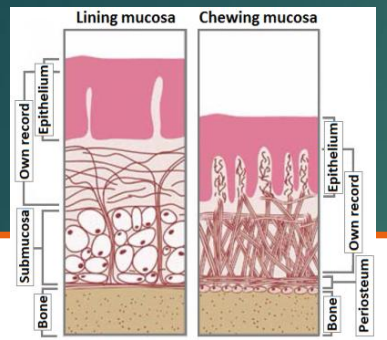

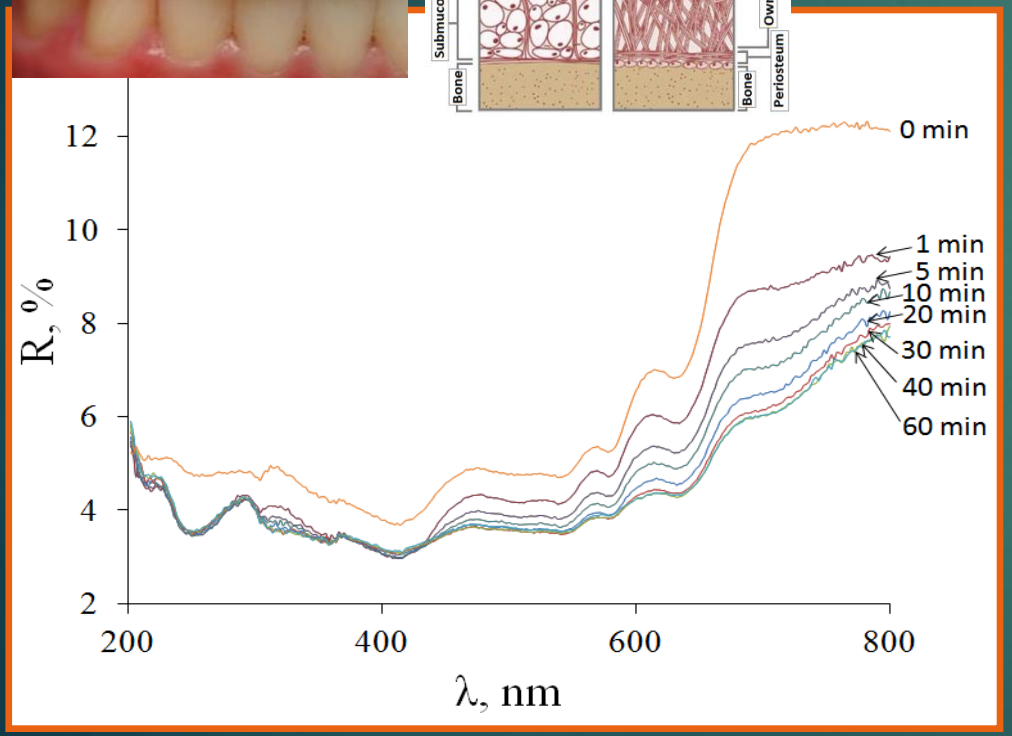

The effectiveness of human gum OC in propylene glycol / glycerol / water mixture E-cigarette vapor liquid

OCA: 99.7% glycerol

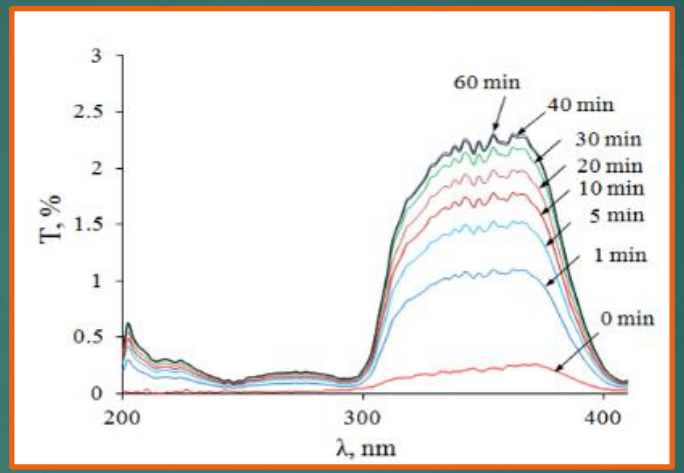

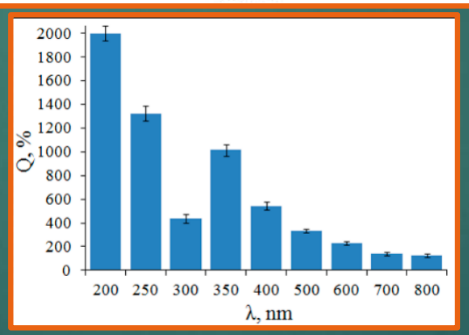

The effective diffusion coefficient in human gum mucous tissue measured *in vitro*:

$D\,(30/70/0) = (2.3\pm0.4)\cdot10^{-6}$ cm²/s
$D\,(50/50/0) = (2.6\pm0.6)\cdot10^{-6}$ cm²/s
$D\,(55/35/10) = (3.2\pm0.8)\cdot10^{-6}$ cm²/s

A.A. Selifonov – PhD thesis on study of biophysics of control optical properties of biological tissue to optimize phototherapy for oral cavity diseases

The UV treatment of 120 patients with chronic stomatitis in children's clinic No. 3 in Saratov showed high efficiency for 4-6 procedures

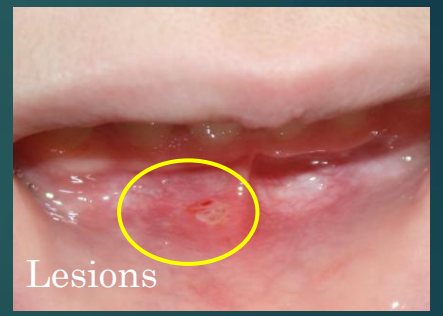

OC of mouse scalp skin

OCA: 70%-Glycerol + 5% DMSO

Laser beam
1268 nm

Scalp skin
Skull bone
Dura mater
CSF
Cortex
Gray matter
White matter

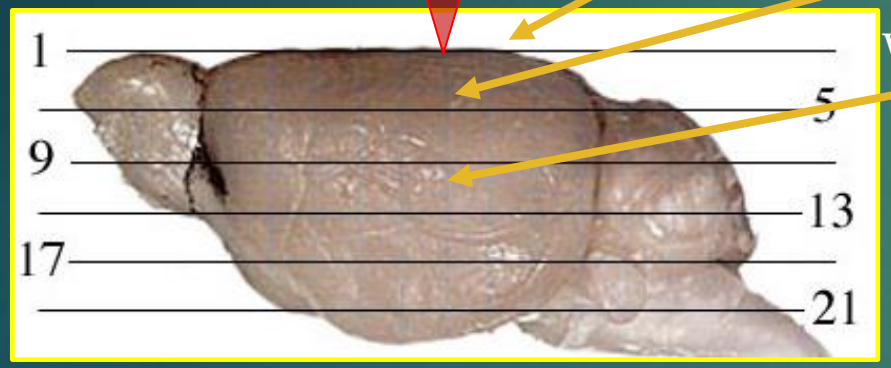

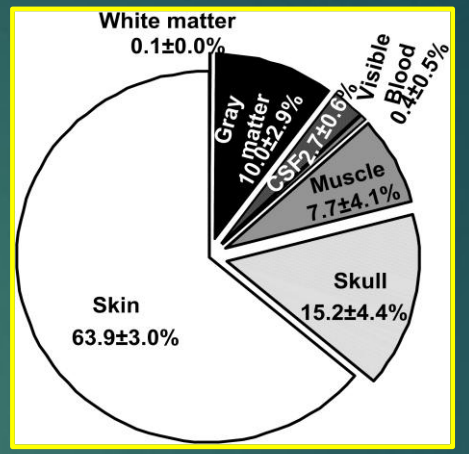

T. Li, et al. JIOHS 10(5), 1743002 (2017).

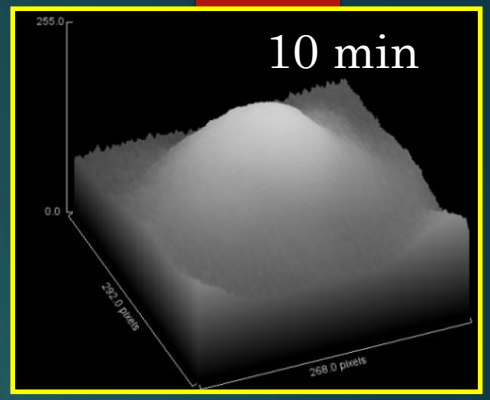

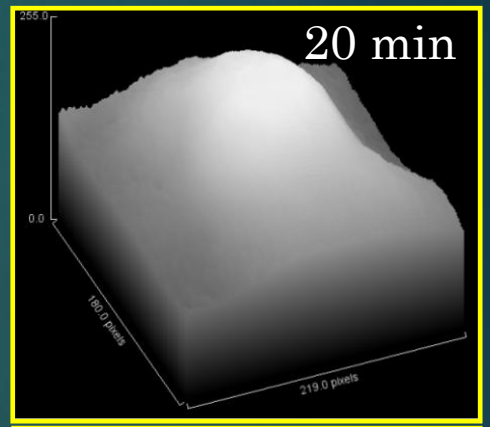

The thickness of the mouse head from skin surface to plane 13 was 7 mm

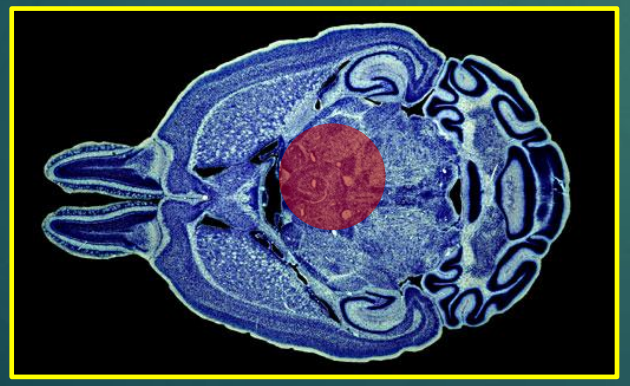

- Optogenetics
- Biomodulation
- Imaging

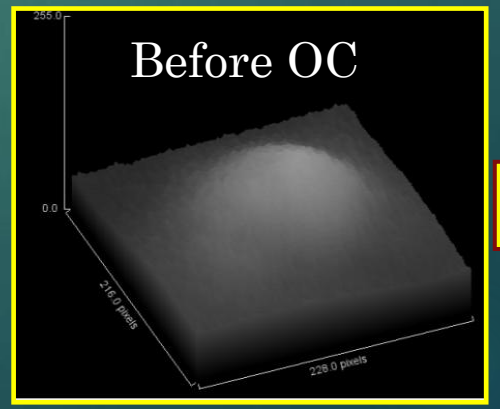

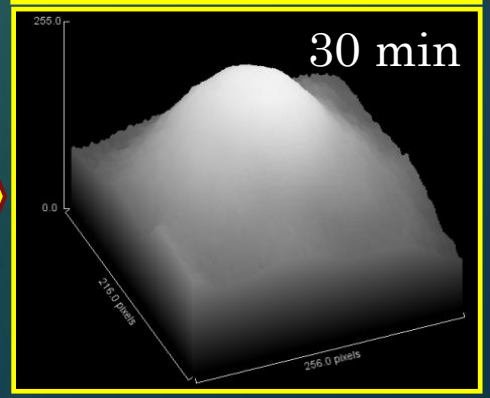

Monte Carlo simulation of radiative transfer for a four-layer mouse head model

P.A. Timoshina, D.K. Tuchina, Y.A. Zhavoronkov, S.V. Ul'yanov, V.L. Kuzmin, V.V. Tuchin, Transmission of NIR radiation through multi-layer mouse head at scalp skin optical clearing, *Academic Radiology* (2025)

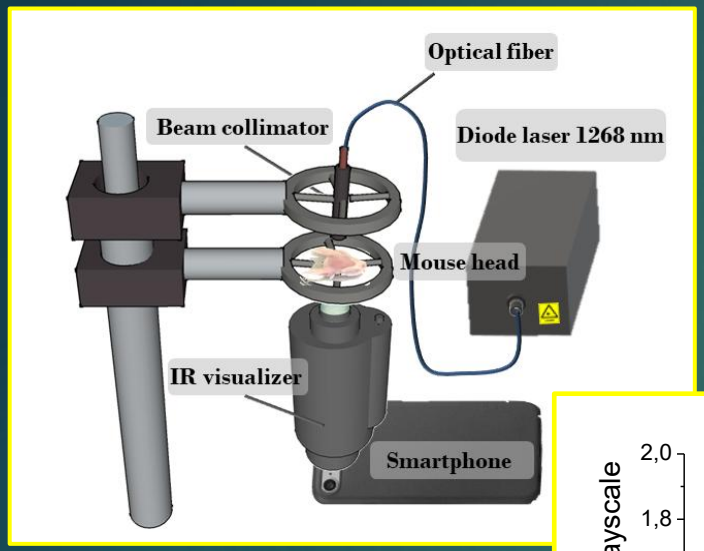

λ=1268 nm

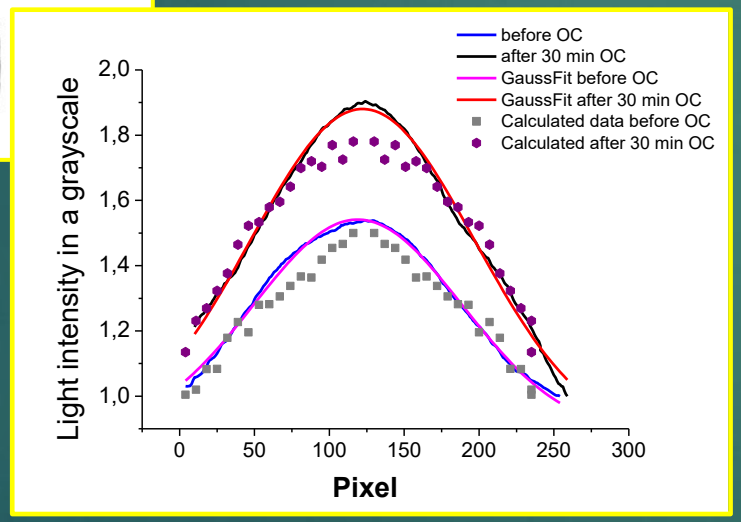

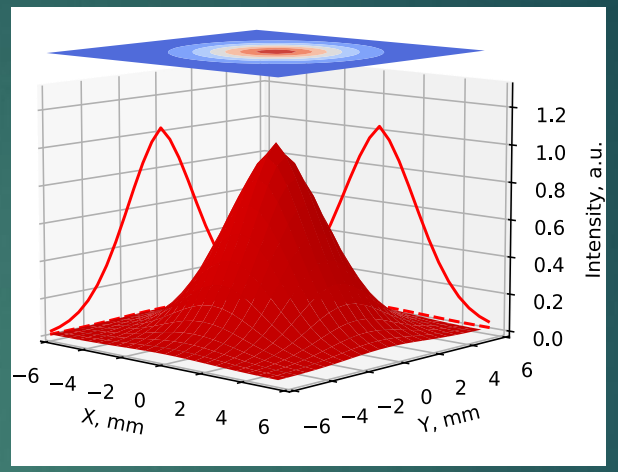

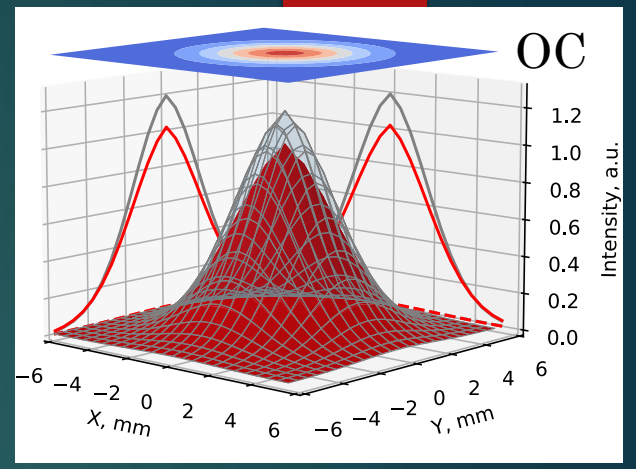

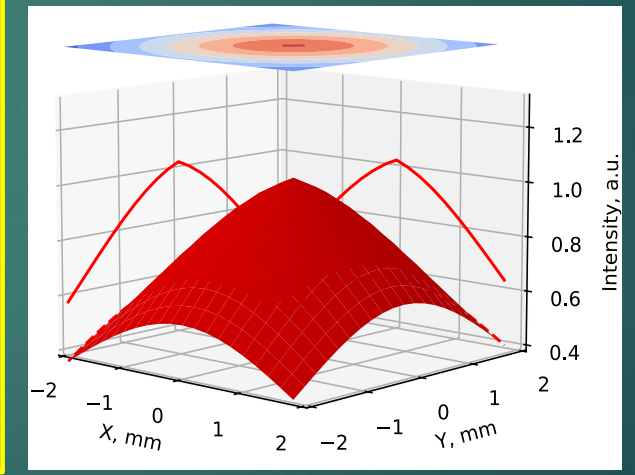

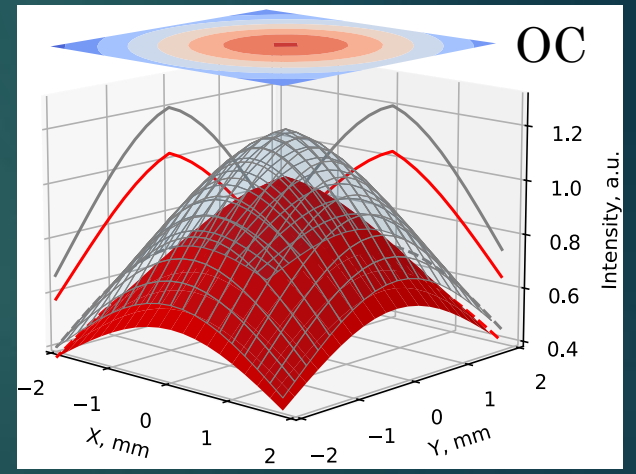

Intensity distribution of a 2 mm diameter incident beam (1268 nm) transmitted through half of the mouse head before (left) and after (right) the OC: the entire transmitted beam (12x12 mm2) (top), its central part (4x4 mm2) (bottom)

Skin OC allows to significantly increase the power density of laser beams in the internal parts of the mouse brain, up to 2.2 times

Kinetics of OC of tissues in rats with diabetes mellitus

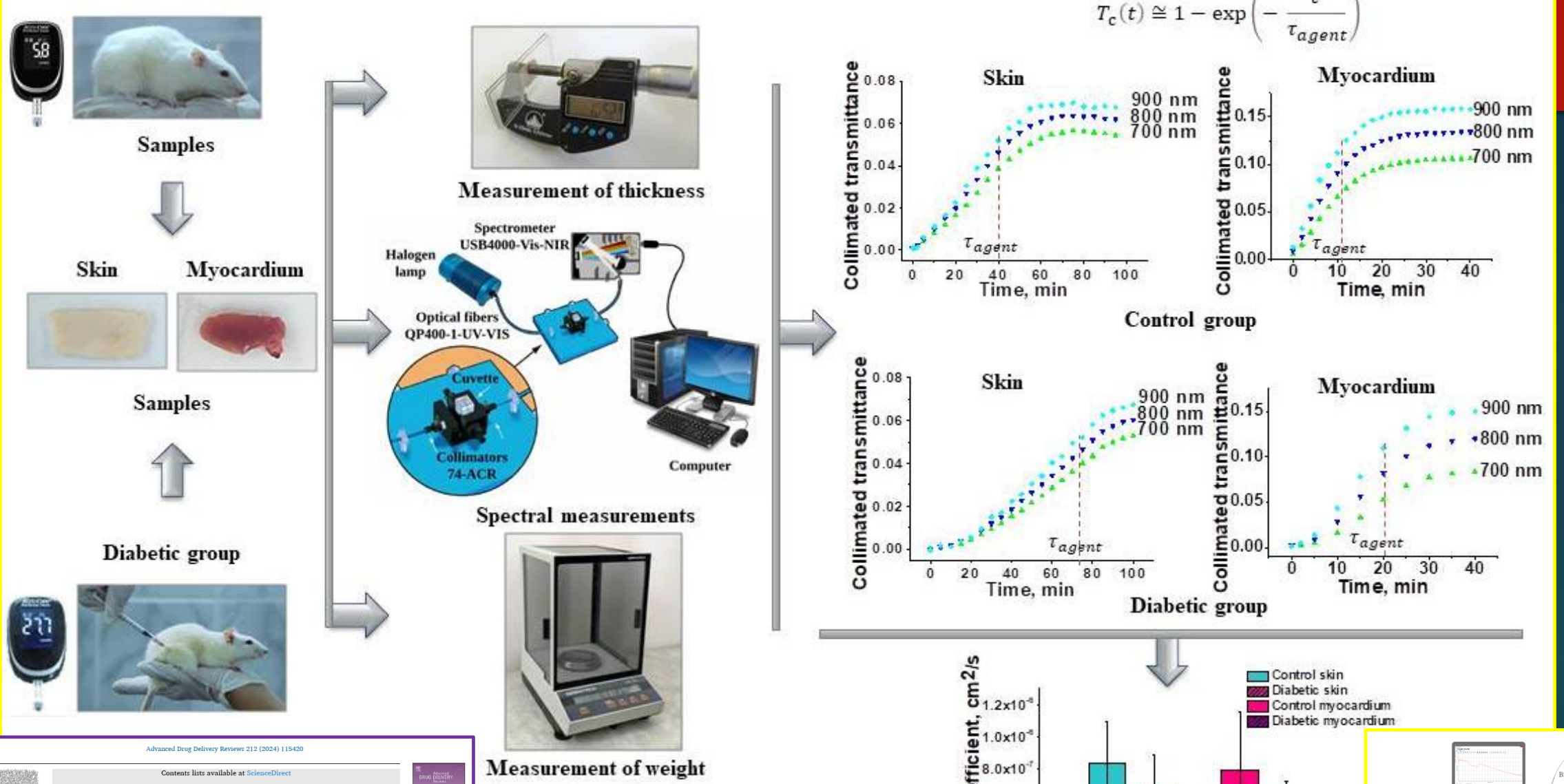

Advanced Drug Delivery Reviews 212 (2024) 115420

Contents lists available at ScienceDirect

Advanced Drug Delivery Reviews

journal homepage: www.elsevier.com/locate/adr

Light in evaluation of molecular diffusion in tissues: Discrimination of pathologies

Luís R. Oliveira[a,1], Maria R. Pinheiro[b,1], Daria K. Tuchina[c,d,1], Polina A. Timoshina[c,d,e,1], Maria I. Carvalho[b,f,2], Luís M. Oliveira[b,g,*,2]

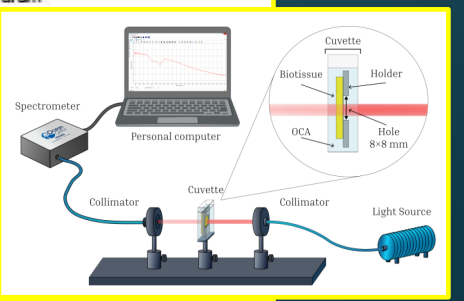

Kinetics of optical clearing of head tissues in rats with diabetes mellitus

A. S. Shanshul, E. N. Lazareva, Yu. I. Surkov, et al., *Izv. Sarat. Univer.*, 2025

Control (C) Gray matter of the brain Diabetes (D)

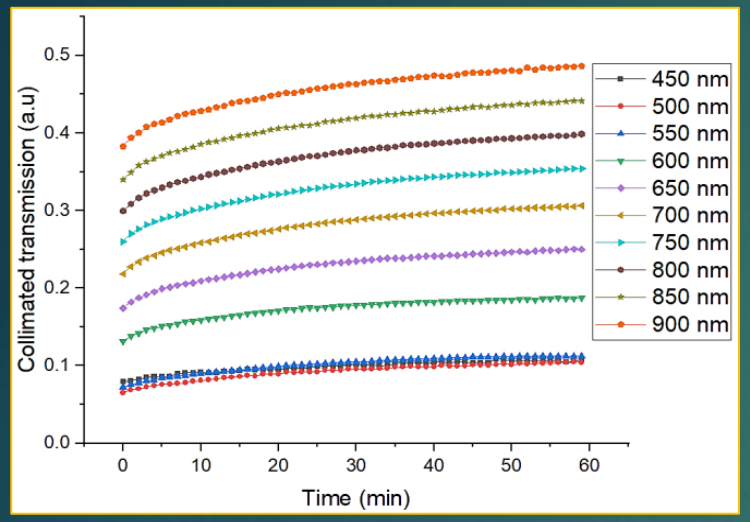

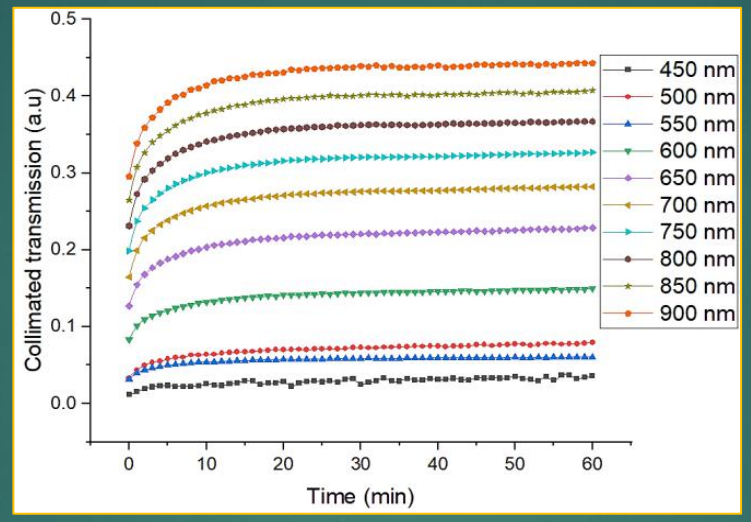

Control (C) White matter of the brain Diabetes (D)

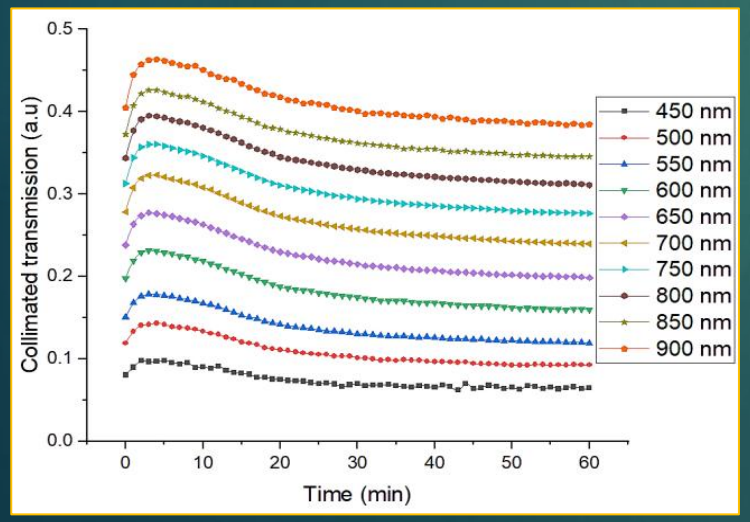

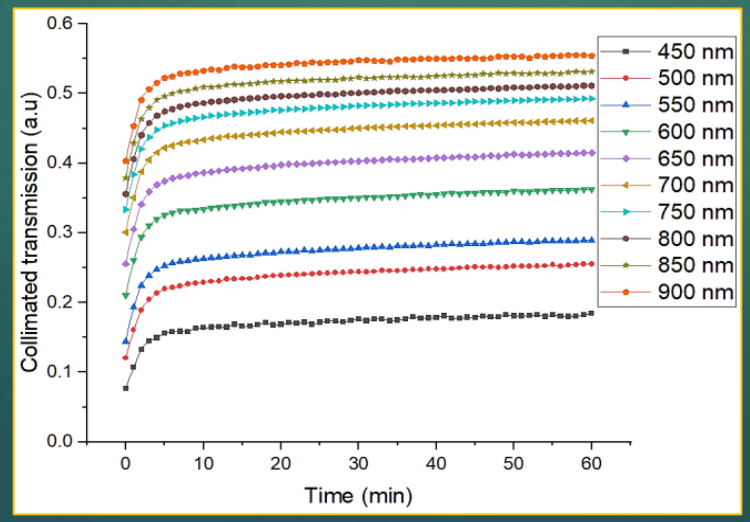

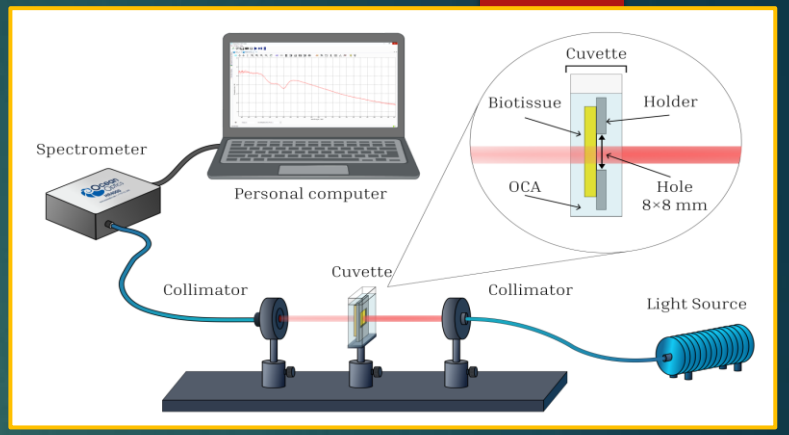

Tissue	C/D	τ, min	Growth τ, %	*l*, mm (before/after)
Scalp skin	C	14±10	14	0.45/0.51
	D	16±11		0.44/0.50
Skull bone	C	32±15	12,5	0.90/0.94
	D	36±15		0.94/0.97
Dura mater	C	13±10	15	0.25/0.27
	D	15±11		0.21/0.23
Gray matter	C	11±5	18	0.21/0.23
	D	13±8		0.22/0.24
White matter	C	12±8	17	0.15/0.17
	D	14±6		0.12/0.14

Frontiers of Optoelectronics (2025) 18:6
https://doi.org/10.1007/s12200-025-00149-3
Frontiers of Optoelectronics
RESEARCH ARTICLE

Age as a limiting factor for effectiveness of photostimulation of brain drainage and cognitive functions

Terskov Andrey[1] · Shirokov Alexander[1,2] · Blokhina Inna[1] · Zlatogorskaya Daria[1] · Adushkina Viktoria[1] · Semiachkina-Glushkovskaia Anastasiia[3] · Atul Kumar[4] · Fedosov Ivan[5] · Evsukova Arina[1] · Semyachkina-Glushkovskaya Oxana[1]

Fluorescent imaging of mouse cancer cells *in vivo*

D.K. Tuchina, I.G. Meerovich, O.A. Sindeeva, V. V. Zherdeva, A. P. Savitsky, A. A. Bogdanov Jr, V. V. Tuchin, Magnetic resonance contrast agents in optical clearing: Prospects for multimodal tissue imaging. *J. Biophotonics* 13(11) e201960249 (2020); *Quantum Electronics* (2021)

20 days after tumor cell enucleation (HEp2-TagRFP) in BALBc/nude mice

OCA: 70% glycerol, 5% DMSO, 25% water

Profiles for fluorescence signal

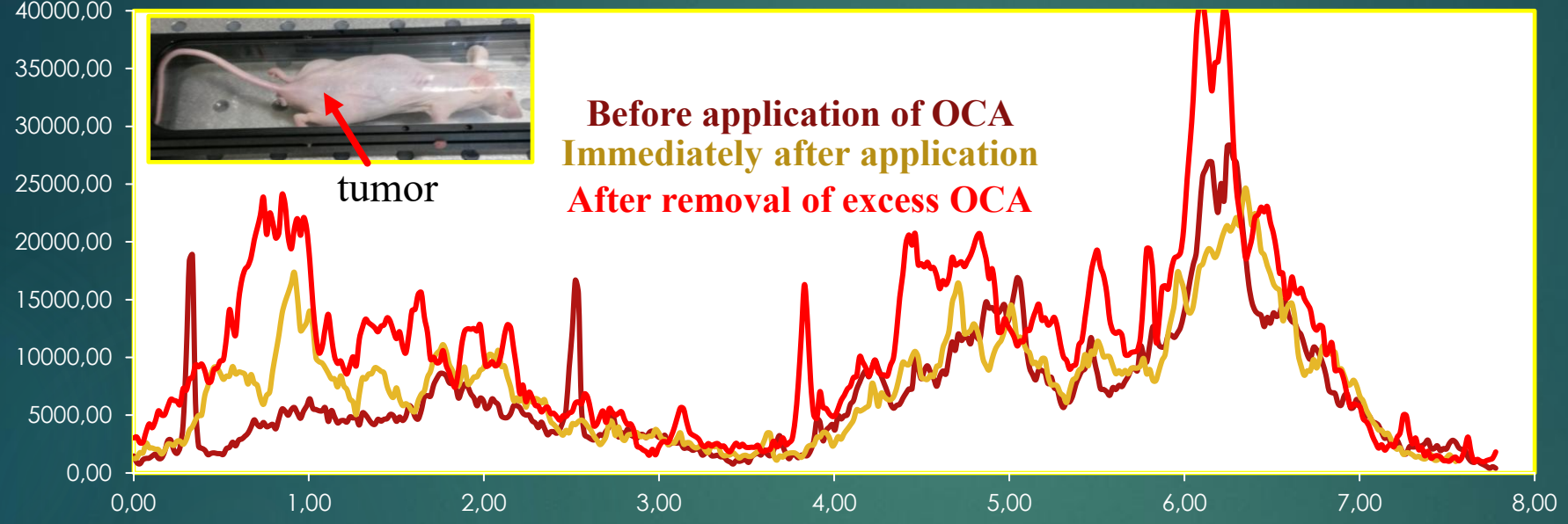

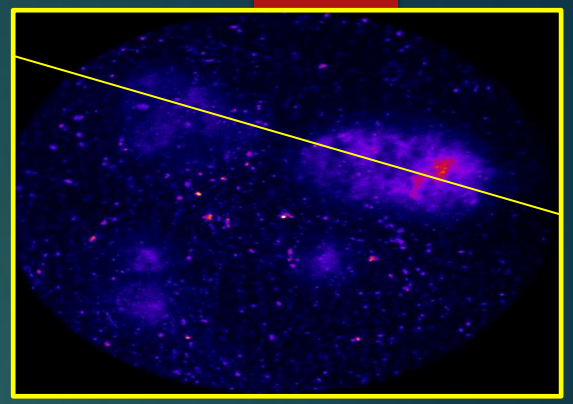

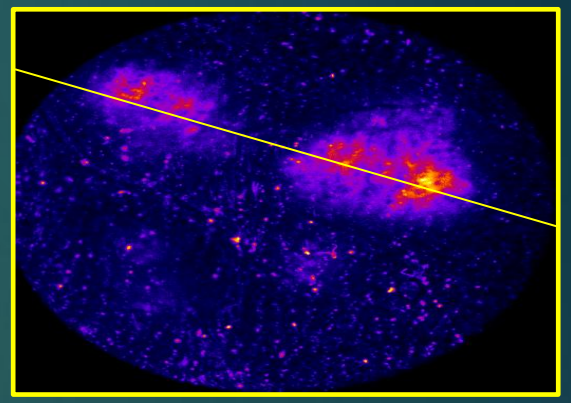

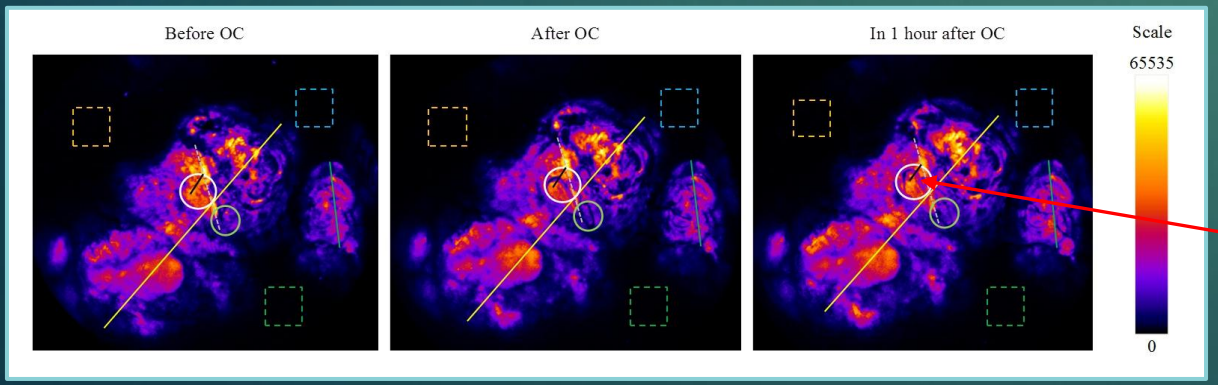

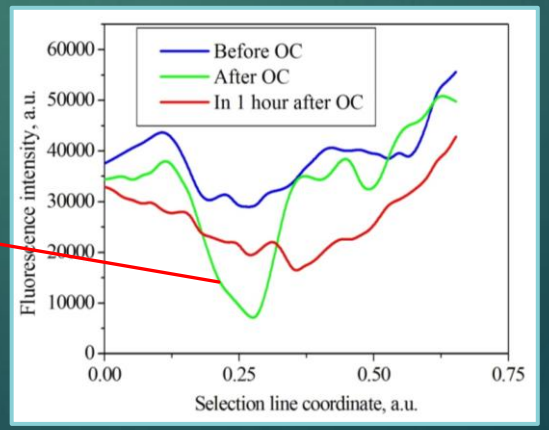

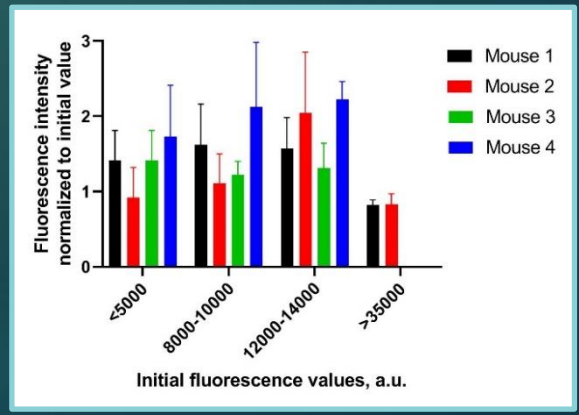

MRI contrast agents can be successfully used as OCA to improve optical imaging

This is a fundamentally new approach to multimodal imaging using MRI and optical methods

D.K. Tuchina, I.G. Meerovich, O.A. Sindeeva, V. V. Zherdeva, A. P. Savitsky, A. A. Bogdanov Jr, V. V. Tuchin, Magnetic resonance contrast agents in optical clearing: Prospects for multimodal tissue imaging. *J. Biophotonics* **13**(11) e201960249 (2020); *Quantum Electronics* (2021)

V.V. Tuchin, D.K. Tuchina, A.P. Savitsky, A.A. Bogdanov Jr. Method for visualizing biological tissues and/or organs, patent RU 2 735 463 dated 03.09.2020.

$$\frac{l_d}{L} = \sqrt{\frac{D_a^{free}}{D_a^{tissue}}}$$

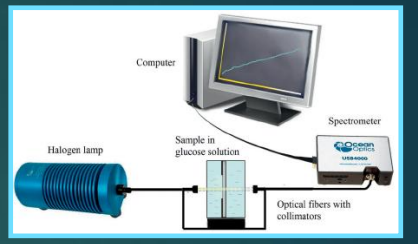

MRI image of the head

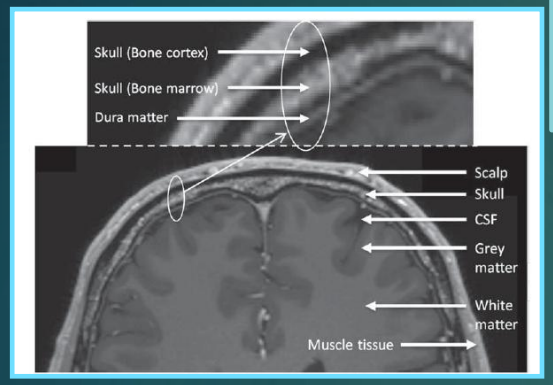

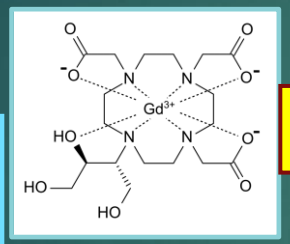

Gadovist (Gadobutrol 604.72)

Introduction of MRI and CT agents and saline into mouse skin

MR CA	0 min	30min	60 min
Gadovist®			
Magnevist®			
Dotarem®			
CT CA Visipaque®			
Saline			

Agent	MR
Trademark	Gadovist
D_a^{tissue}, cm^2/s	$(4.29 \pm 0.39) \times 10^{-7}$
D_a^{free}, cm^2/s	3.9×10^{-6}
Tortuosity, l_d/L	3.0

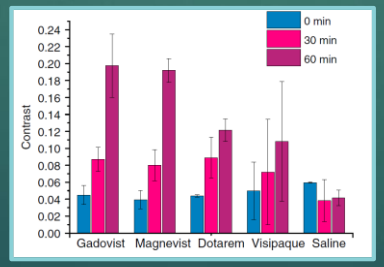

MRI agents increase skin transmittance up to 20-30 times

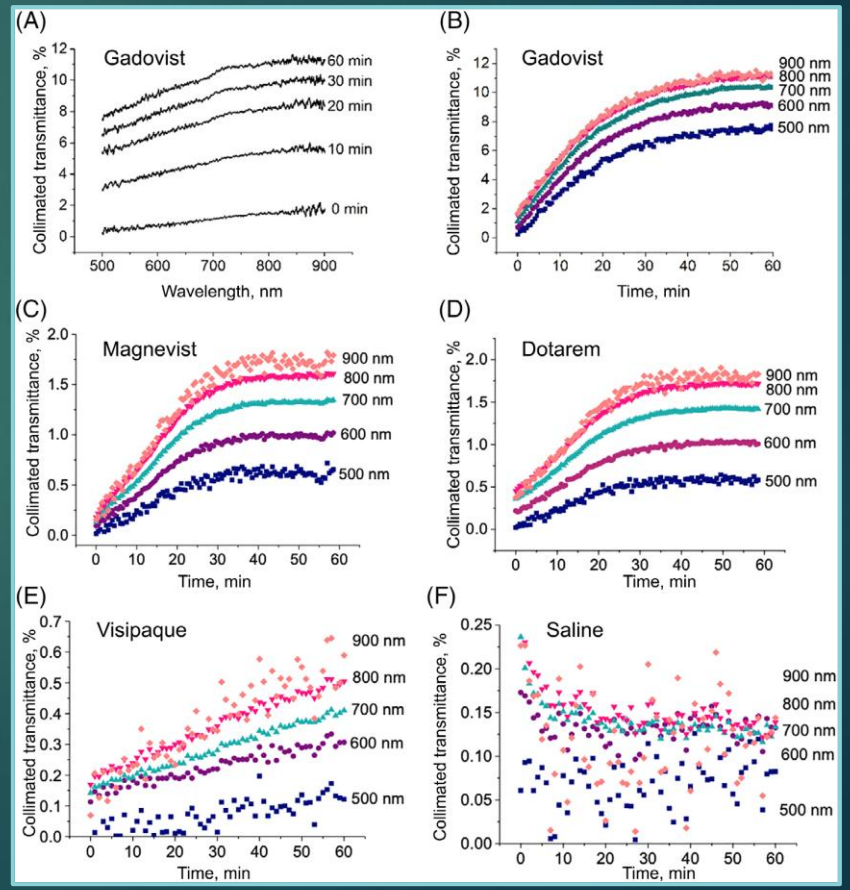

H.F. Silva, I.S. Martins, A.A. Bogdanov Jr., V.V. Tuchin, L.M. Oliveira, Characterization of optical clearing mechanisms in muscle during treatment with glycerol and gadobutrol solutions, ***J. Biophotonics*** 16(1), e202200205 (2023)

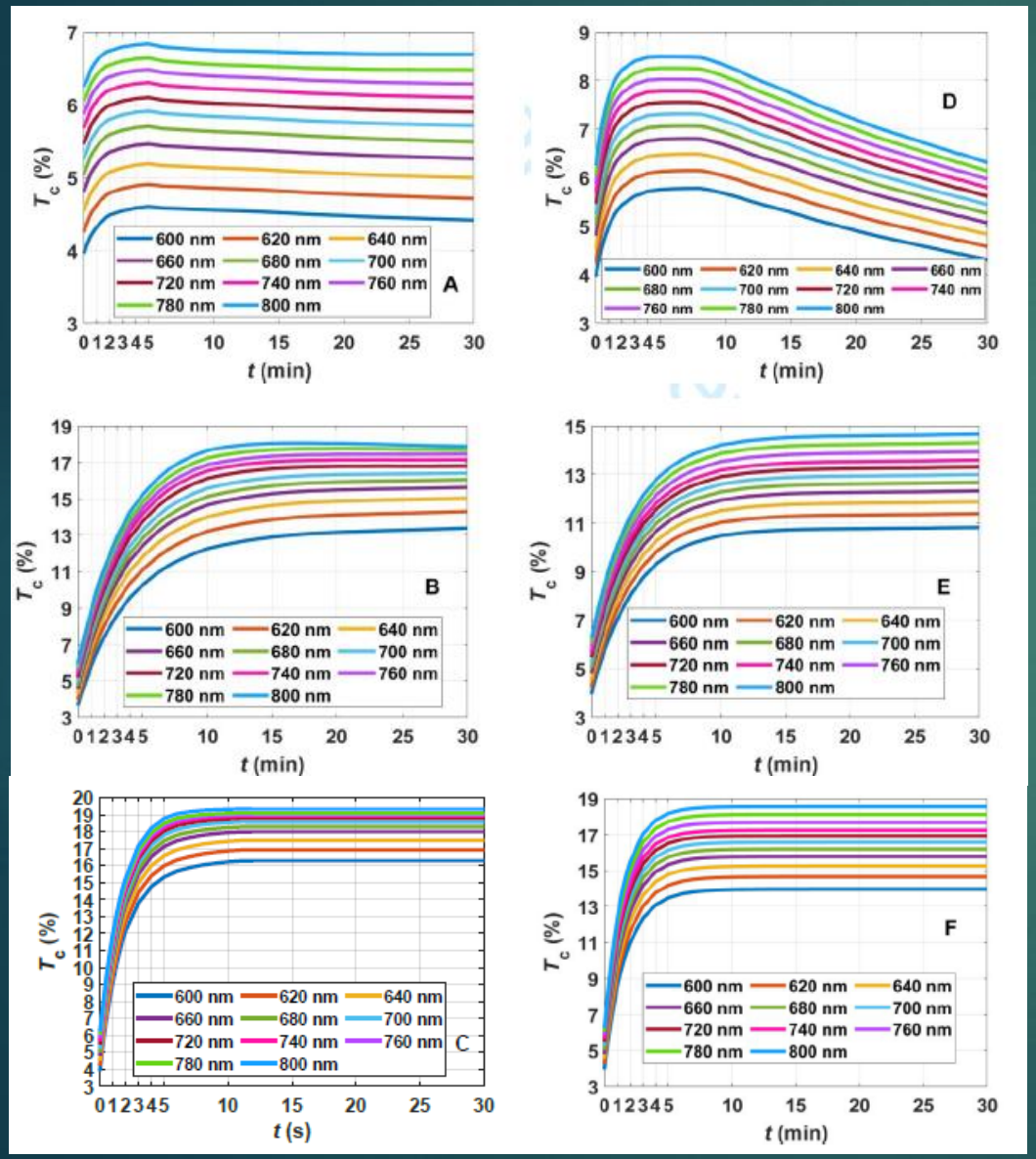

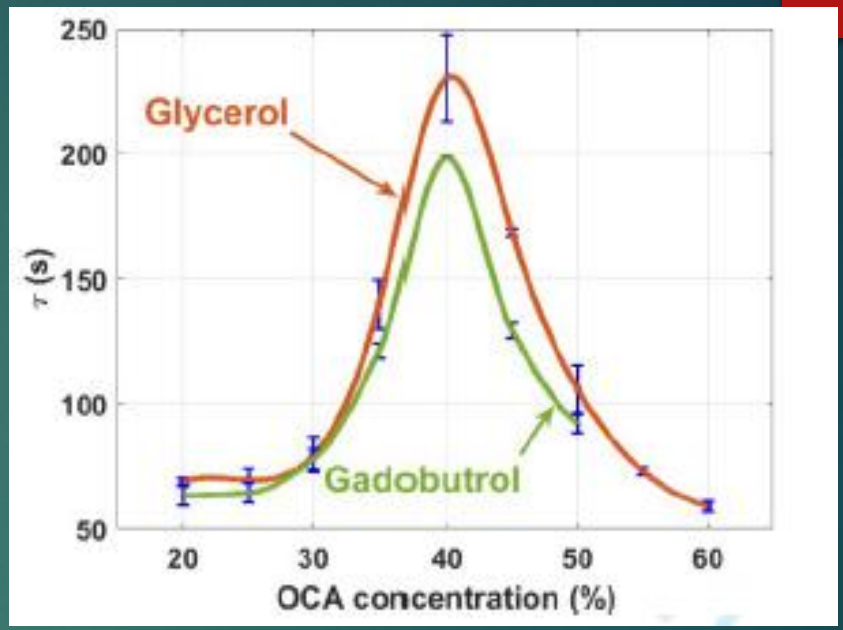

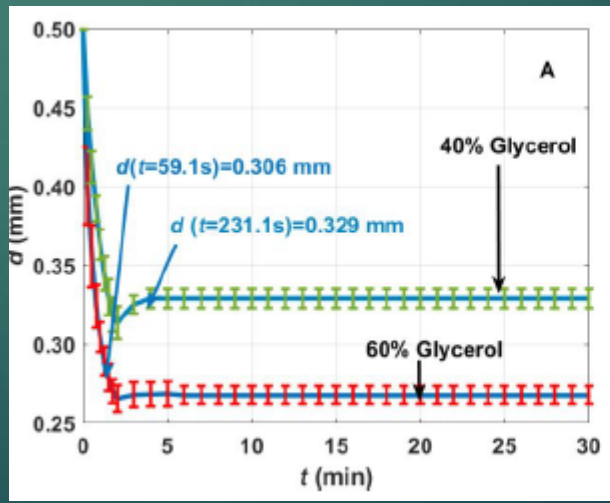

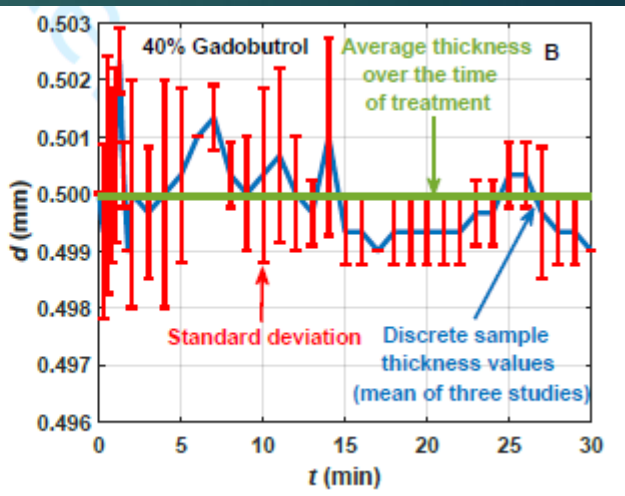

Tag-RFP fluorescence and MRI of tumor xenografts in mice after intravenous injection of gadobutrol (GB) (MRI contrast)

N.I. Kazachkina, V.V. Zherdeva, I.G. Meerovich, A.N. Saydasheva, I.D. Solovyev, D.K. Tuchina, A.P. Savitsky, V.V. Tuchin, A.A. Bogdanov Jr., "MR and fluorescence imaging of gadobutrol-induced optical clearing of red fluorescent protein signal in an in vivo cancer model," NMR in Biomedicine, e4708-1-13 (2022).

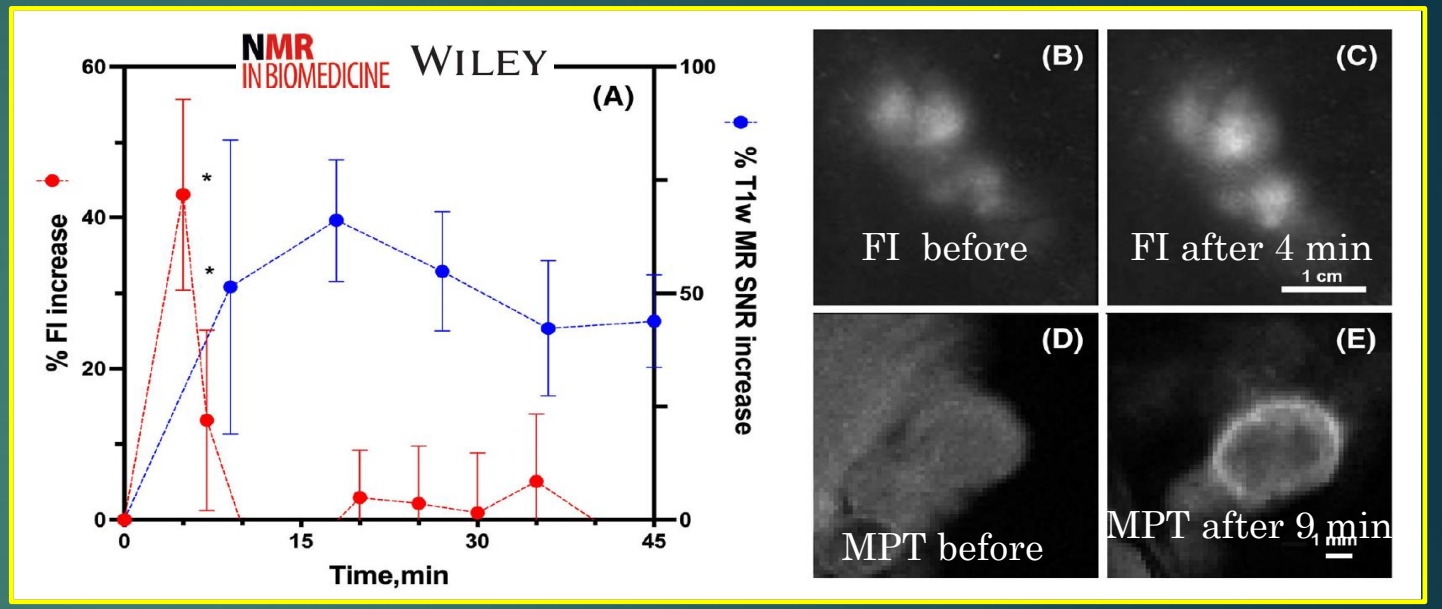

A: FI and T1w MRI SNR kinetics measured using the whole tumor ROI after intravenous GB injection (0.3 mmol/kg, n = 3). Data are presented as mean ± SD. Asterisks indicate that the measured mean values are statistically significant compared with baseline values ($P < 0.01$).
B: Tag-RFP FI imaging before intravenous GB injection.
C: Tag-RFP FI imaging 4 min after intravenous GB injection
D: One sagittal T1w GRE MRI slice of the tumor before GB injection.
E: Corresponding sagittal T1w GRE MRI slice of the tumor 9 min after GB injection; scale bar, 1 mm

Nonlinear Microscopy

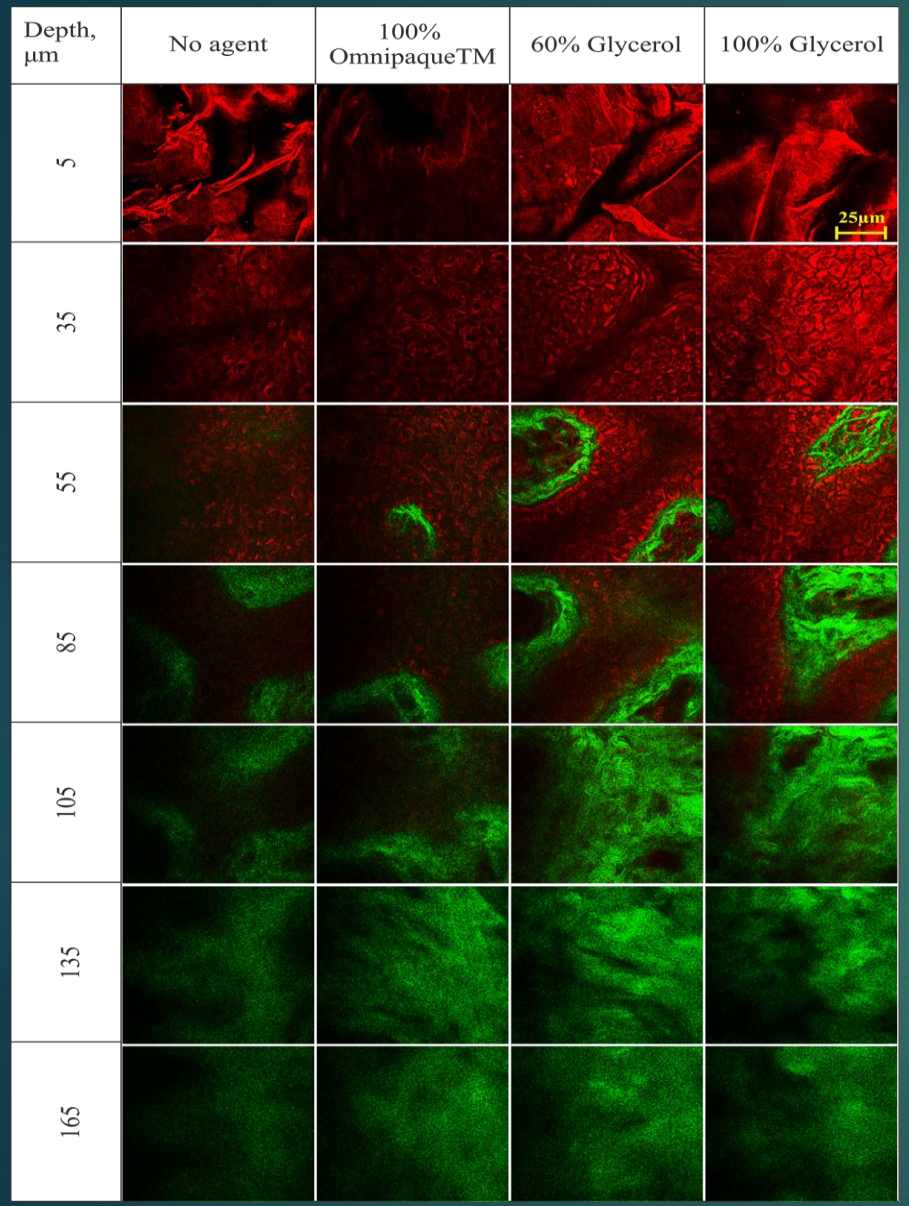

Red – TPEAF signal
Green – SHG signal

TPEAF and SHG images of skin layers obtained *ex vivo* on porcine ear skin samples for Omnipaque™ and glycerol solutions

A. Sdobnov, M. E. Darvin, J. Lademann, V. Tuchin, *J. Biophotonics* (2017)

OCA	Glycerol			Omnipaque	
Concentration,%	40	60	100	60	100
Refractive index, n	1.384	1.413	1.474	1.392	1.432
Osmolarity, Osm/L	5.5	8.2	10.9	0.33	0.465
Viscosity, cp	3.7	10.8	1410	3.1	11.8

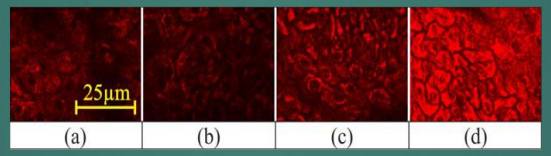

Epidermis on 35 μm depth OCA treatment (b)–(d): 100% Omnipaque, 40% glycerol, 100% glycerol.

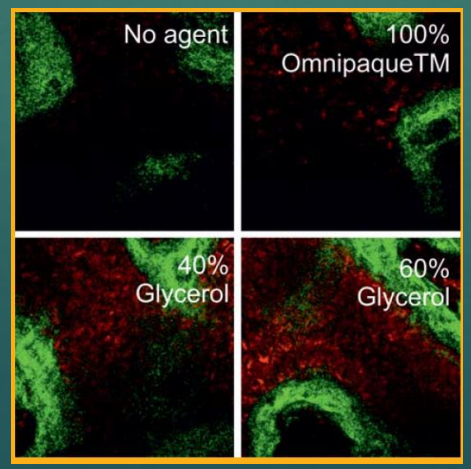

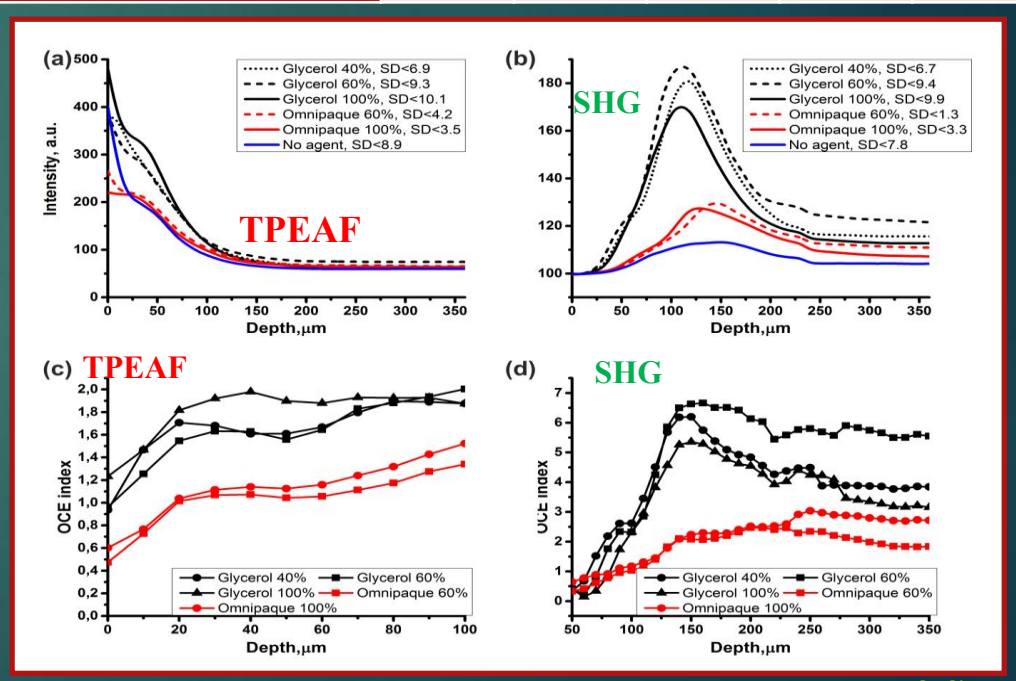

Averaged depth-dependent intensity profiles and OCE indices for TPEAF (a, c) and SHG (b, d) signals

Impact of E-cigarette liquid on *ex vivo* porcine lung optical properties studied by confocal Raman micro-spectroscopy

Ali Jaafar, et al. *J. Biophotonics* 17(2) e202300336 (2024)

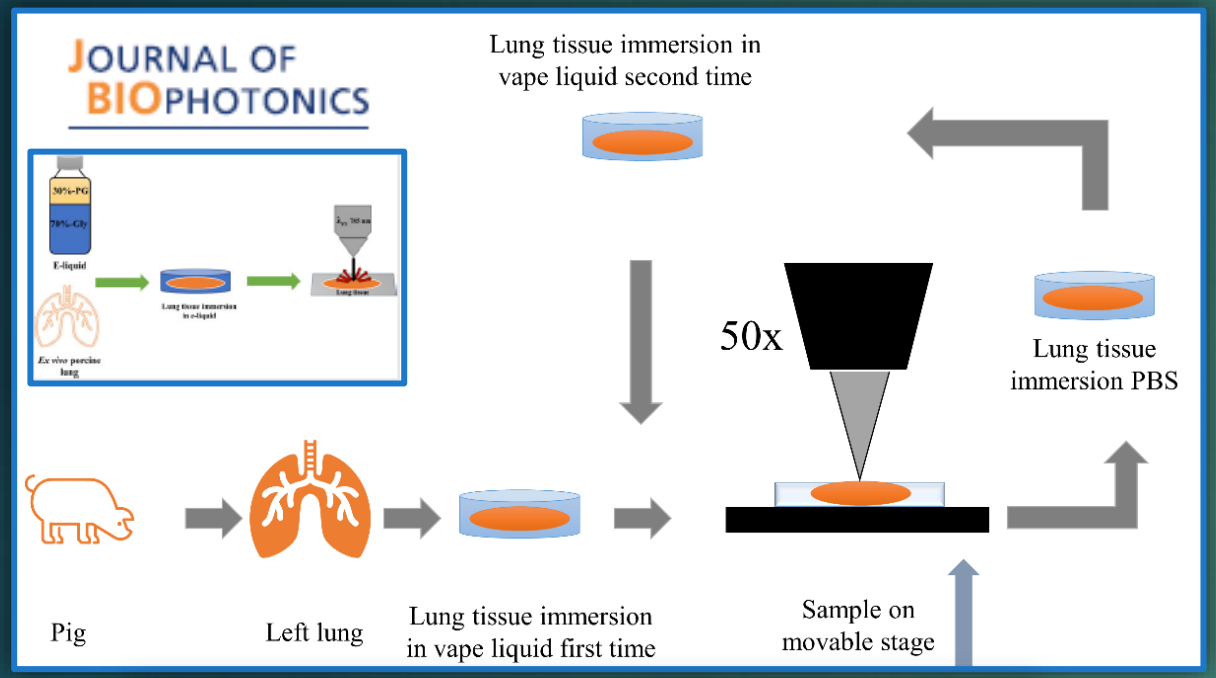

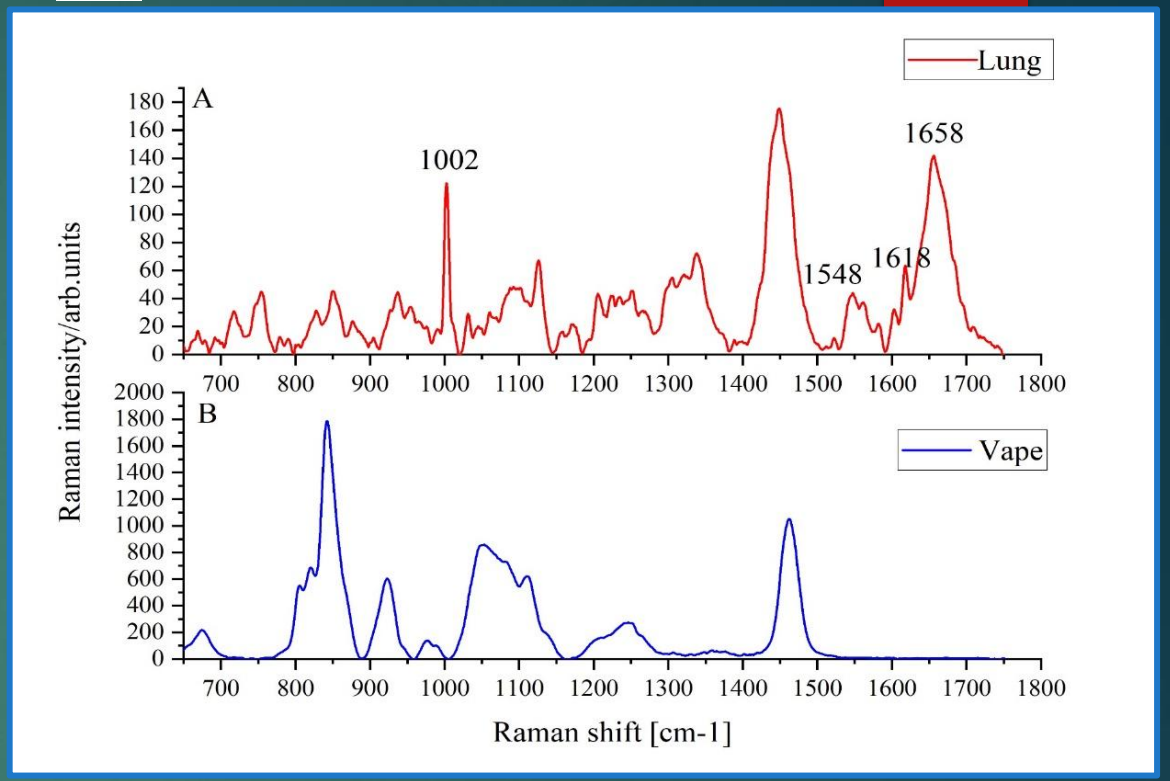

Average Raman spectra of control lung tissue (A), and vape containing of 70%Gly and 30% PG (B)

Lung tissue:

1002 Ring breathing Proteins (Phe)

1548 Proteins (Trp), deoxy-Hb

1618 (C=C), tryptophan

1658 Proteins (α-helix), lipids (unsat. FA) (Amide I)

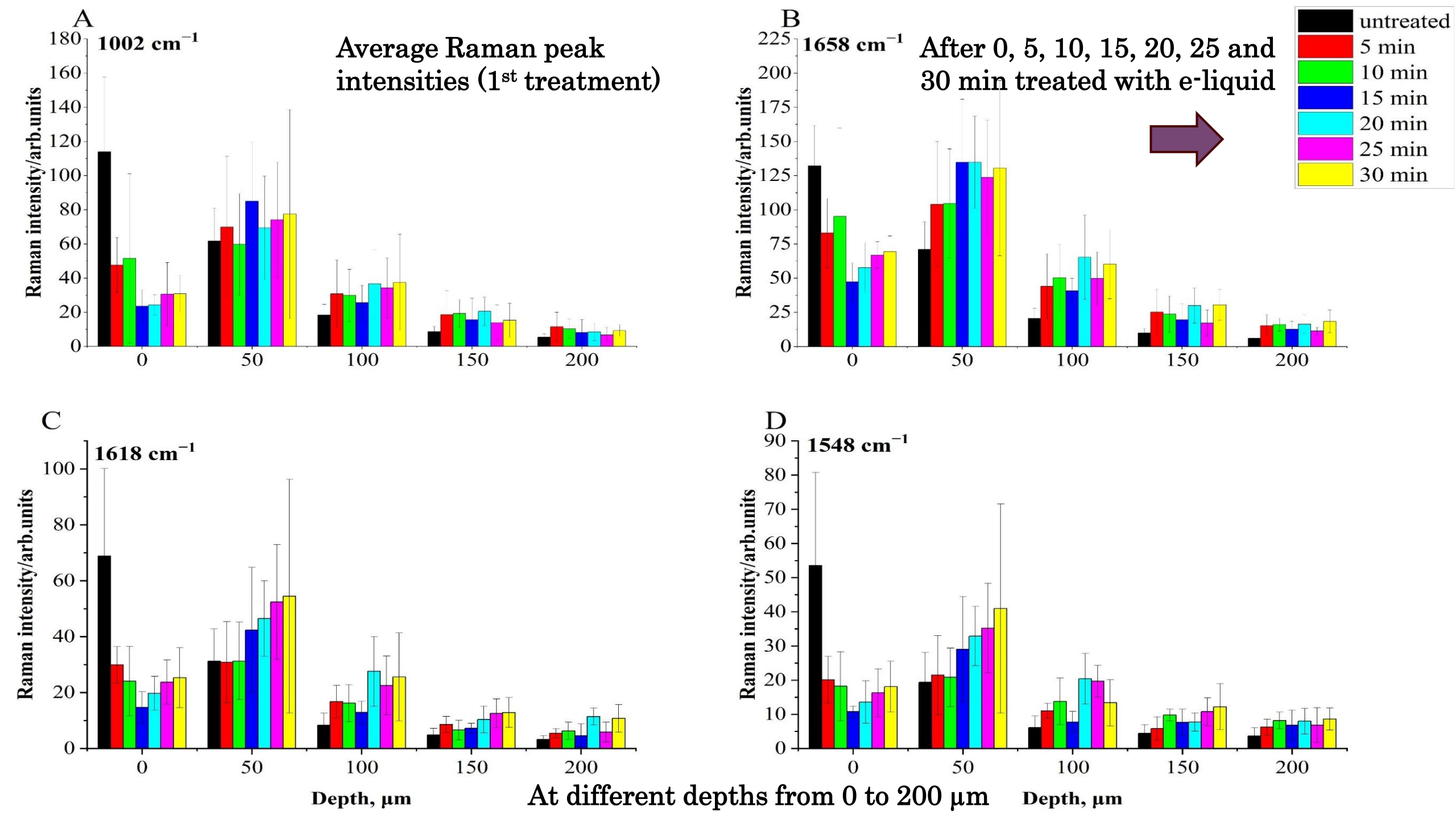
A
1002 cm⁻¹
Raman intensity/arb.units
Average Raman peak intensities (1st treatment)
B
1658 cm⁻¹
Raman intensity/arb.units
After 0, 5, 10, 15, 20, 25 and 30 min treated with e-liquid
untreated
5 min
10 min
15 min
20 min
25 min
30 min
C
1618 cm⁻¹
Raman intensity/arb.units
Depth, µm
D
1548 cm⁻¹
Raman intensity/arb.units
Depth, µm
At different depths from 0 to 200 µm

Kinetics of OC of human skin studied *in vivo* using a fiber Raman probe

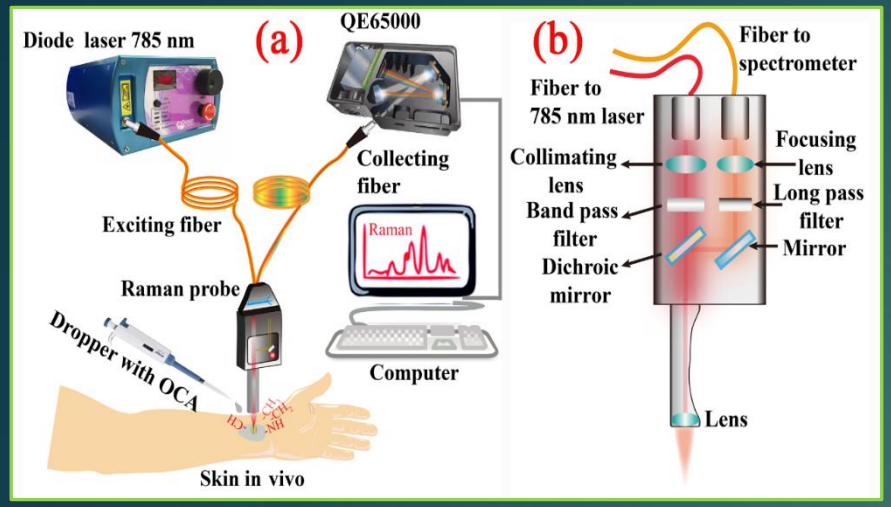

Diagram of the Raman experimental device (a) and detail of Raman probe (b)

Q. Lin et al., *Laser Phys. Lett.* (2020)

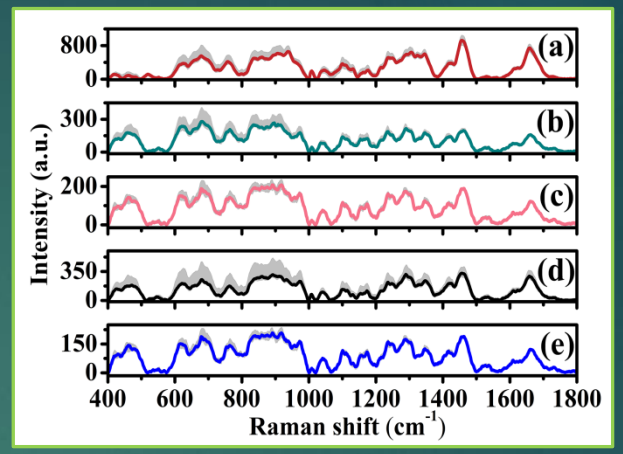

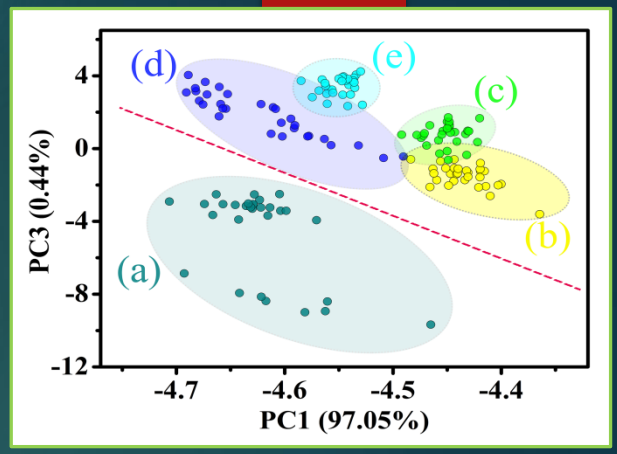

In vivo Raman spectra and PC scores scatter plots for the Raman spectra acquired from different body sites: : fingernail (a), finger (b), arm (c), palm (d), and wrist (e)

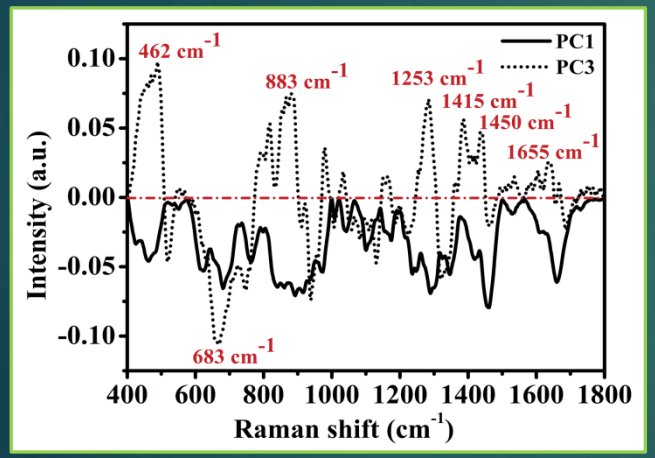

PC loading plots of the 1st (solid-line) and 3rd PCs (dotted-line) for the Raman spectra of different body sites

Raman spectra contribute differently to the classification

The PC variations of the different skin sites were largely dominated by bands at:

- **462 cm^{-1} (δ(CCC), proteins)**
- 683 cm^{-1} (ν(CS), amino acid)
- 883 cm^{-1} (ρ(CH$_2$)/ν(CC)/ν(CN), collagen)
- 1253 cm^{-1} (δ(CH$_2$)/ν(CN), nucleus)
- **1415 cm^{-1} (δ(CH$_3$), lipids)**
- 1450 cm^{-1} (δ(CH$_2$)/δ(CH$_3$); keratin, collagen)
- 1655 cm^{-1} (ν(C=O), keratin)

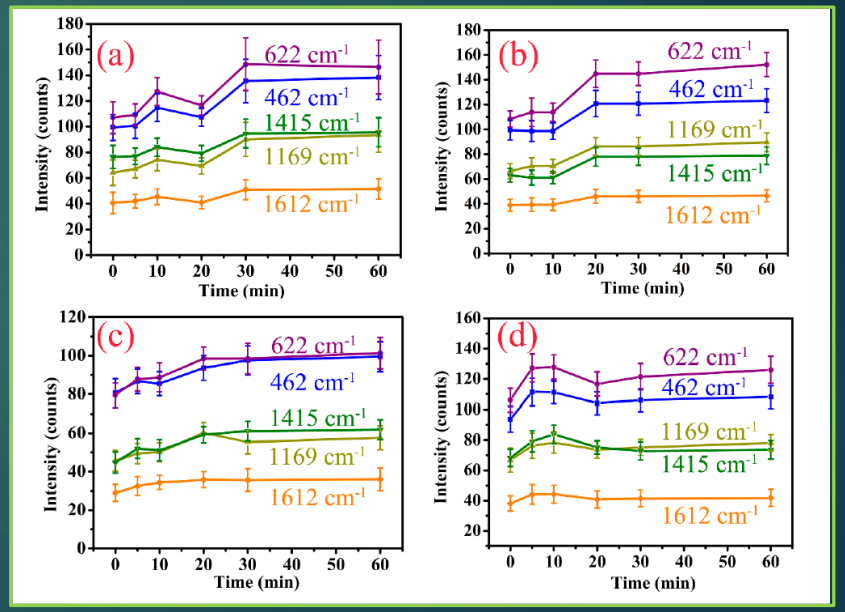

The time dependencies of wrist skin Raman peaks after application of glycerol with different concentration: 30% (a), 50% (b), 70% (c), and 99.9% (d).

Frontiers of Optoelectronics (2026) 19:1
https://doi.org/10.15302/foe.2026.0001

Frontiers of Optoelectronics

RESEARCH ARTICLE

Impact of glycerol solution on myocardium tissue – *Ex vivo* deep-UV Raman spectroscopy study

Ali Jaafar (✉)[1] · Tamas Vaczi[2] · Nicolae Tarcea[3] · Denis Akimov[4] · Tobias Meyer-Zedler[3,4] · Michael Schmitt[3] · Jürgen Popp[3,4*] · Valery V. Tuchin[5,6*] · Miklós Veres[2*]

Myocardium samples before, after 30 min, 60 min treatment with 70%-Gly

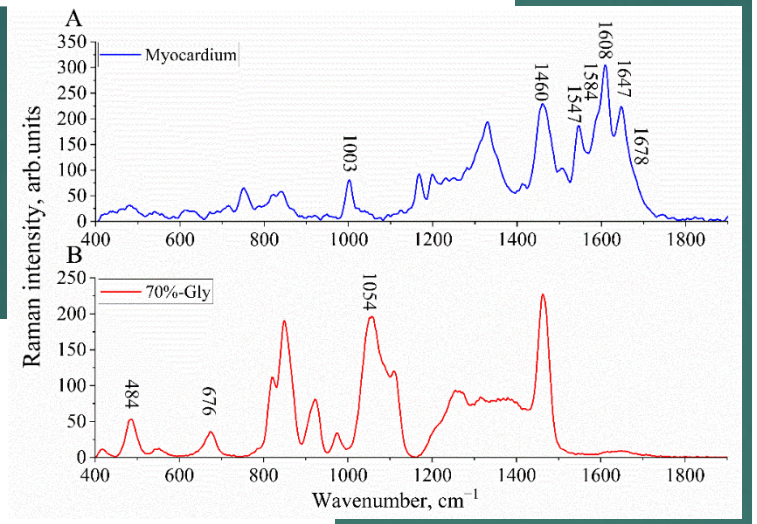

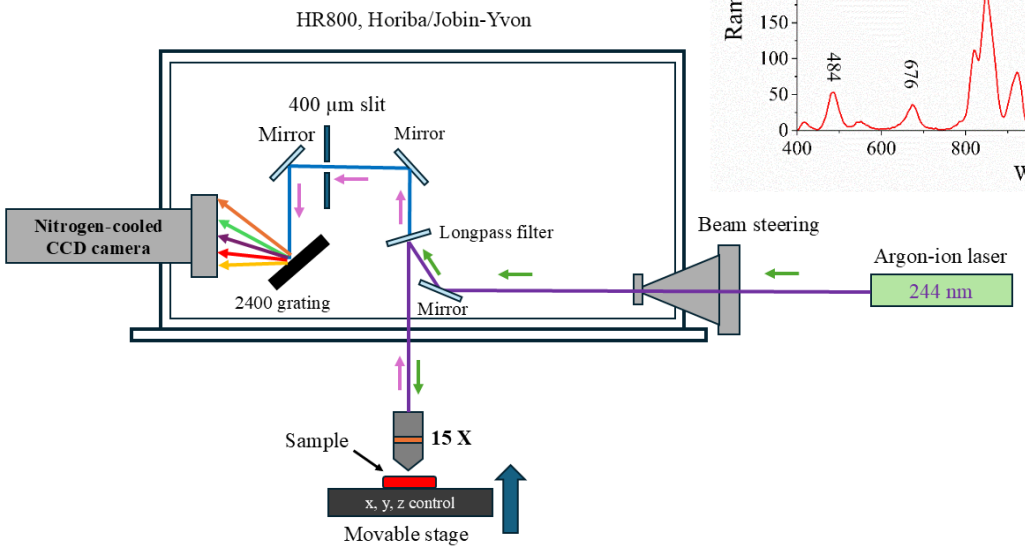

Raman micro-spectrometer Horiba/Jobin-Yvon. The paths of the laser and Raman signal are showed by arrows

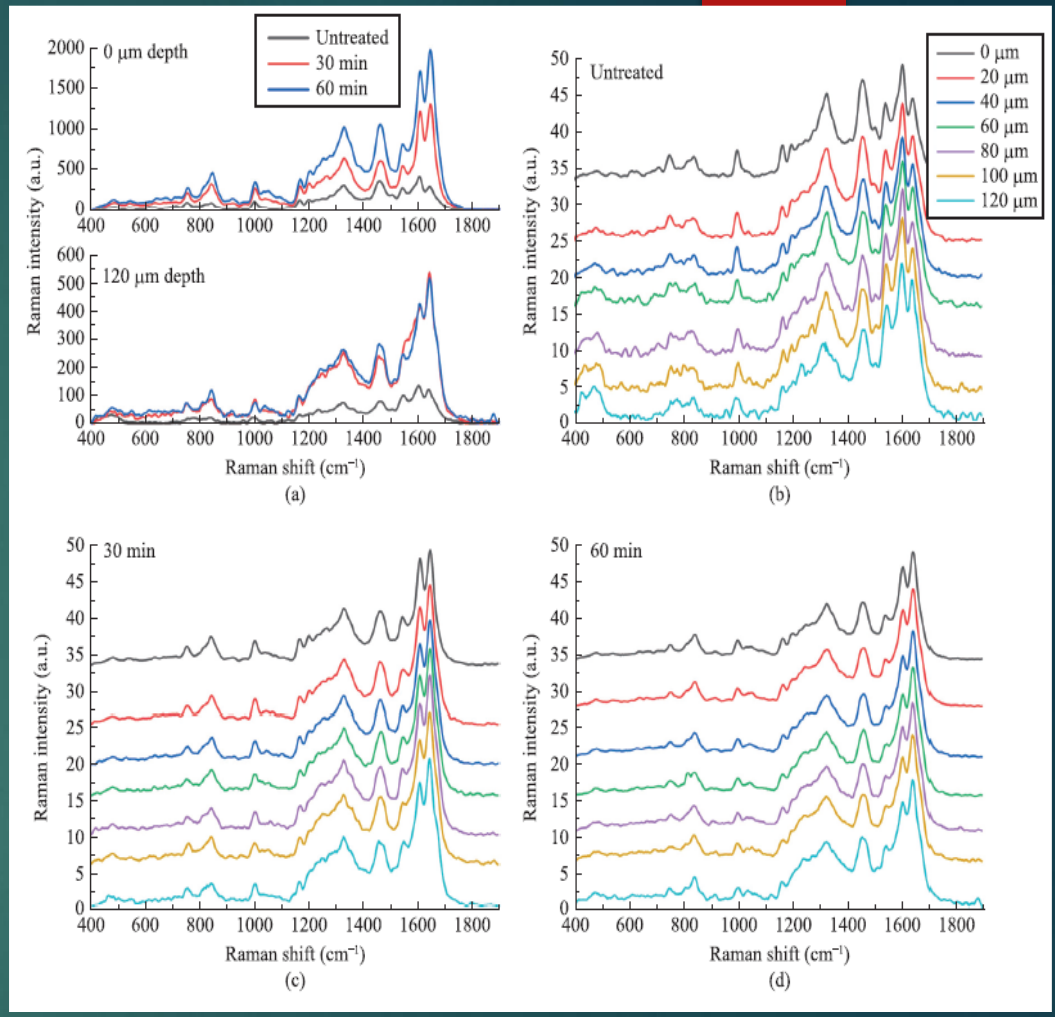

Averaged Raman spectra of *ex vivo* myocardium before and after treatment with 70%-Gly: (a) depths at 0 and 120 μm, (b) untreated, (c) 30 and (d) 60 min treatment. Spectra were offset along the ordinate

OCT/Cartilage/Omnipaque/PG as OCAs

A. Bykov et.al. , Imaging of subchondral bone by OCT upon optical clearing of articular cartilage, J. Biophotonics, 2015

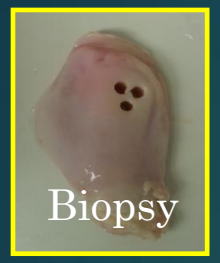

OC cartilage

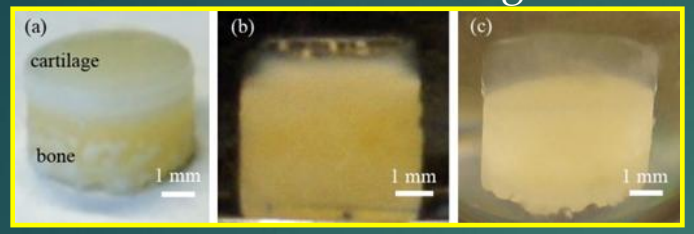

PG Omnipaque

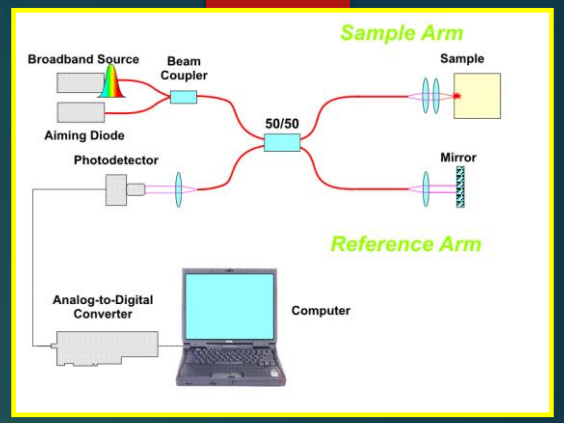

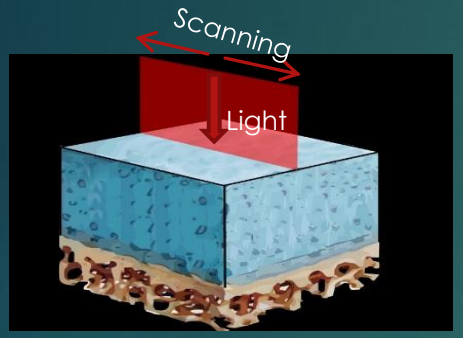

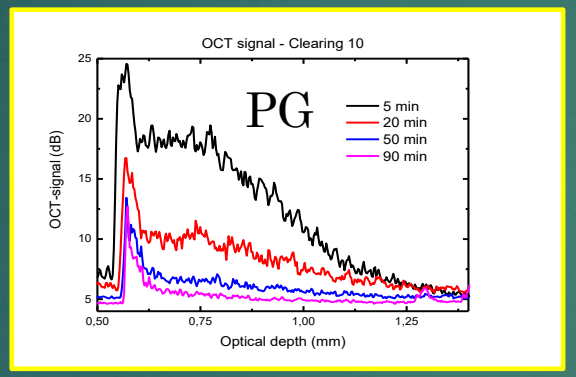

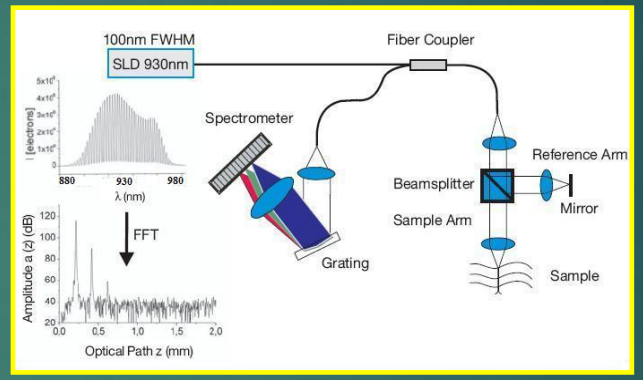

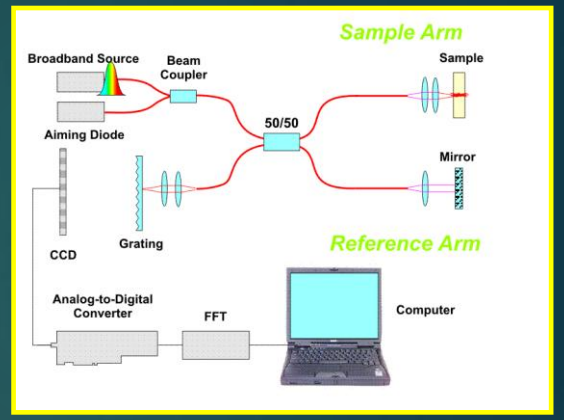

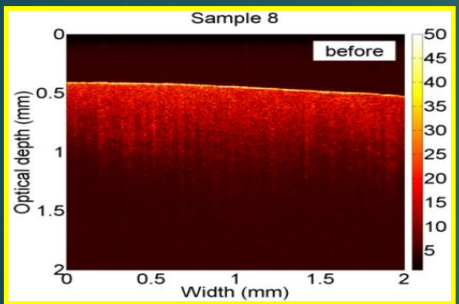

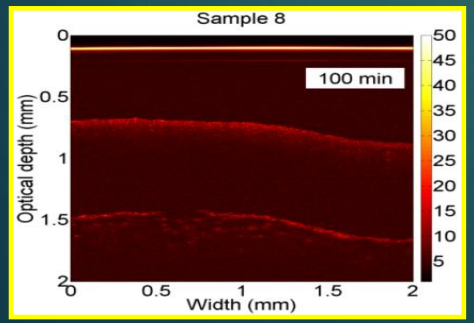

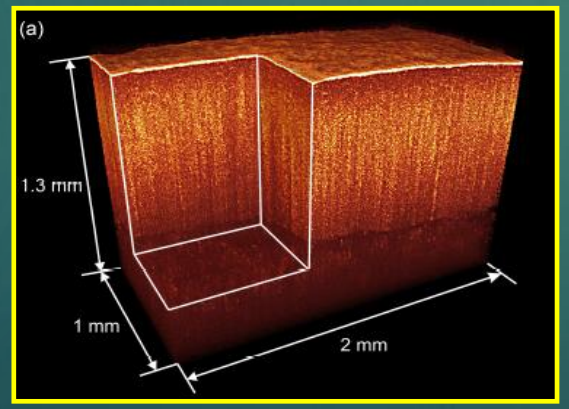

3D OCT image

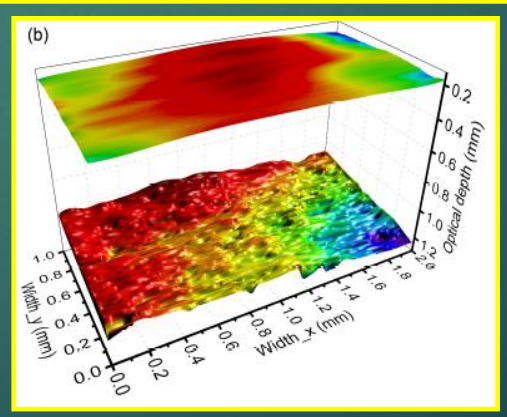

Roughness of the cartilage-bone interface Sa = 10 μm

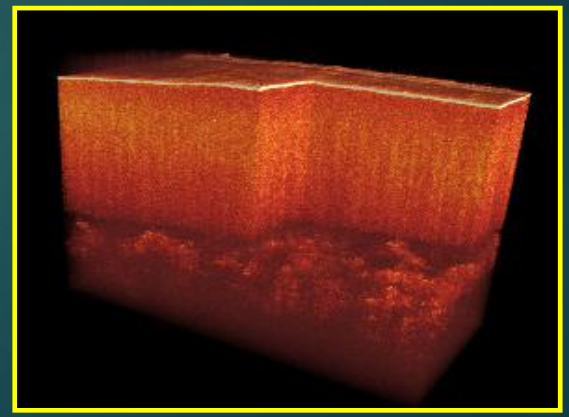

3D OCT image

A rapid Stokes imaging method

Jiawei Song, Nan Zeng, Hui Ma, and Valery V. Tuchin, A rapid Stokes imaging method for characterizing the optical properties of tissue during immersion optical clearing, IEEE Journal of Selected Topics in Quantum Electronics (2023)

$$S = \begin{bmatrix} S_0 \\ S_1 \\ S_2 \\ S_3 \end{bmatrix} = \begin{bmatrix} I_H + I_V \\ I_H - I_V \\ I_{45^\circ} - I_{135^\circ} \\ I_R - I_L \end{bmatrix}$$

Stokes parameters

$$\delta = \cos^{-1}\left(\frac{\vec{S_{in}} \cdot \vec{S_{out}}}{\left|\vec{S_{in}}\right| \left|\vec{S_{out}}\right|} \right)$$

Linear retardance

$$\Delta_c = 1 - \sqrt{s_1^2 + s_2^2 + s_3^2}$$

Depolarization

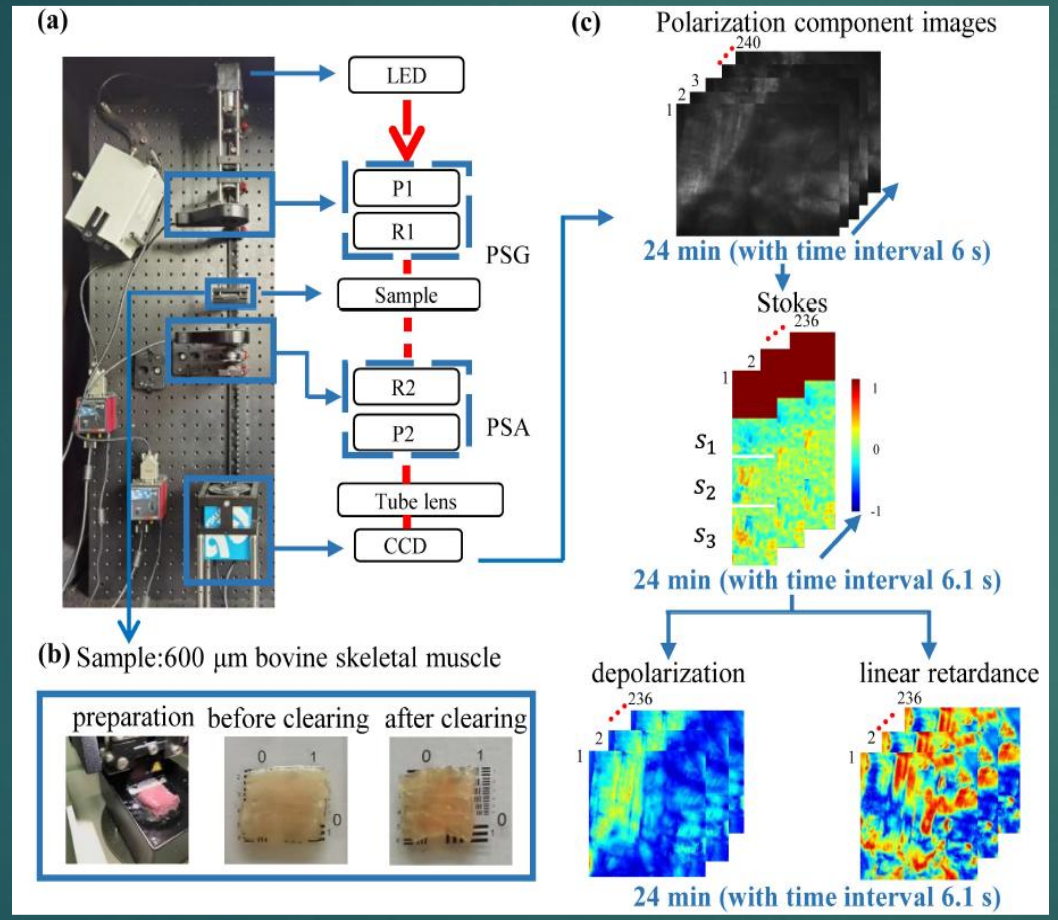

Schematic diagram of the assessment of OC with rapid Stokes imaging, bovine skeletal muscle for 24 min with 80% glycerol solution The flow chart of data analysis, from light intensity images, Stokes images to the derived polarization parameter images

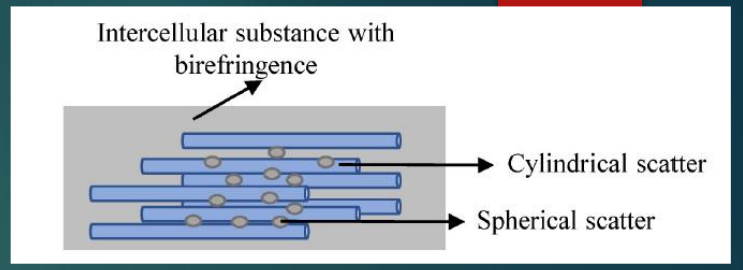

Sphere-cylinder birefringence model (SCBM) to mimic the TOC process

Three-dimensional SHG images of the sample before (left) and after (right) being immersed in 80% glycerol for 10 min

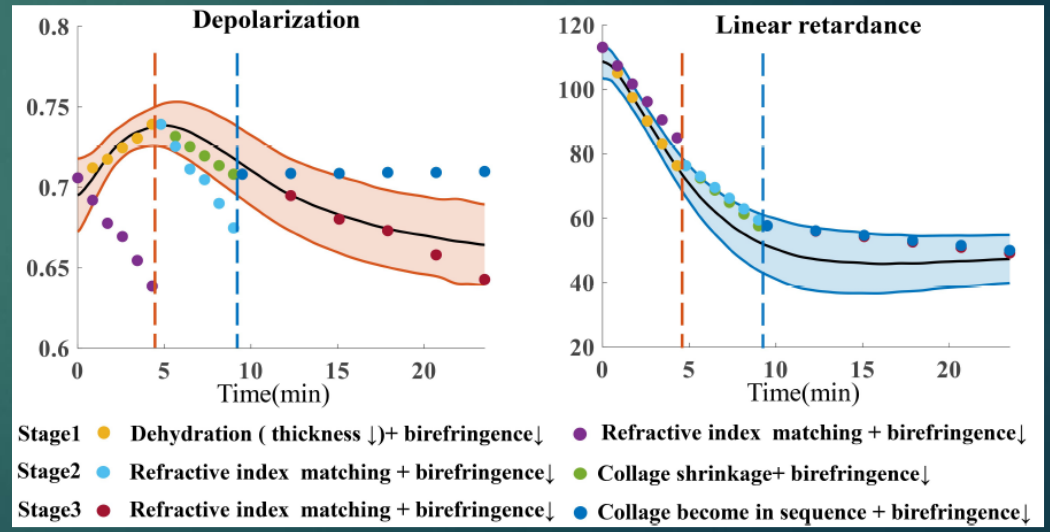

Monte Carlo simulations for three-stage characteristics with 80% glycerol solution during tissue clearing, changes of two polarization parameters depolarization and linear retardance are simulated

In vivo optoacoustic (OA) cytometry

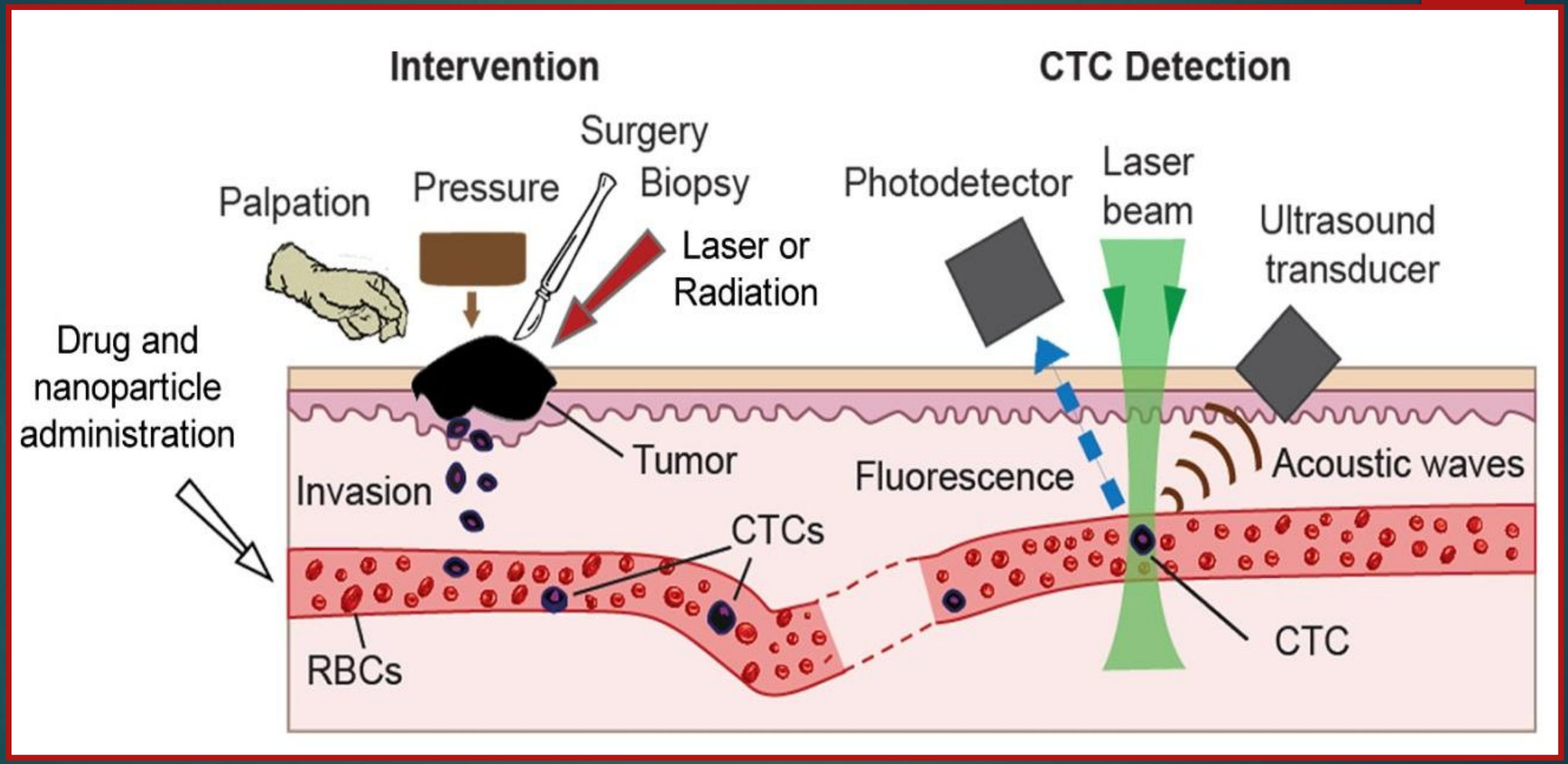

Optoacoustic (OA) cytometry *in vivo*, lympho- and angiography

M.V. Novoselova et al., Optical clearing for PA lympho- and angiography beyond conventional depth limit in vivo, *Photoacoustics* 20 100186 (2020)

OA *in vivo* cytometry

Y.A. Menyaev et al., Skin optical clearing for in vivo photoacoustic flow cytometry, Biomed. Opt. Express 4 (12), 3030-3041 (2013)

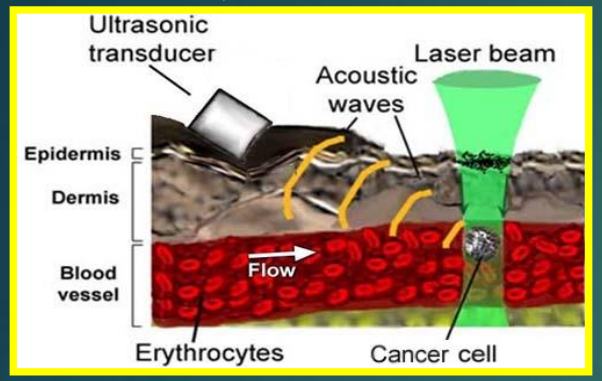

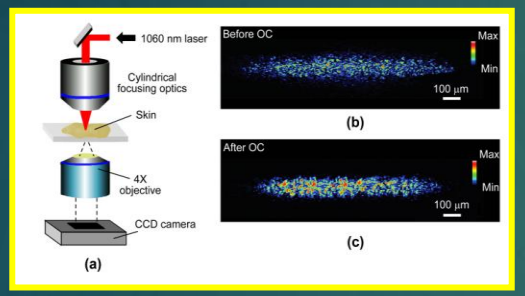

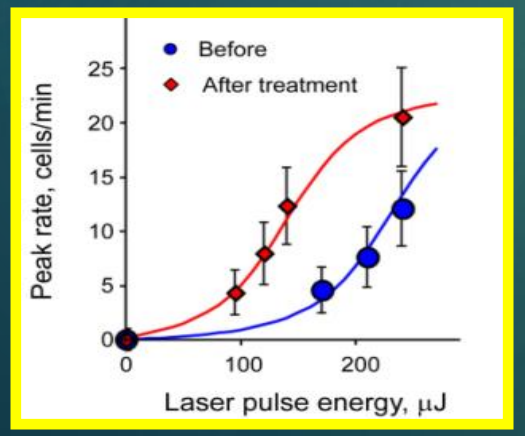

3D OA lympho-/angiography of mouse limb *in vivo*

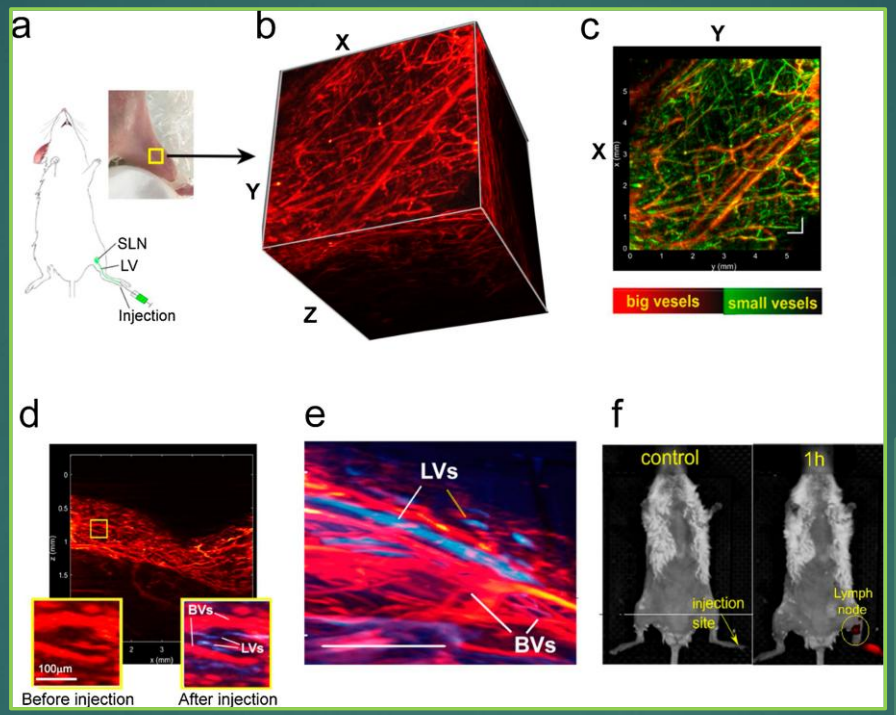

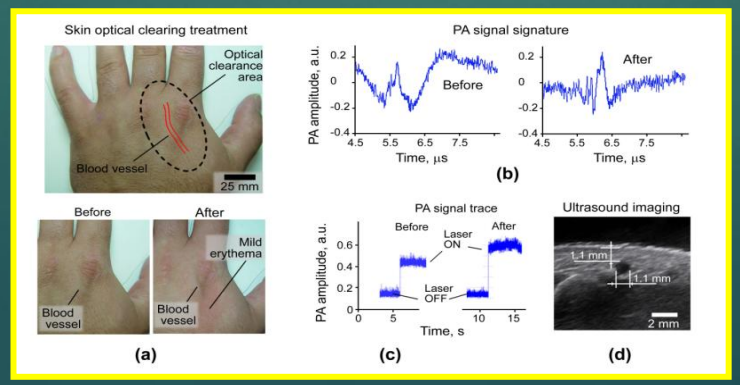

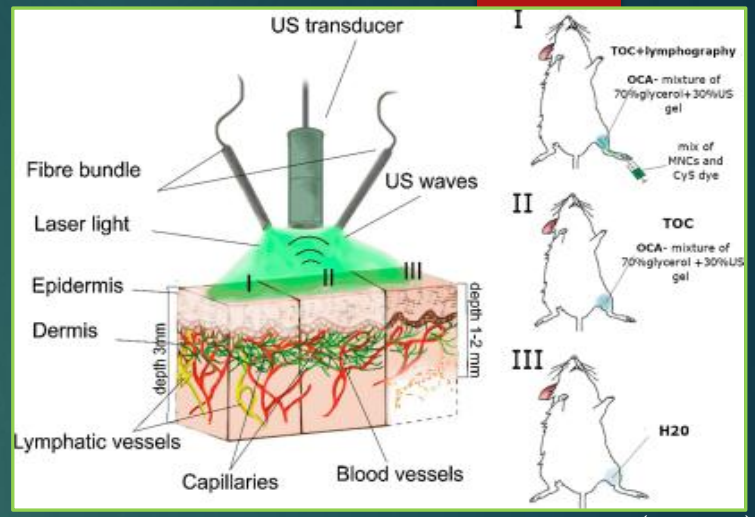

Raster scanning optical-acoustic mesoscopy (RSOM) scheme and experimental protocol

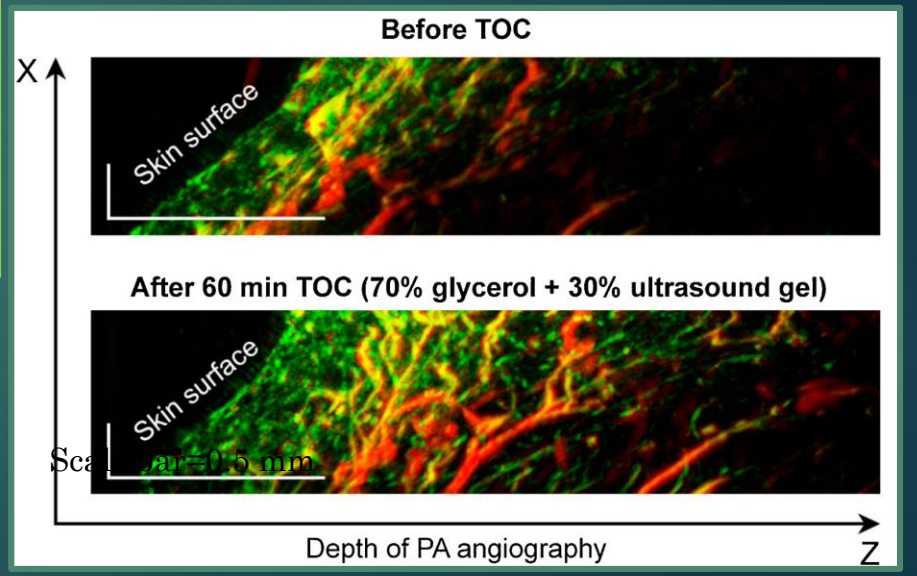

Topical application of OCA to the skin surface of a mouse limb during RSOM imaging

Laser speckle contrast imaging microscopy

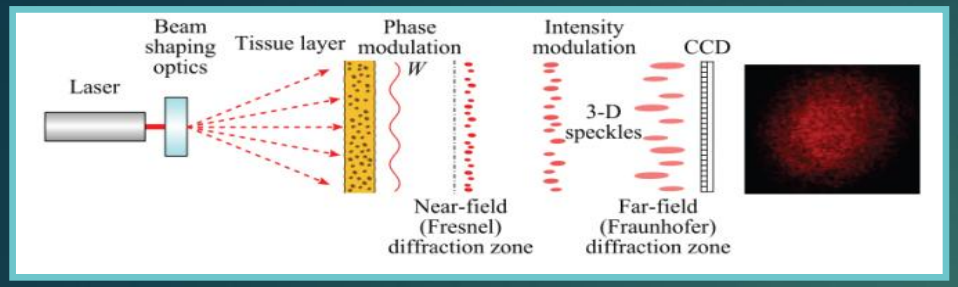

$$K = \sigma / \langle I \rangle \sim 1 / \langle V \rangle,$$

σ is the standard deviation of the intensity fluctuations

<I> is the mean intensity, and <V> is the mean velocity

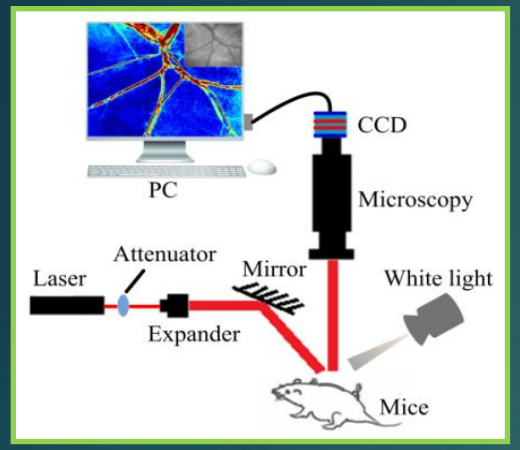

Blood vessel visibility at topical treatment of rat skin *in vivo* by a mixture of PEG-400 and thiazone

Zhu D., et al. *J. Biomed. Opt.* 15(2), 026008 (2010)

Imaging of brain blood vessels

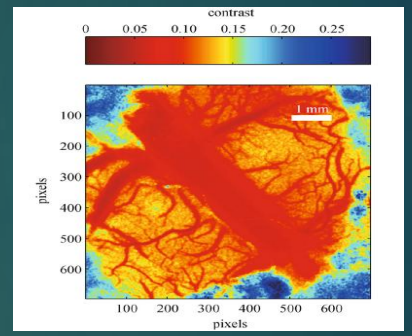

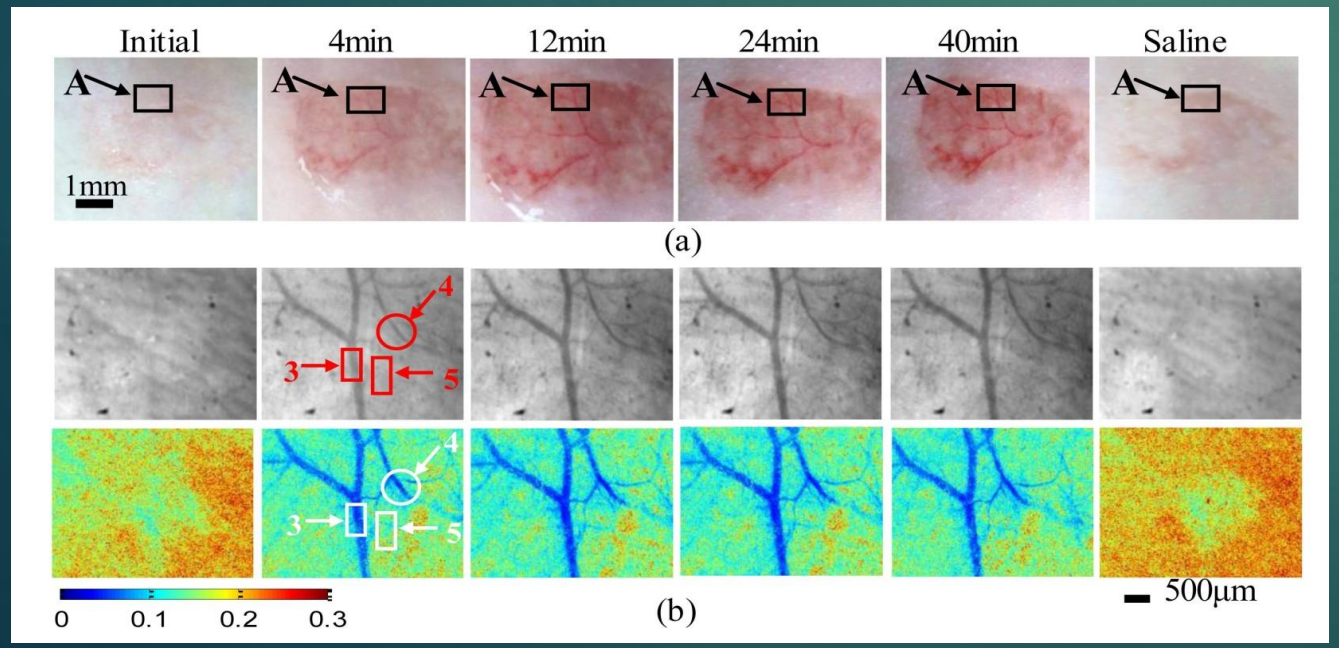

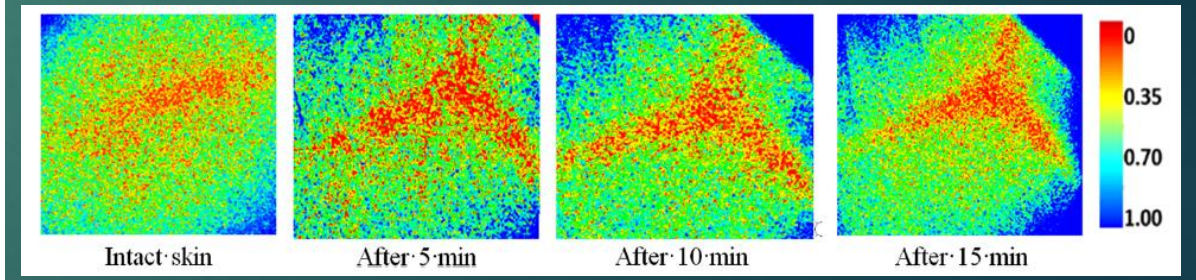

LSCI of cerebral vessels at application of 60% glycerol solution to skin surface of the newborn mouse in the fontanelle area

Advanced Drug Delivery Reviews 212 (2024) 115420

Contents lists available at ScienceDirect

Advanced Drug Delivery Reviews

journal homepage: www.elsevier.com/locate/adr

Light in evaluation of molecular diffusion in tissues: Discrimination of pathologies

Luís R. Oliveira [a,1], Maria R. Pinheiro [b,1], Daria K. Tuchina [c,d,1], Polina A. Timoshina [c], Maria I. Carvalho [b,f,2], Luís M. Oliveira [b,g,*,2]

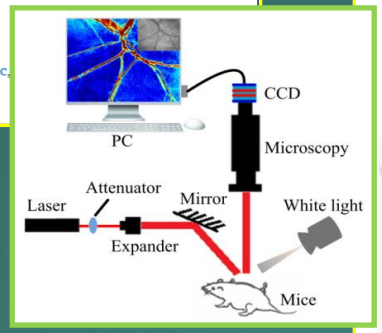

Schematic representation of the stages of studying pancreatic microcirculation in rats with alloxan-induced diabetes mellitus using laser speckle-contrast imaging with OCA application:

- Experimental type 1 diabetes in rats was induced by a single subcutaneous injection of alloxan at a dose of 220 mg/kg body weight
- Setup for studying pancreatic microcirculation in rats with diabetes
- Analysis and processing of the obtained results

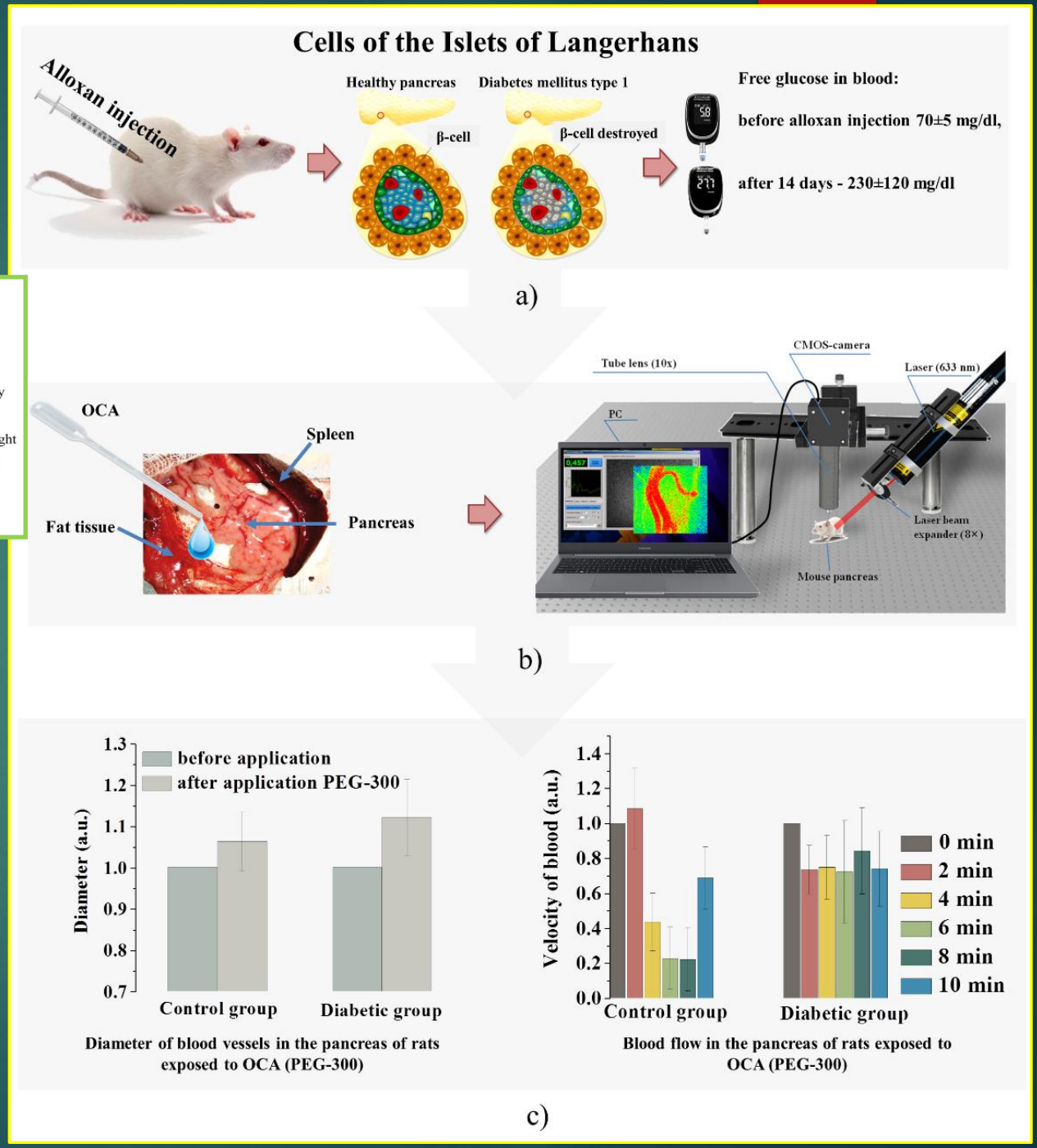

RESEARCH ARTICLE SUMMARY

BIOLOGICAL IMAGING

Achieving optical transparency in live animals with absorbing molecules

Zihao Ou, Yi-Shiou Duh, Nicholas J. Rommelfanger, Carl H. C. Keck, Shan Jiang, Kenneth Brinson Jr., Su Zhao, Elizabeth L. Schmidt, Xiang Wu, Fan Yang, Betty Cai, Han Cui, Wei Qi, Shifu Wu, Adarsh Tantry, Richard Roth, Jun Ding, Xiaoke Chen, Julia A. Kaltschmidt, Mark L. Brongersma*, Guosong Hong*

Ou et al., Science 385, 1061 (2024), 6 September 2024

INTRODUCTION: A challenge in trying to image biological matter is that its complex structure causes opacity because of unwanted light scattering. This scattering results from refractive index mismatches among the components of biological tissues, limiting the penetration depth of optical imaging. The desire to see inside biological tissue and uncover the fundamental processes of life has spurred extensive research into deep-tissue optical imaging methods, such as two-photon microscopy, near-infrared-II fluorescence imaging, and optical tissue clearing. However, these methods either lack sufficient penetration depth and resolution or are unsuitable for living animals. Therefore, the ability to achieve optical transparency in live animals holds promise for transforming many of imaging techniques.

RATIONALE: We hypothesized that strongly absorbing molecules can achieve optical transparency in live biological tissues. By applying the Lorentz oscillator model for the dielectric properties of tissue components and absorbing molecules, we predicted that dye molecules with sharp absorption resonances in the near-ultraviolet spectrum (300 to 400 nm) and blue region of the visible spectrum (400 to 500 nm) are effective in raising the real part of the refractive index of the aqueous medium at longer wavelengths when dissolved in water, which is in agreement with the Kramers-Kronig

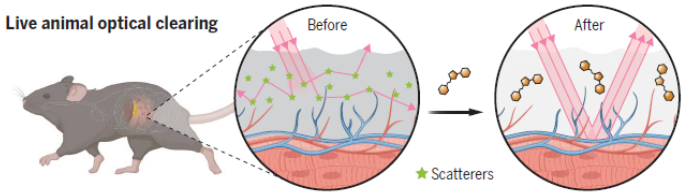

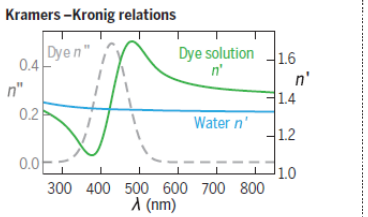

Achieving optical transparency in live mice with absor
dissolved in water can modify the RI of the aqueous med
match that of lipids. This approach can render various sa
chicken breast tissue, and live mouse body for visualizing
Scale bars, 5 mm. [The schematic was prepared using Bi

communications biology Research highlight

https://doi.org/10.1038/s42003-024-07012-9

'Transparent mice': deep-tissue live imaging using food dyes

Tartrazine cannot make live tissues transparent

Shigenori Inagaki[1] & Takeshi Imai[1]*

Affiliations:

[1] Department of Developmental Neurophysiology, Graduate School of Medical Sciences, Kyushu University, Higashi-ku, Fukuoka 812-8582, Japan.

Optical Clearing with Tartrazine Enables Deep Transscleral Imaging with Optical Coherence Tomography

Amit Narawane[1,†,*], Robert Trout[1,†], Christian Viehland[1], Anthony N. Kuo[2,3], Lejla Vajzovic[2], Al-Hafeez Dhalla[1], Cynthia A. Toth[2,3]

[1]Department of Biomedical Engineering, Duke University, Durham, NC 27708, USA
[2]Department of Ophthalmology, Duke University Medical Center, Durham, NC 27710, USA
[†]These authors contributed equally to this work.
*amit.narawane@duke.edu

Submitted to bioRxiv on 10/25/2024

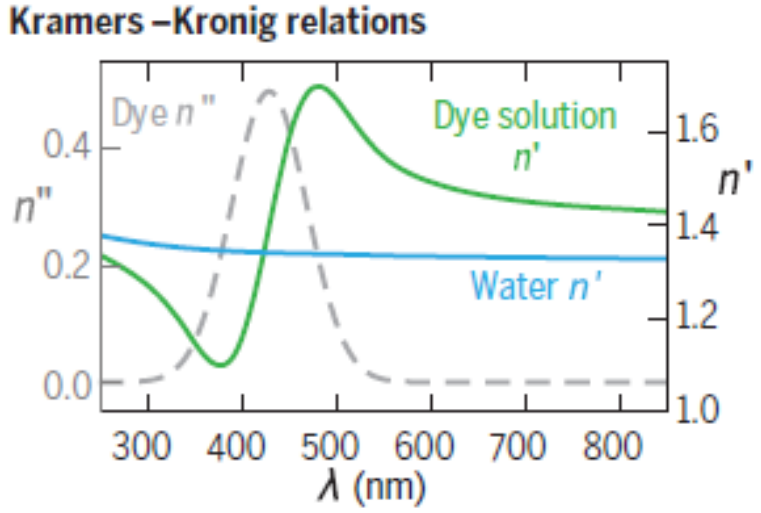

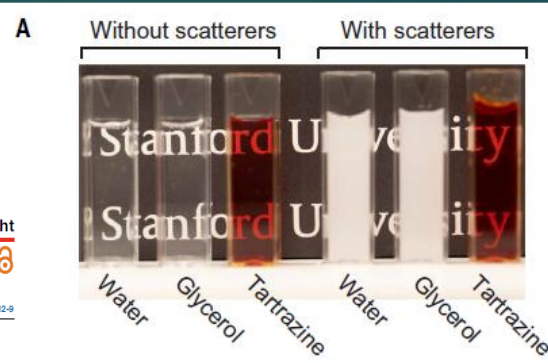

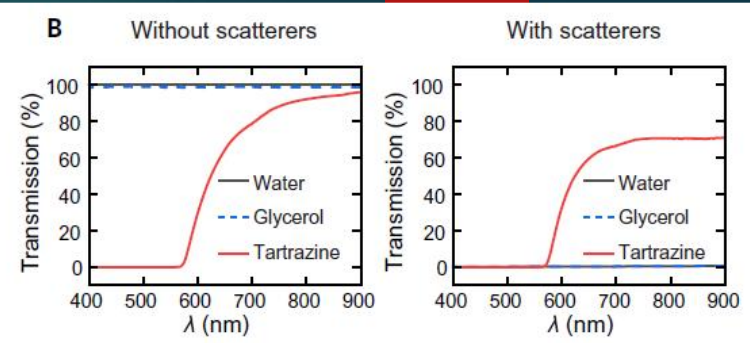

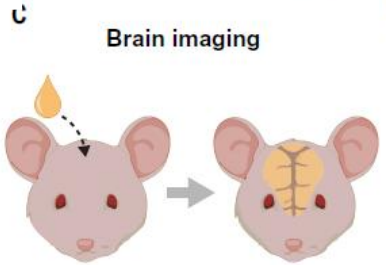

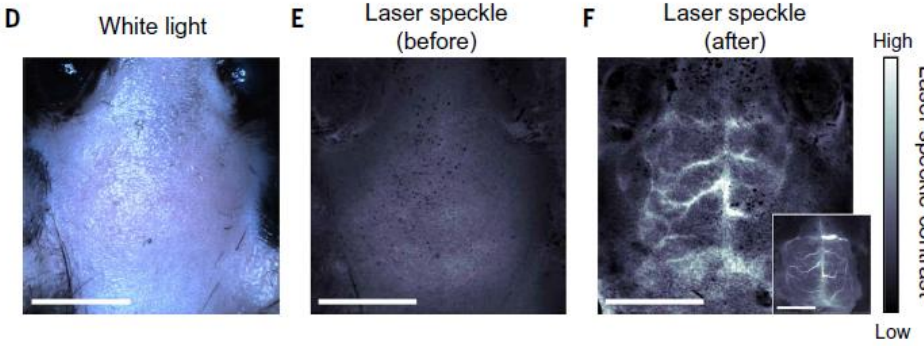

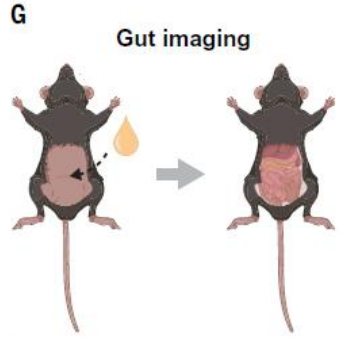

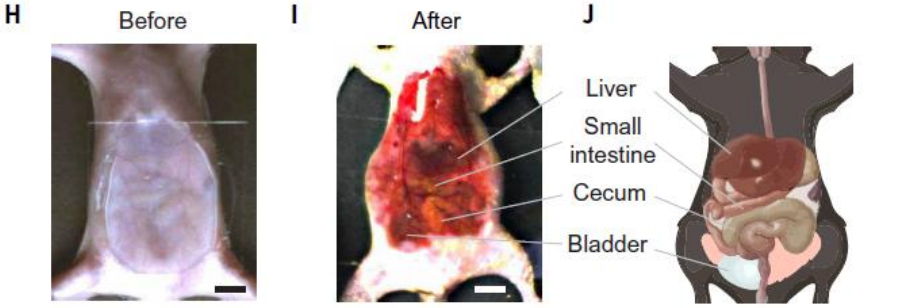

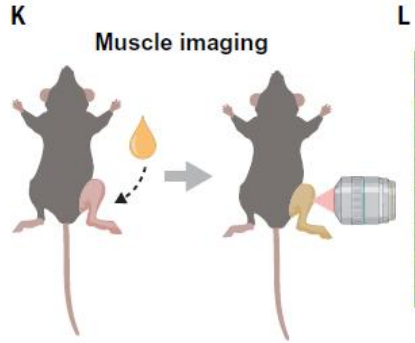

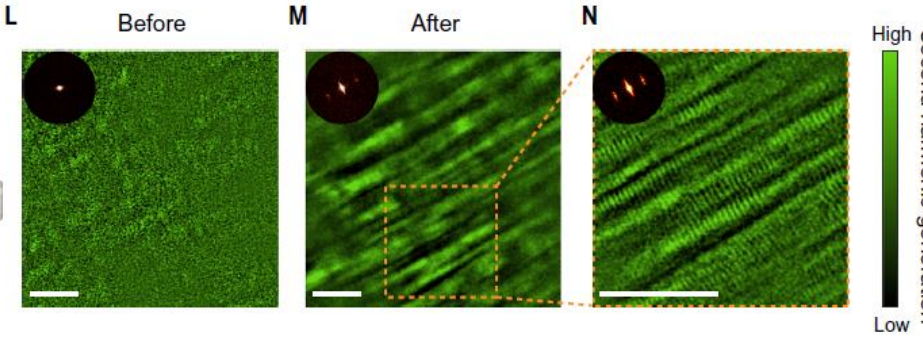

Self optical clearing at RBC hemolysis

V.V. Tuchin, et al. Optics Express 2004

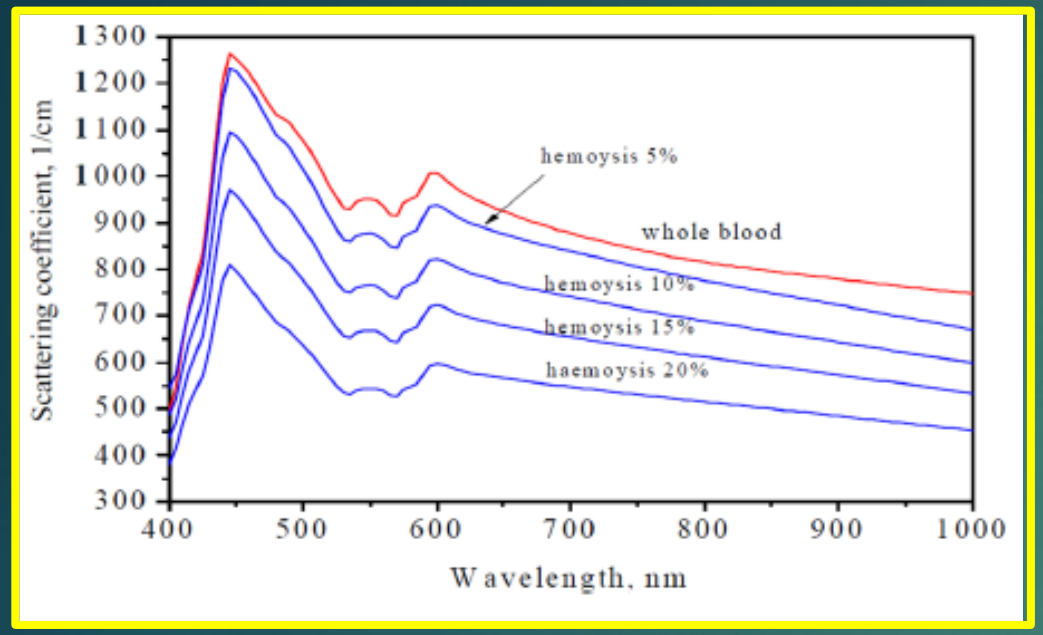

G.Popescu,…M. Feld, J. Biomed. Opt. 2005

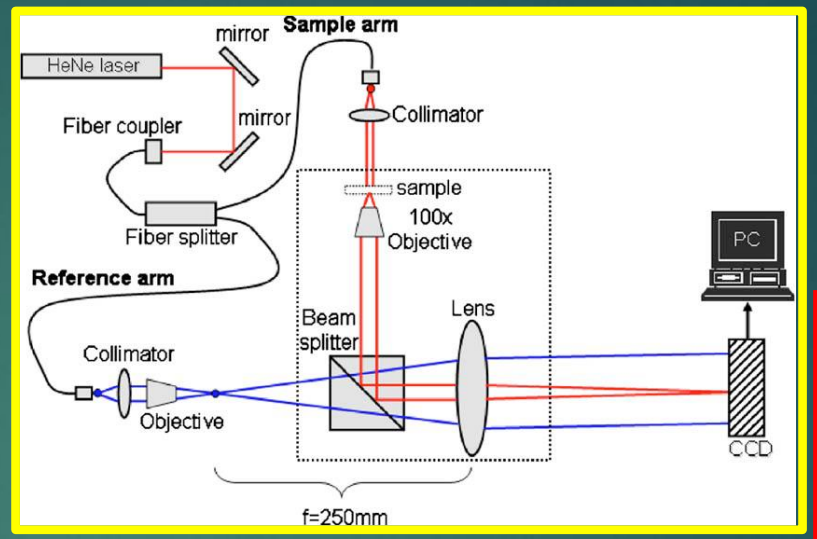

SWIR tissue windows

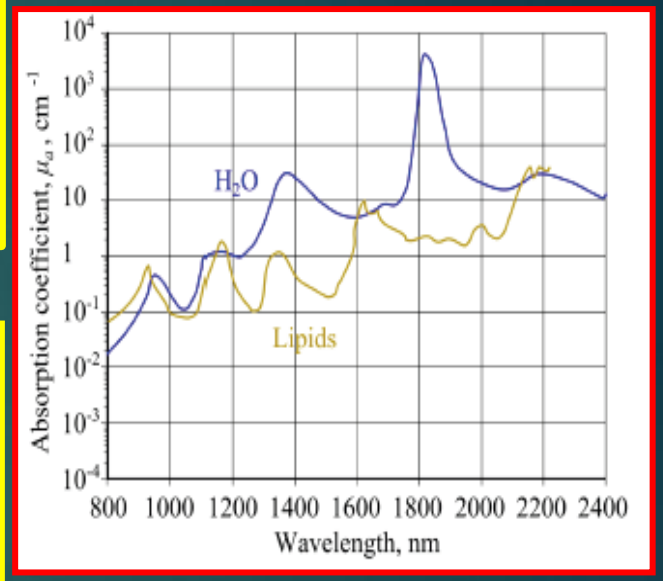

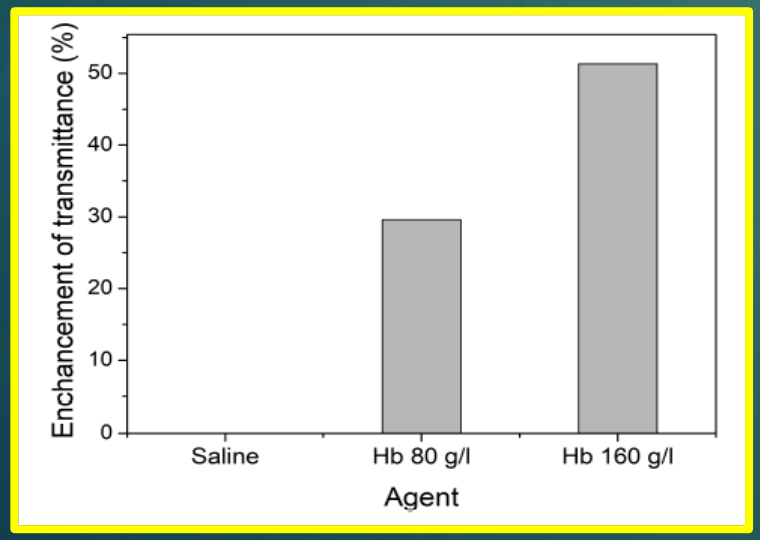

Hilbert phase microscopy

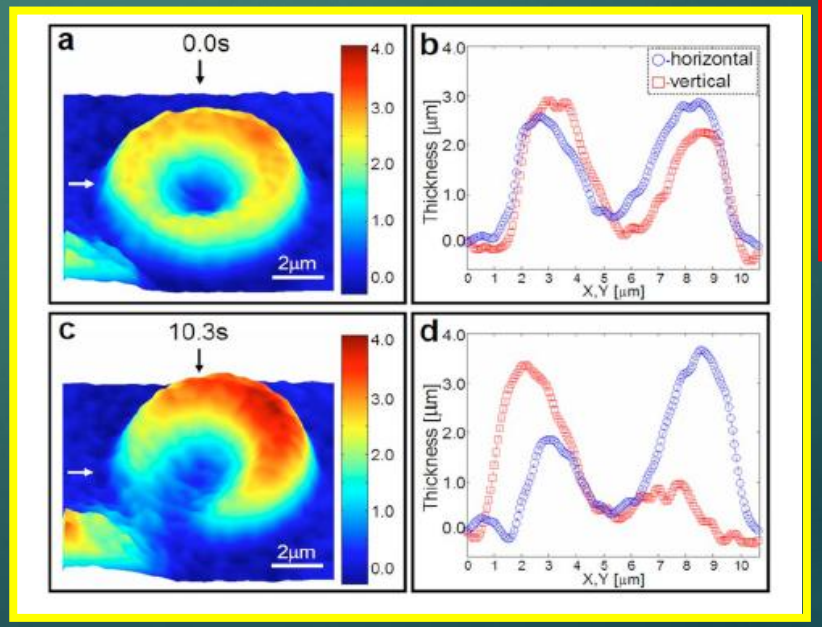

20 2022

Optical clearing of blood and tissues using blood components

Olga S. Zhernovaya, Elina A. Genina, Valery V. Tuchin, and Alexey N. Bashkatov

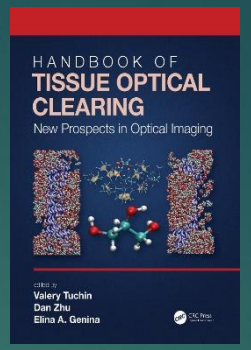

Temporal NIR reflectance of rat skin after injection of hemoglobin (120 g/L) and blood (2:1, in heparin)

Reflectance of skin before injection

Reflectance of skin immediately after injection

Hematoma (bruise) change color with time – hemoglobin transfer to bilirubin

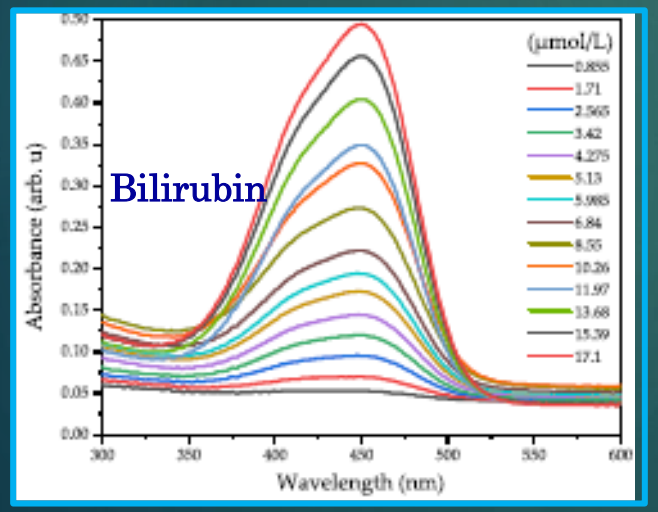

Ye *et al. Nanoscale Research Letters (2022) 17:111*

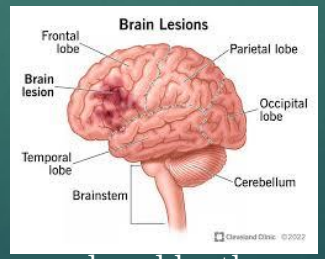

Piglet brain after cortical injury produced by the intracranial balloon, Paiva *et al*: Experimental and therapeutic medicine 25: 20, 2023

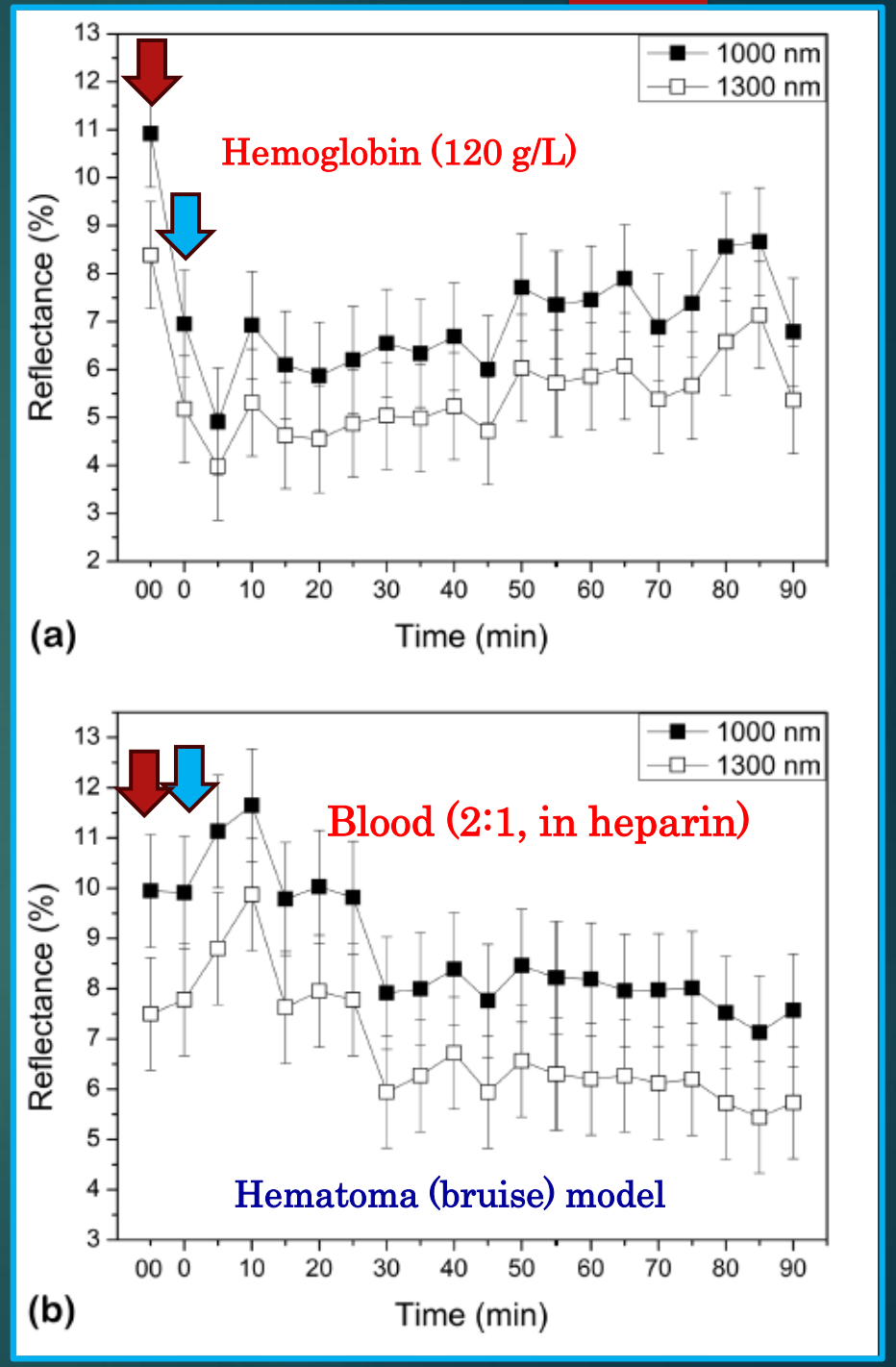

Journal of Biophotonics

JOURNAL OF BIOPHOTONICS

Journal of Biophotonics, 2025; 0:e202500160
https://doi.org/10.1002/jbio.202500160

RESEARCH ARTICLE

Tartrazine for Optical Clearing of Tissues: Stability and Diffusion Issues

Ana R. Guerra[1] | Luís R. Oliveira[1] | Gonçalo O. Rodrigues[1,2] | Maria R. Pinheiro[1,3] | Maria I. Carvalho[1,3] | Valery V. Tuchin[4,5,6] | Luís M. Oliveira[1,2]

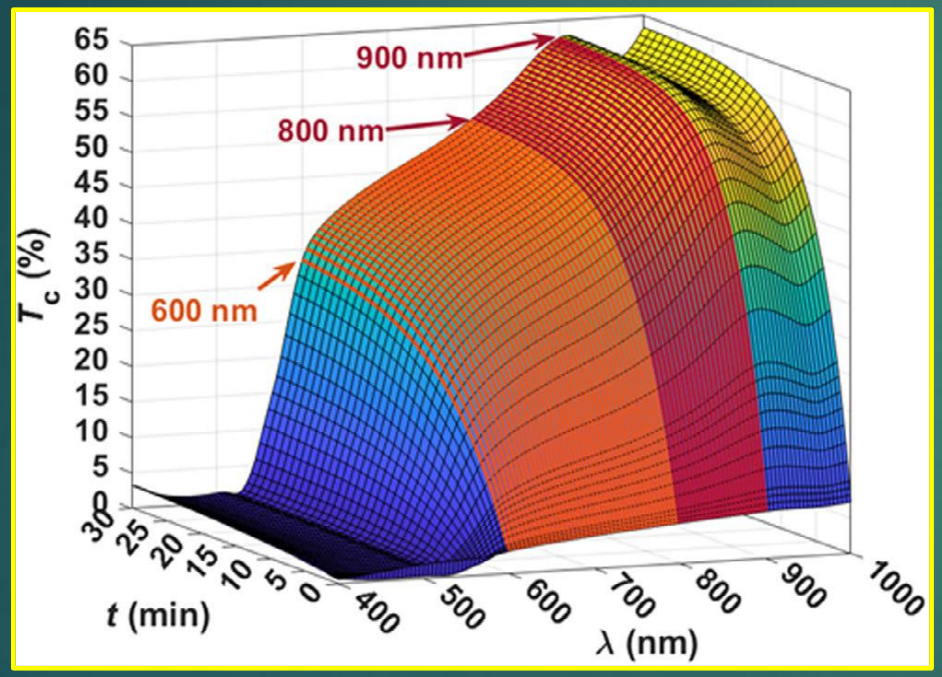

Kinetics of $Tc(\lambda)$ at treatment with TZ solution (40%)

Luís M. Oliveira et al. "Ultraviolet transparency windows created by bonding tartrazine molecules to tissue proteins" (SFM-25)

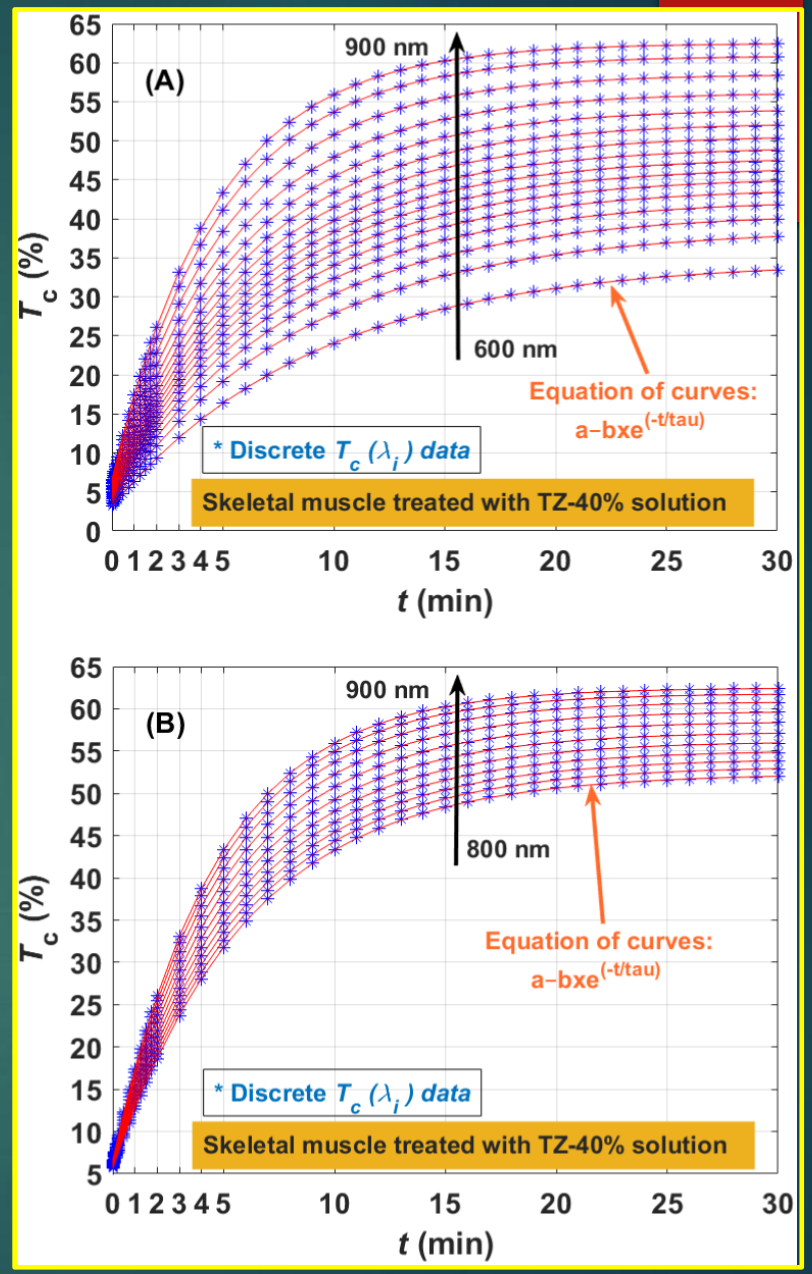

Kinetics of Tc for wavelengths between 600 and 900 nm (A) and between 800 and 900 nm (B)

A.R. Guerra, L.R. Oliveira, G.O. Rodrigues, M.R. Pinheiro, M.I. Carvalho, V.V. Tuchin, L.M. Oliveira, Assessment of tartrazine diffusion properties in skeletal muscle, IEEE Journal of Selected Topics in Quantum Electronics (2026)

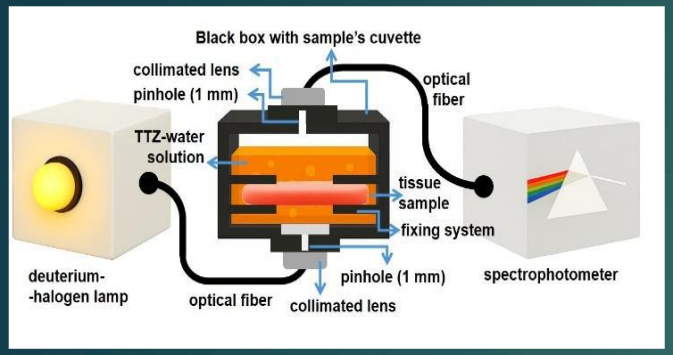

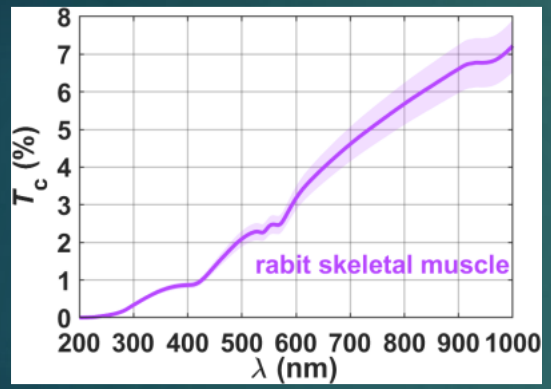

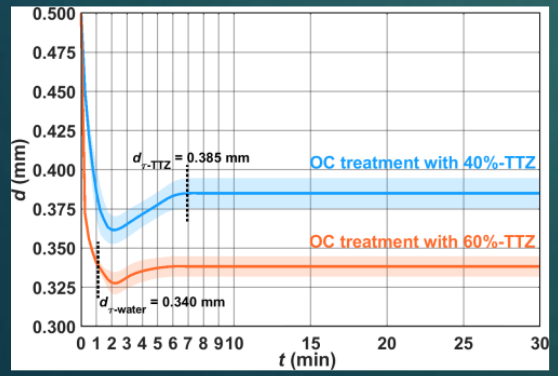

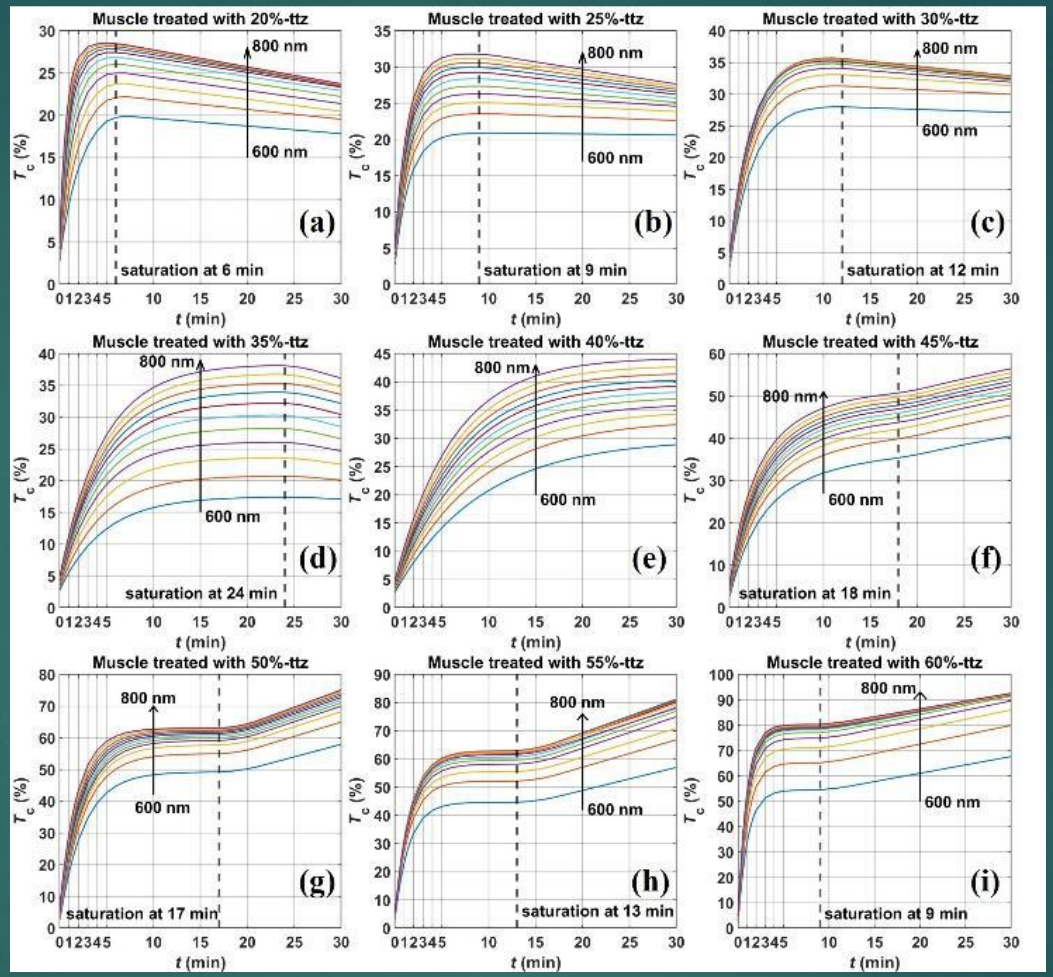

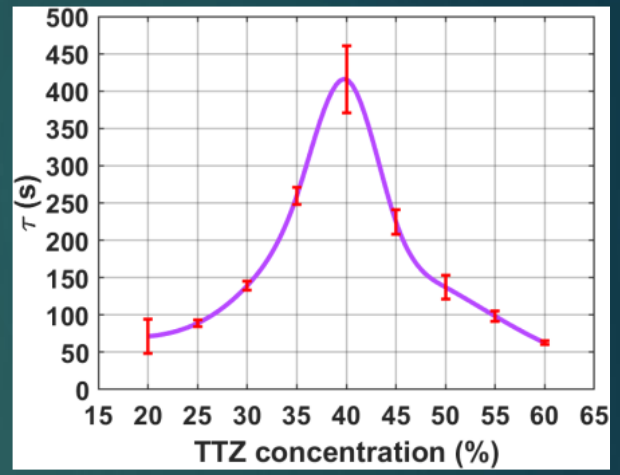

For TTZ, the value of $D_{TTZ,water}$ ~4.8×10^{-6} cm^2/s, i.e. about 13.6× higher than the $D_{TTZ,tissue}$ = 3.6×10^{-7} cm^2/s that is obtained experimentally in this study
For water diffusion, this ratio is 12.1 (2.3×10^{-5} cm^2/s /1.9×10^{-6} cm^2/s).
Consequently, the impact of tissue structure (barrier) on water transport is only slightly less than on transport of TTZ molecules (534 g/mol)

Computer-guided optical clearing for transcranial laser speckle imaging of cortical blood flow through synergistic tartrazine-induced cranial bone transparency

(Yu. Surkov et al., JIOHS, accepted, October 2025)

Mouse scalp was surgically excised without damaging the periosteum

Equipment: LSCI system (632 nm), OCT (930 nm) and OCT (1325 nm)

Static speckle-contrast maps (K_{static}) were calculated from the reconstructed static raw speckle image stack

Dynamic speckle contrast: $K_{dynamic} = K_{full} - K_{static}$

Relative blood flow index ($rBFI$) maps:

$$rBFI_{full} = 1/K_{full}^2, \qquad rBFI_{dynamic} = 1/K_{dynamic}^2$$

$$CNR(t) = \left(\langle K_{\mathrm{ROI}}(t)\rangle - \langle K_{\mathrm{bg}}(t)\rangle\right)/\sigma_{\mathrm{bg}}$$

$\langle \cdot \rangle$ the mean value within the vessel ROI

bg – neighboring parenchymal background area free of large vessels

σ_{bg} – standard deviation within that background

COC – computational optical clearing (PCA-based filtering that selectively removes static scattering, like physical optical clearing implemented algorithmically)

OCT-1325 nm

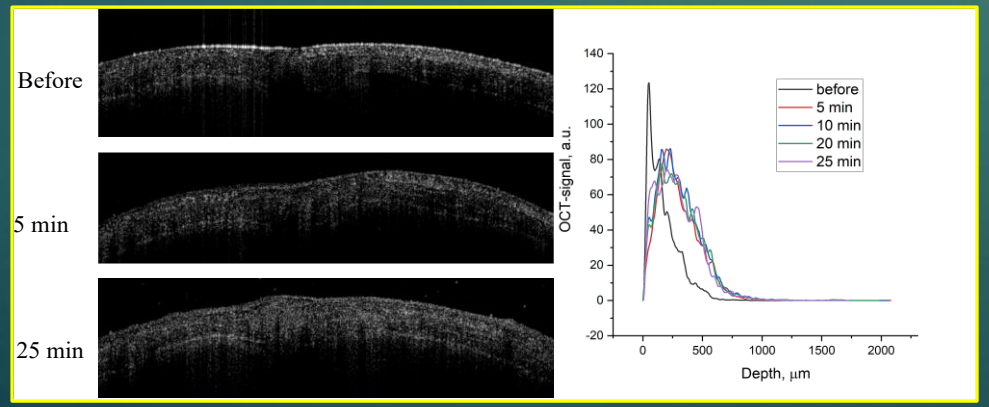

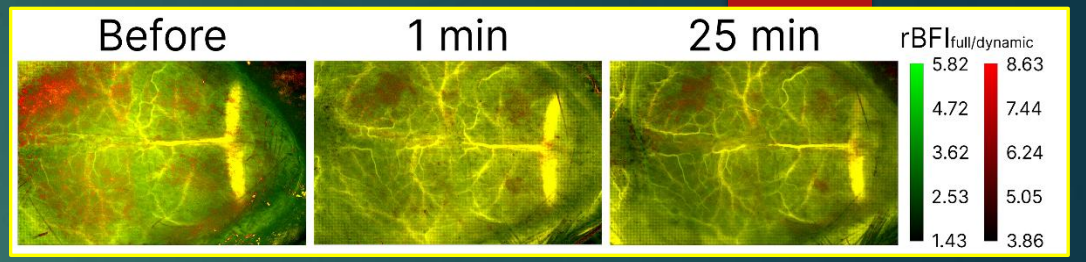

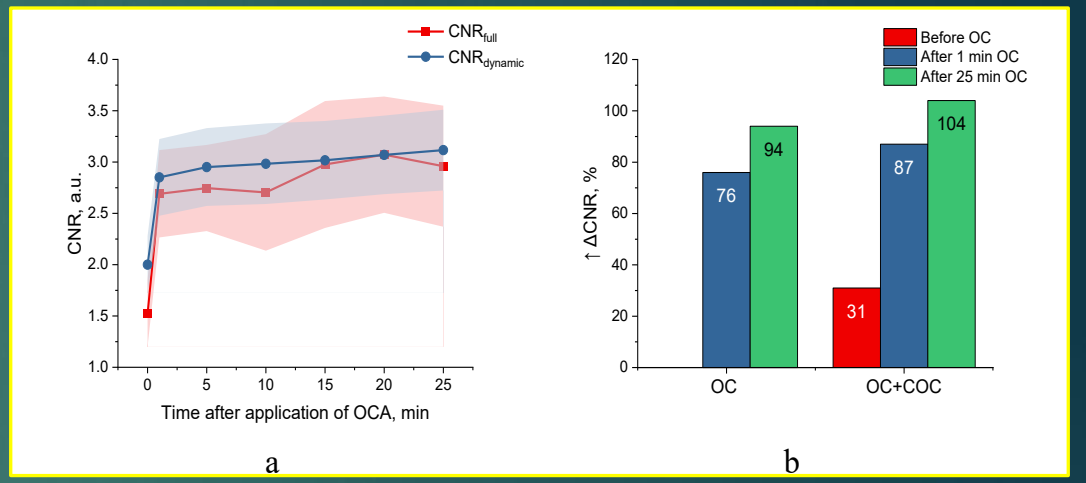

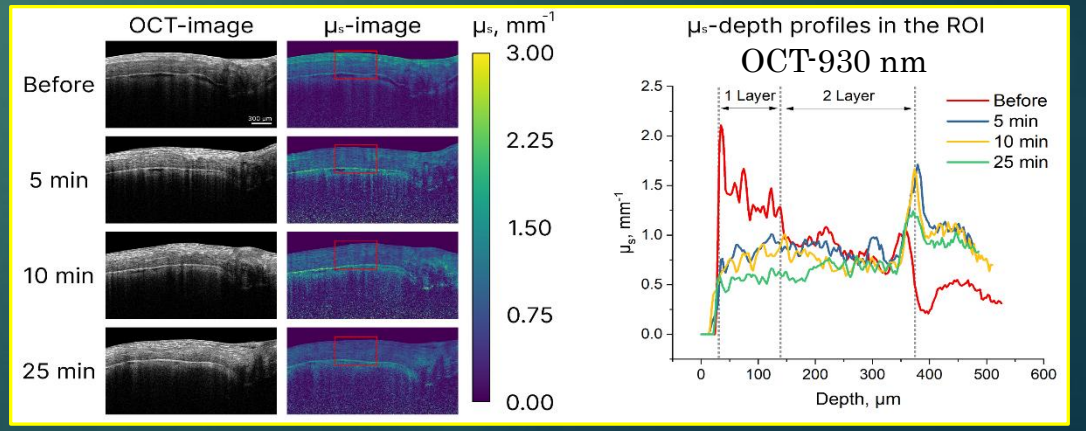

Dispersion of ICG in water, ethanol, glycerol, and albumin (presented on LALS -24)

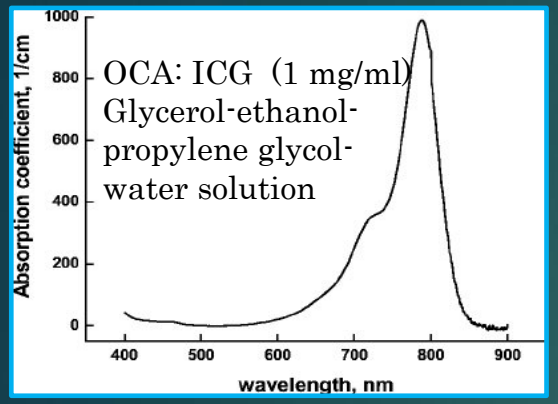

E. Genina et al., JBO 9(4) (2004)

Multi-wavelength refractometer

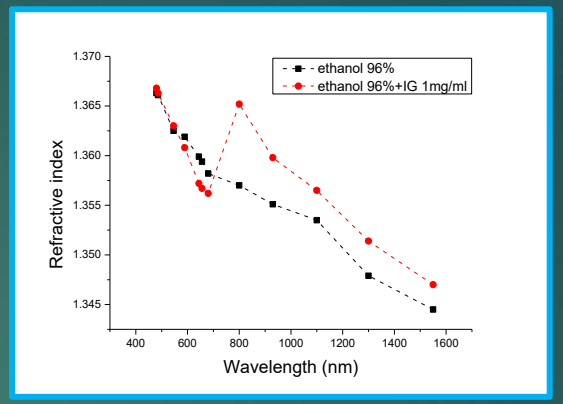

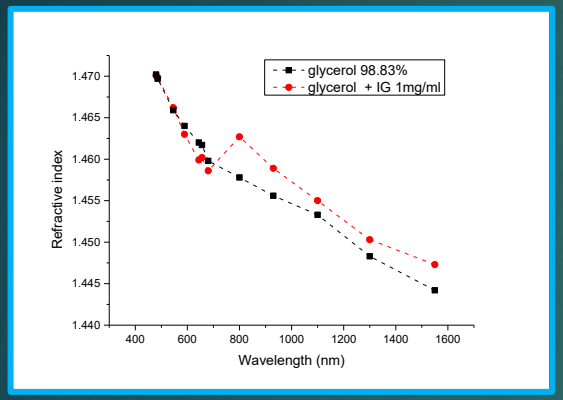

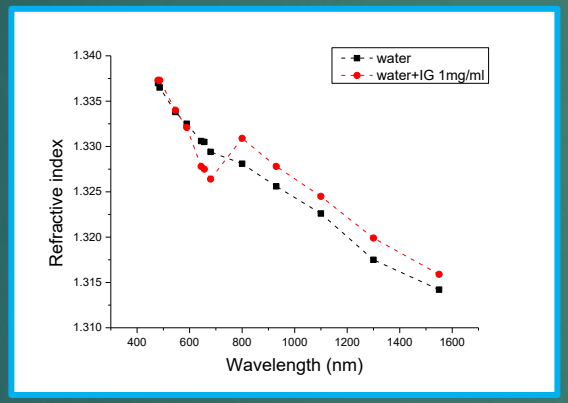

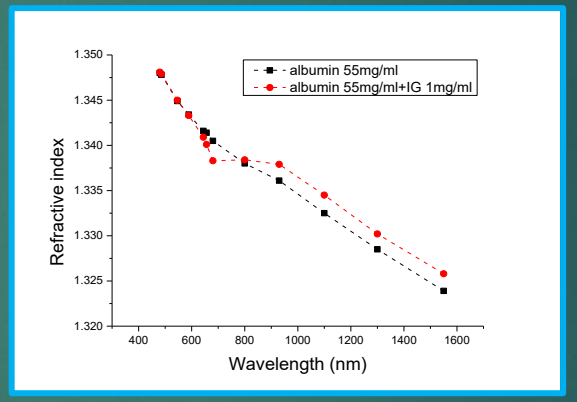

Мышечная ткань крысы, ОПА 70%-раствор глицерина (25% воды и 5% ДМСО + ICG 5×10^{-3} мг/мл)

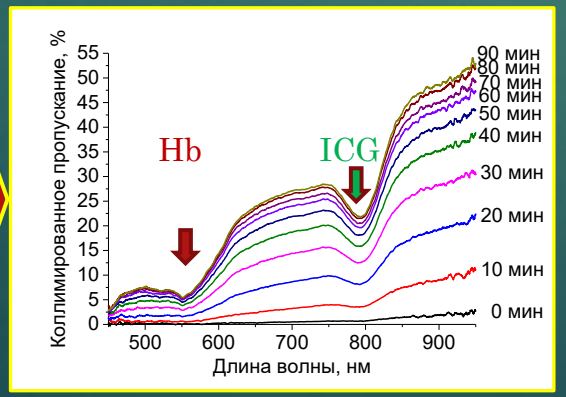

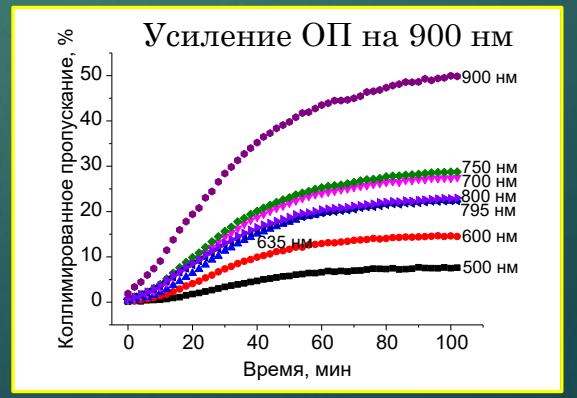

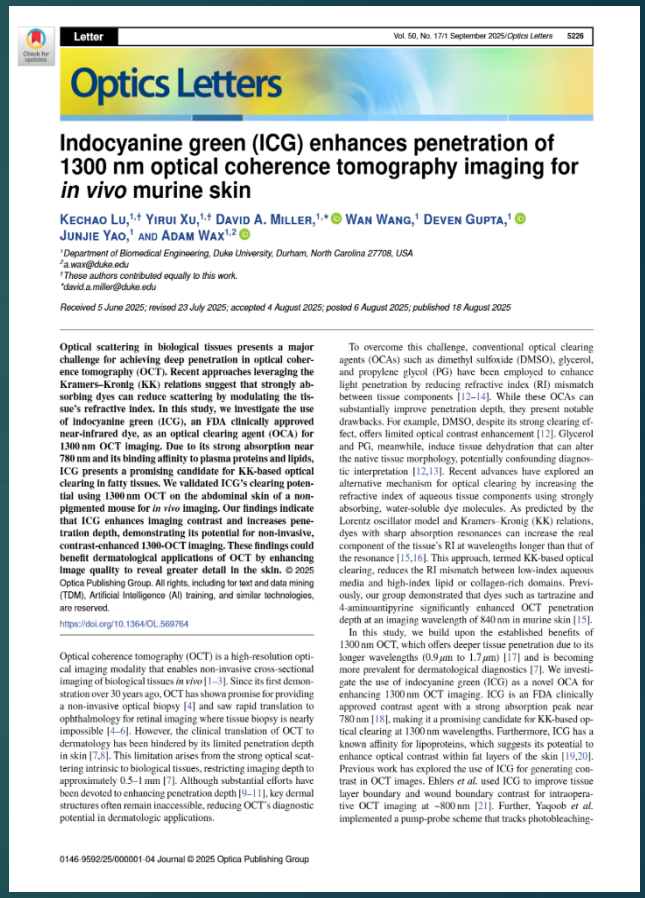

Letter

Vol. 50, No. 17/1 September 2025/Optics Letters 5229

Optics Letters

Indocyanine green (ICG) enhances penetration of 1300 nm optical coherence tomography imaging for *in vivo* murine skin

Kechao Lu,[1,†] Yirui Xu,[1,†] David A. Miller,[1,*] Wan Wang,[1] Deven Gupta,[1] Junjie Yao,[1] and Adam Wax[1,2]

[1]Department of Biomedical Engineering, Duke University, Durham, North Carolina 27708, USA
[2]a.wax@duke.edu
[†]These authors contributed equally to this work.
[*]david.a.miller@duke.edu

Received 5 June 2025; revised 23 July 2025; accepted 4 August 2025; posted 6 August 2025; published 18 August 2025

Optical scattering in biological tissues presents a major challenge for achieving deep penetration in optical coherence tomography (OCT). Recent approaches leveraging the Kramers–Kronig (KK) relations suggest that strongly absorbing dyes can reduce scattering by modulating the tissue's refractive index. In this study, we investigate the use of indocyanine green (ICG), an FDA clinically approved near-infrared dye, as an optical clearing agent (OCA) for 1300 nm OCT imaging. Due to its strong absorption near 780 nm and its binding affinity to plasma proteins and lipids, ICG presents a promising candidate for KK-based optical clearing in fatty tissues. We validated ICG's clearing potential using 1300 nm OCT on the abdominal skin of a non-pigmented mouse for *in vivo* imaging. Our findings indicate that ICG enhances imaging contrast and increases penetration depth, demonstrating its potential for non-invasive, contrast-enhanced 1300-OCT imaging. These findings could benefit dermatological applications of OCT by enhancing image quality to reveal greater detail in the skin. © 2025 Optica Publishing Group. All rights, including for text and data mining (TDM), Artificial Intelligence (AI) training, and similar technologies, are reserved.

https://doi.org/10.1364/OL.569764

Optical coherence tomography (OCT) is a high-resolution optical imaging modality that enables non-invasive cross-sectional imaging of biological tissues *in vivo* [1–3]. Since its first demonstration over 30 years ago, OCT has shown promise for providing a non-invasive optical biopsy [4] and saw rapid translation to ophthalmology for retinal imaging where tissue biopsy is nearly impossible [4–6]. However, the clinical translation of OCT to dermatology has been hindered by its limited penetration depth in skin [7,8]. This limitation arises from the strong optical scattering intrinsic to biological tissues, restricting imaging depth to approximately 0.5–1 mm [7]. Although substantial efforts have been devoted to enhancing penetration depth [9–11], key dermal structures often remain inaccessible, reducing OCT's diagnostic potential in dermatologic applications.

To overcome this challenge, conventional optical clearing agents (OCAs) such as dimethyl sulfoxide (DMSO), glycerol, and propylene glycol (PG) have been employed to enhance light penetration by reducing refractive index (RI) mismatch between tissue components [12–14]. While these OCAs can substantially improve penetration depth, they present notable drawbacks. For example, DMSO, despite its strong clearing effect, offers limited optical contrast enhancement [12]. Glycerol and PG, meanwhile, induce tissue dehydration that can alter the native tissue morphology, potentially confounding diagnostic interpretation [12,13]. Recent advances have explored an alternative mechanism for optical clearing by increasing the refractive index of aqueous tissue components using strongly absorbing, water-soluble dye molecules. As predicted by the Lorentz oscillator model and Kramers–Kronig (KK) relations, dyes with sharp absorption resonances can increase the real component of the tissue's RI at wavelengths longer than that of the resonance [15,16]. This approach, termed KK-based optical clearing, reduces the RI mismatch between low-index aqueous media and high-index lipid or collagen-rich domains. Previously, our group demonstrated that dyes such as tartrazine and 4-aminoantipyrine significantly enhanced OCT penetration depth at an imaging wavelength of 840 nm in murine skin [15].

In this study, we build upon the established benefits of 1300 nm OCT, which offers deeper tissue penetration due to its longer wavelengths (0.9 μm to 1.7 μm) [17] and is becoming more prevalent for dermatological diagnostics [7]. We investigate the use of indocyanine green (ICG) as a novel OCA for enhancing 1300 nm OCT imaging. ICG is an FDA clinically approved contrast agent with a strong absorption peak near 780 nm [18], making it a promising candidate for KK-based optical clearing at 1300 nm wavelengths. Furthermore, ICG has a known affinity for lipoproteins, which suggests its potential to enhance optical contrast within fat layers of the skin [19,20]. Previous work has explored the use of ICG for generating contrast in OCT images. Ehlers *et al.* used ICG to improve tissue layer boundary and wound boundary contrast for intraoperative OCT imaging at ~800 nm [21]. Further, Yaqoob *et al.* implemented a pump-probe scheme that tracks photobleaching-

0146-9592/25/000001-04 Journal © 2025 Optica Publishing Group

OC of **lung tissue** and **e-liquid** as an OCA

A.B. Bucharskaya, et al., ***Biophys. Rev.*** 14 (2022)

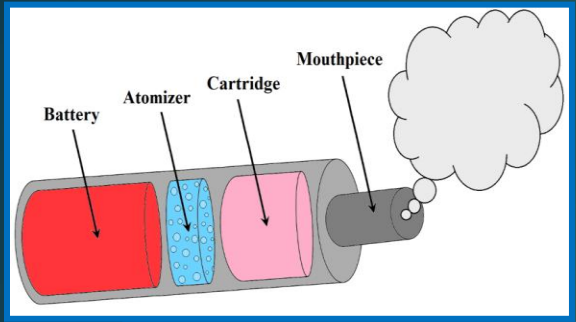

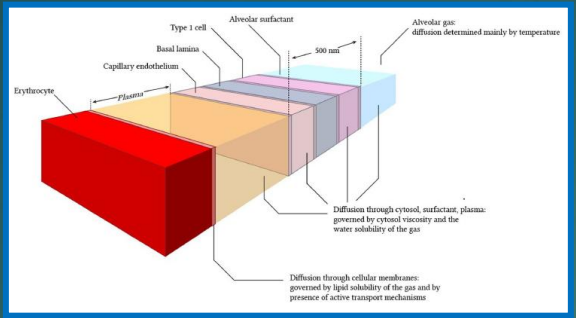

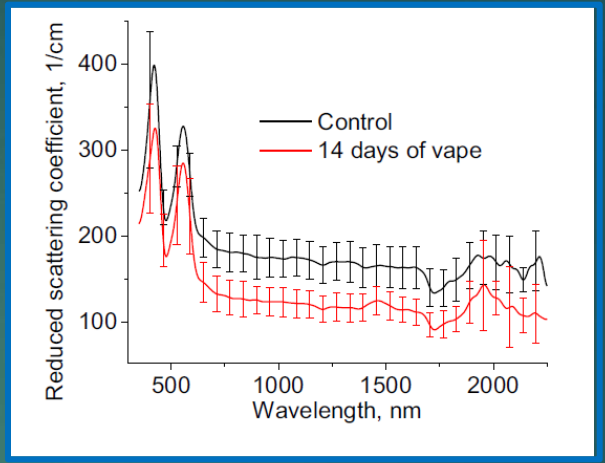

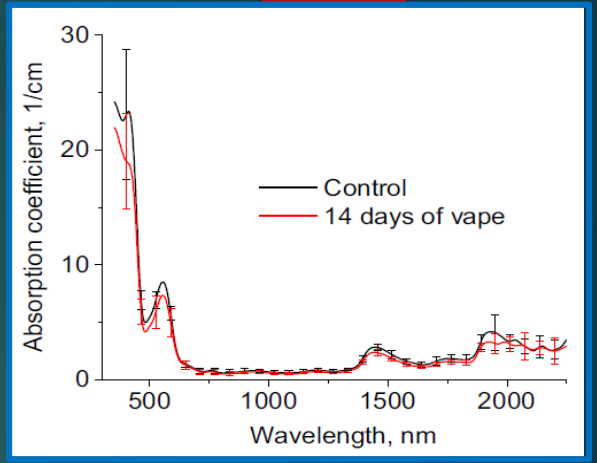

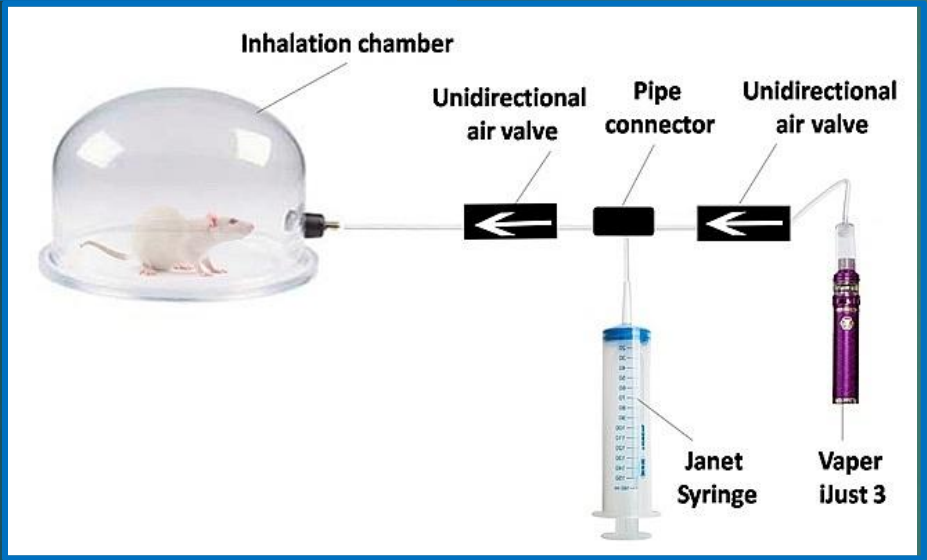

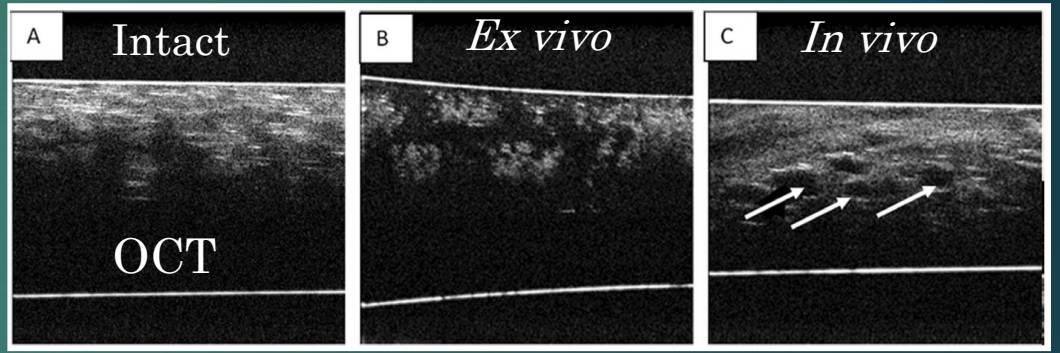

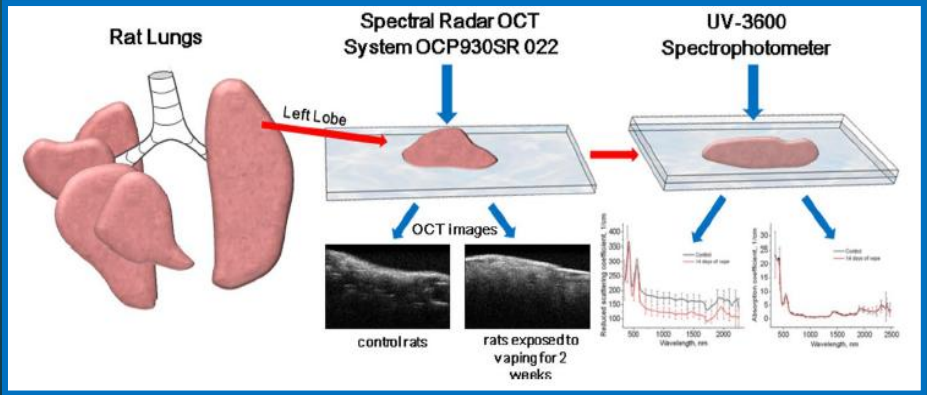

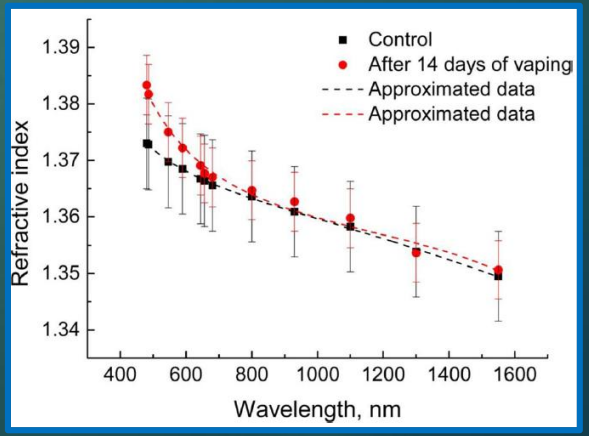

L.R. Oliveira, R.M. Ferreira, M.R. Pinheiro, H.F. Silva, V.V. Tuchin, L.M. Oliveira, Broadband spectral verification of optical clearing reversibility in lung tissue, ***J. Biophotonics*** 15, e202200185, 2023

Rabbit lung tissue

$$OC_{eff}(\%) = \frac{T_c(\lambda, t) - T_c(\lambda, t = 0)}{T_c(\lambda, t = 0)} \times 100\%$$

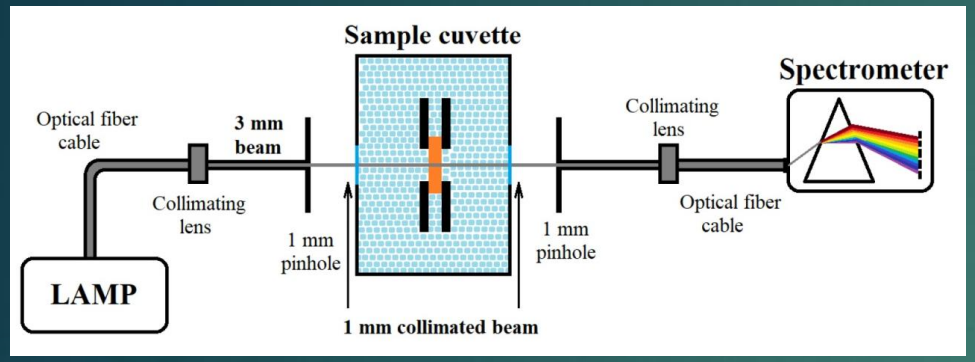

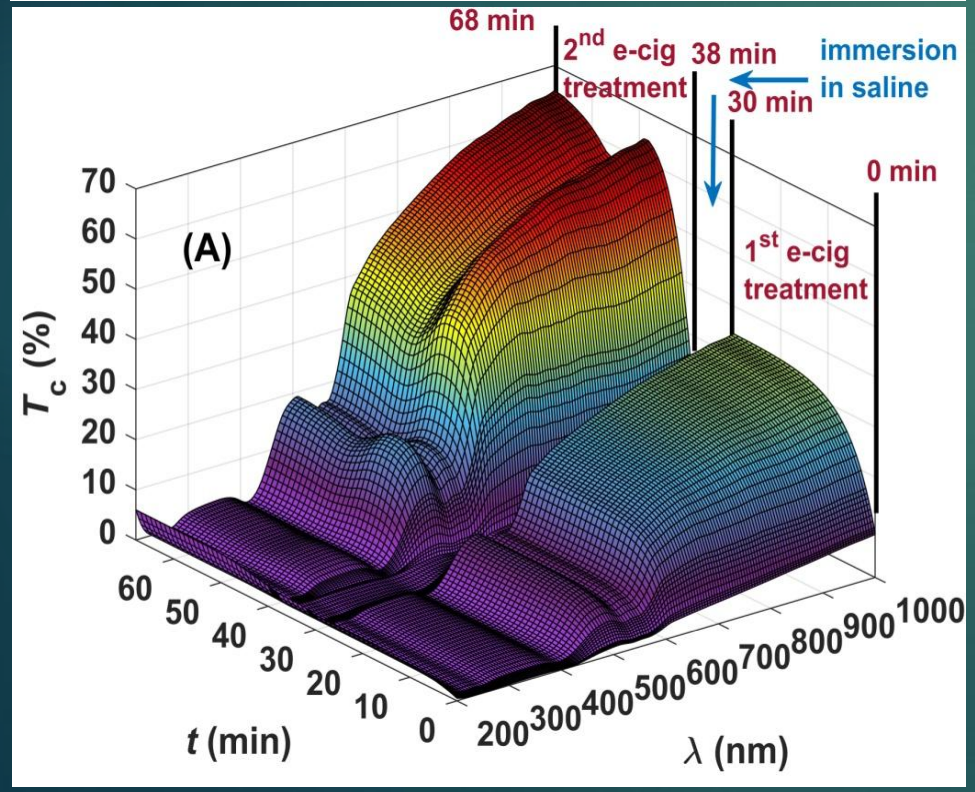

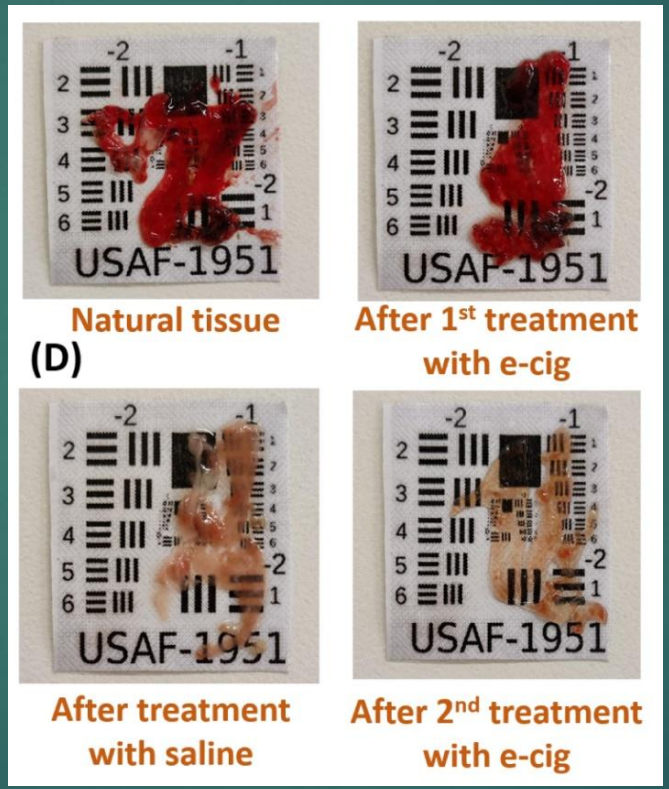

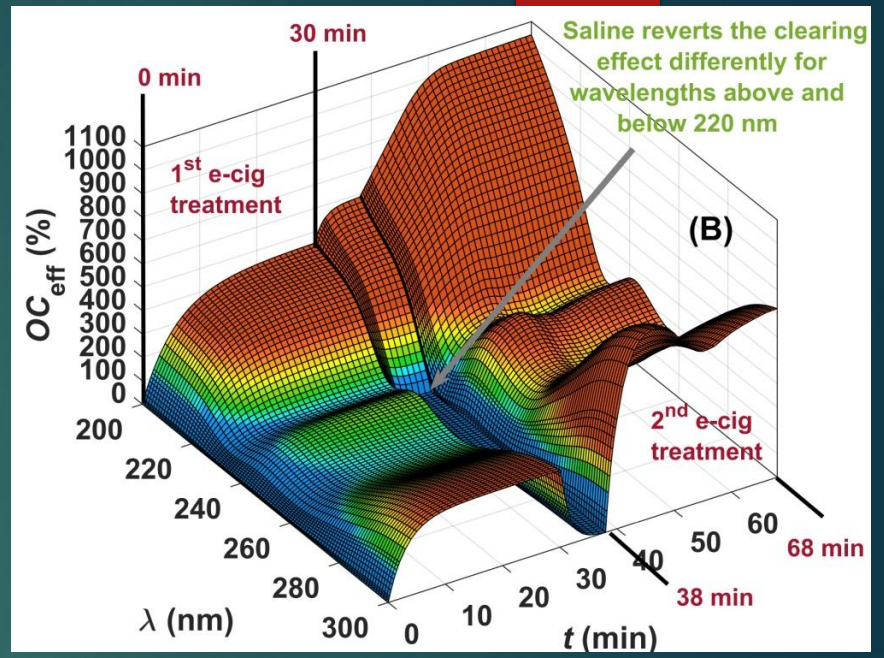

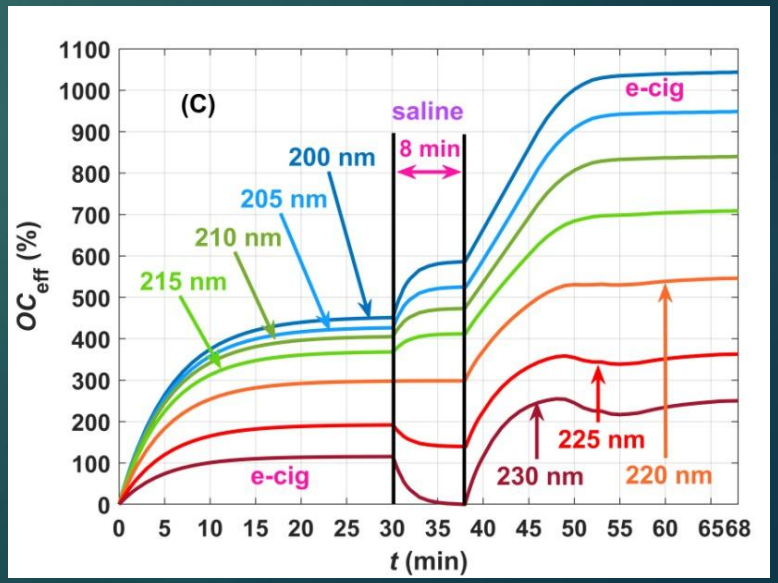

In vivo immersion optical clearing of adipose tissue

Motivation: Conventional or Laser Surgery, to see and avoid dissection of blood vessels

I. Y. Yanina, et al., "Immersion optical clearing of adipose tissue in rats: ex vivo and in vivo studies," *J. Biophotonics* e202100393 (2022)

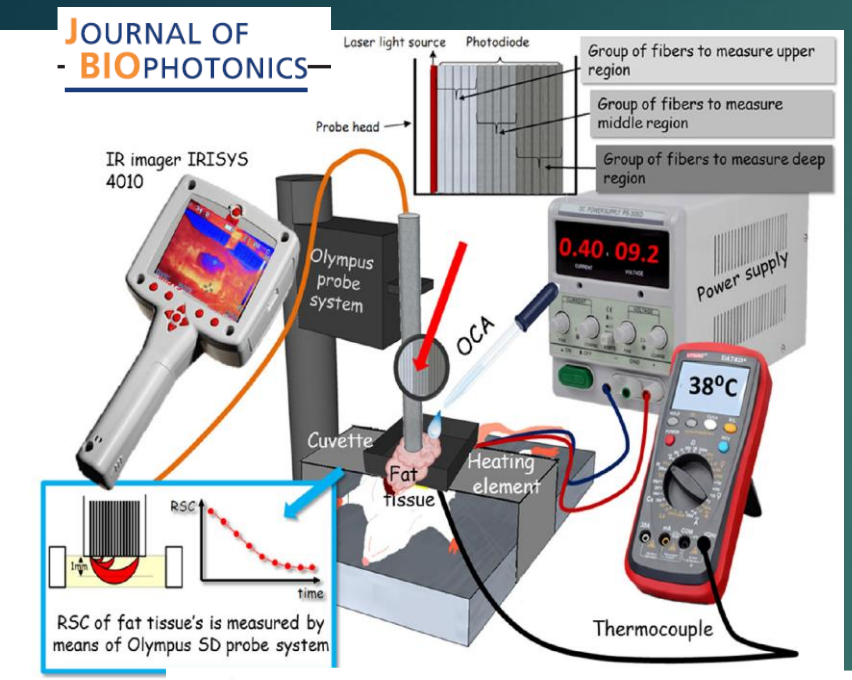

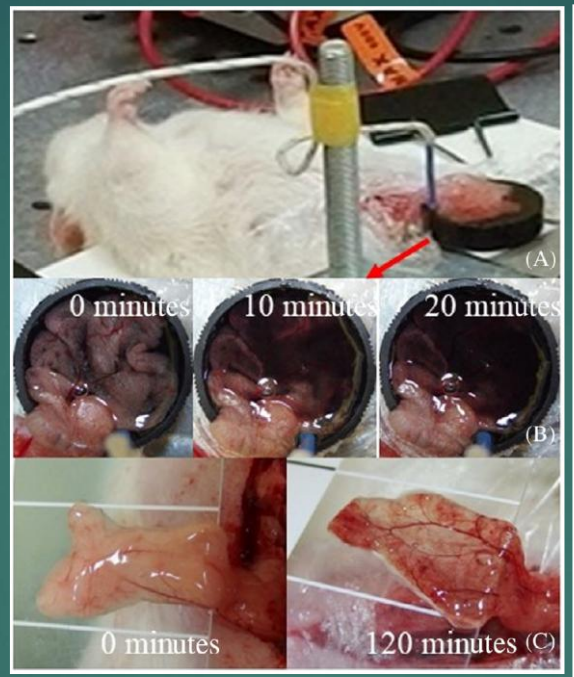

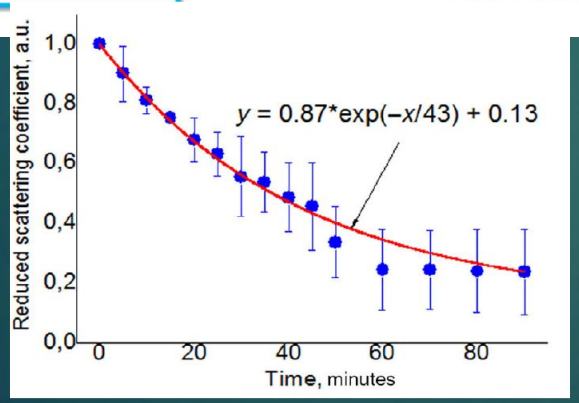

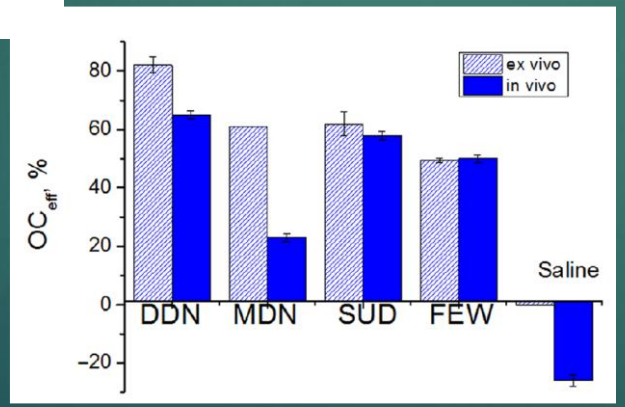

Ex vivo	Intact	FEW	DDN	MDN	SUD
Damage severity		Low	Middle	Middle	Above middle
Signs		Cells have round shape with thickened membranes	Nuclei are absent, membranes are crenulated	Nuclei are absent, membranes are thickened, eosinophilic and thinned	Broken adipocyte septa
Histological images	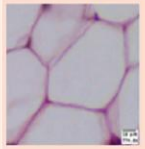	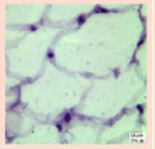	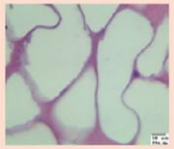	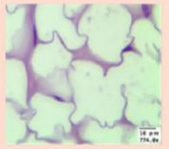	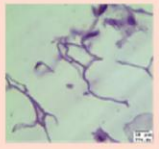

In vivo	Intact	FEW	DDN	MDN	SUD
Damage severity		Low	Middle	Middle	Middle
Signs		Single broken or crenulated adipocyte septa	Swelling of the intercellular membranes of adipose tissue	Severe vascular hyperemia and moderate thickening of membranes	The diapedesis hemorrhages
Histological images	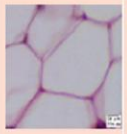	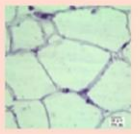	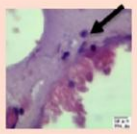		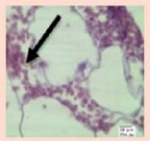

1 FEW: 50% Fructose, 30% Ethanol, 20% Water (n=1.408)

2 DDN: 21% Diatrizoic acid, 66% DMSO, 13% N-methyl-glucamine (n=1.511)

3 MDN: 30% Metrizoic acid, 58% DMSO, N-methyl-glucamine (n=1.529)

4 SUD: 60% Sucrose, 40% DMSO (n=1.509)

IEEE JOURNAL OF SELECTED TOPICS IN QUANTUM ELECTRONICS, VOL. 27, NO. 4, JULY/AUGUST 2021 7200711

Detection of Melanoma Cells in Whole Blood Samples Using Spectral Imaging and Optical Clearing

Polina A. Dyachenko, Leonid E. Dolotov, Ekaterina N. Lazareva, Anastasia A. Kozlova, Olga A. Inozemtseva, Roman A. Verkhovskii, Galina A. Afanaseva, Natalia A. Shushunova, Valery V. Tuchin, Ekaterina I. Galanzha, and Vladimir P. Zharov

(Invited Paper)

Principle of spectral absorbance measurement of a whole blood sample at immersion OC

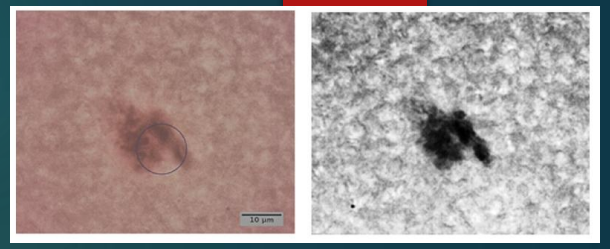

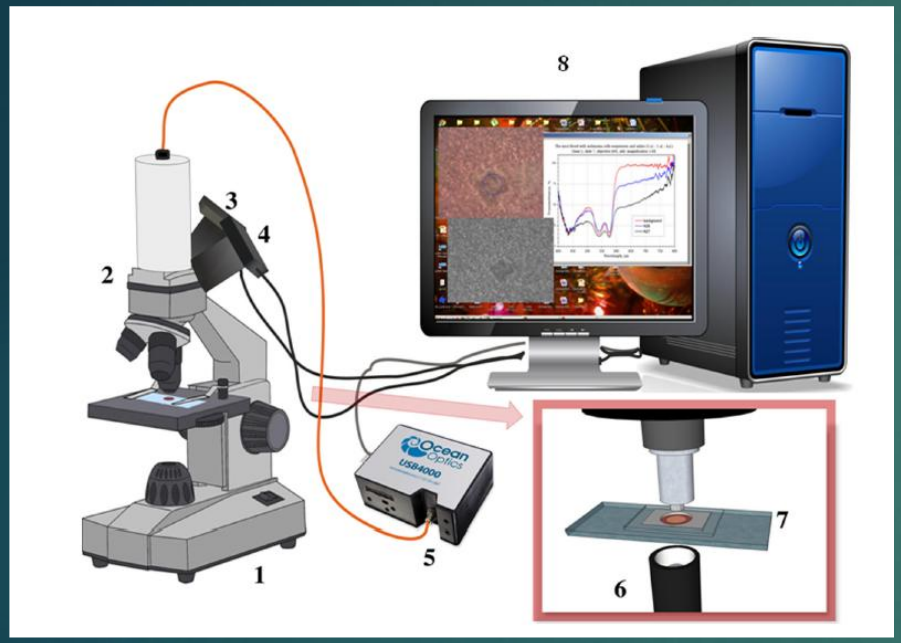

Scheme of experimental setup for spectral study: 3 is the color video camera DCC1645C, 4 is the monochrome camera DCC1545M, 5 is the spectrometer USB4000, 6 is the illumination unit KL-1500Z, 7 is the blood slide

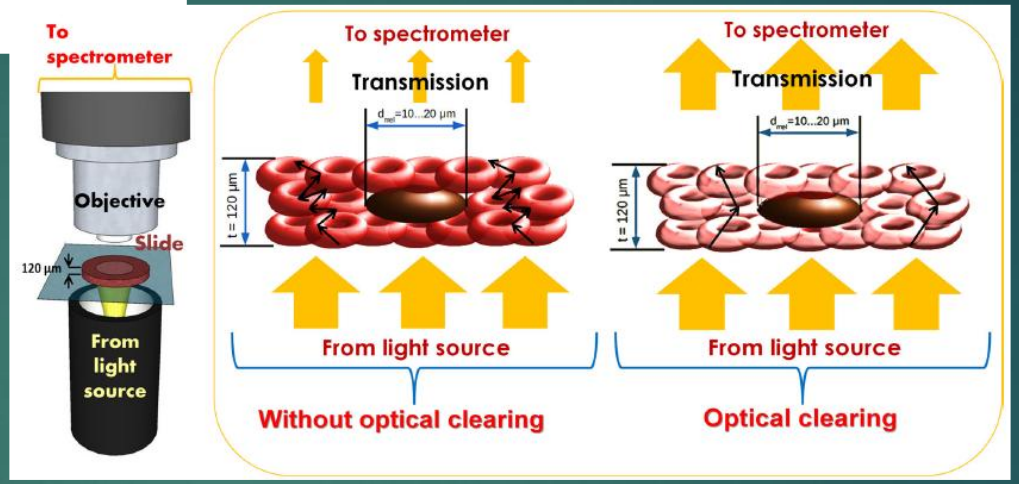

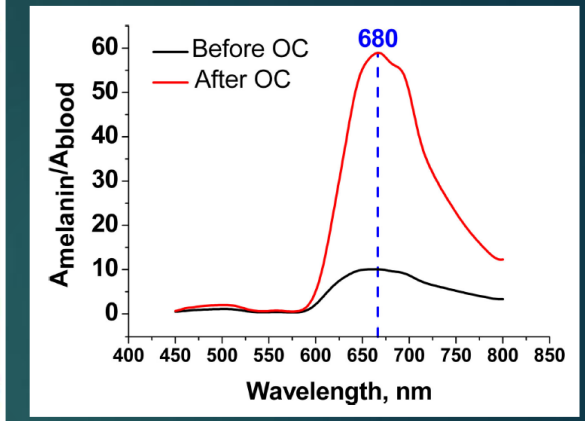

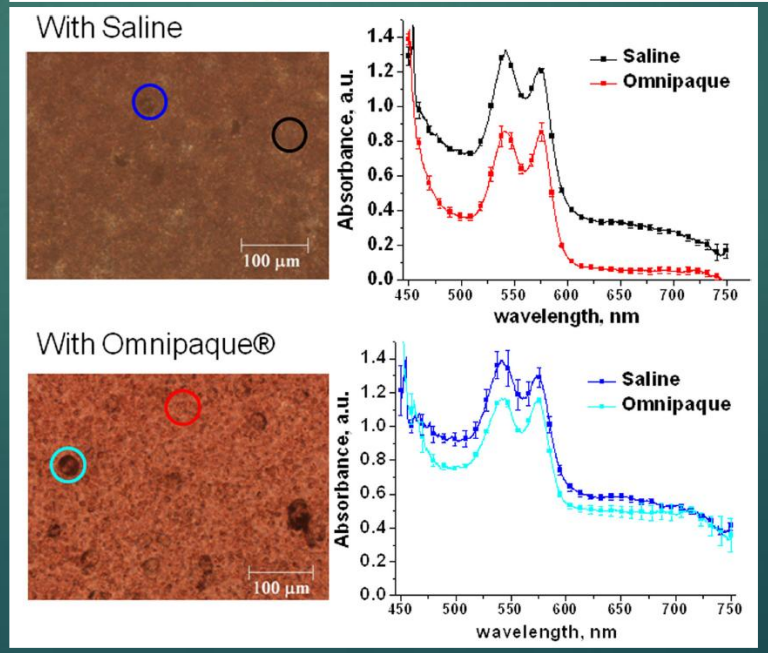

Images of slides of thickness 120 μm with a whole blood (3 μl) of a laboratory mouse and mouse melanoma cells (B16F10) (1 μl) mixed with 4 μl of saline (upper image) or Omnipaque (lower image)

Upconversion nanoparticles (UCNP) for deep-tissue imaging

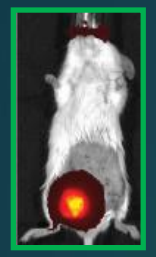

A.P. Popov, E.V. Khaydukov, A.V. Bykov, V.A. Semchishen, V.V. Tuchin, Enhancement of upconversion deep-tissue imaging using optical clearing, Proc. of SPIE-OSA **9540**, 95400B-5, 2015

[NaYF4 matrix is doped with ions of ytterbium, erbium and thulium)]

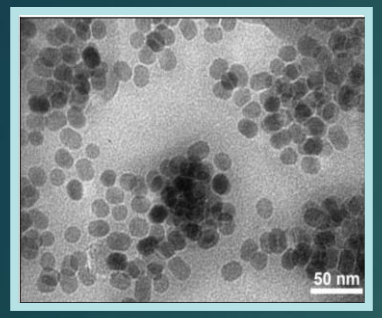

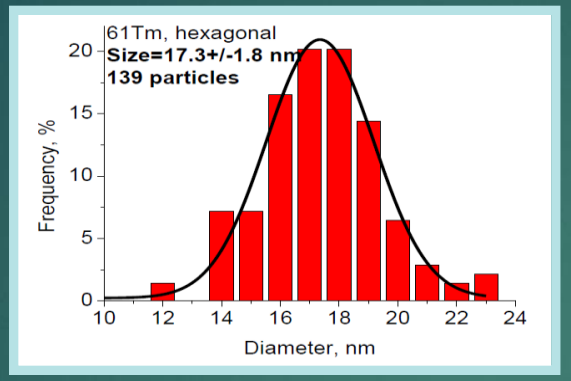

Size distribution

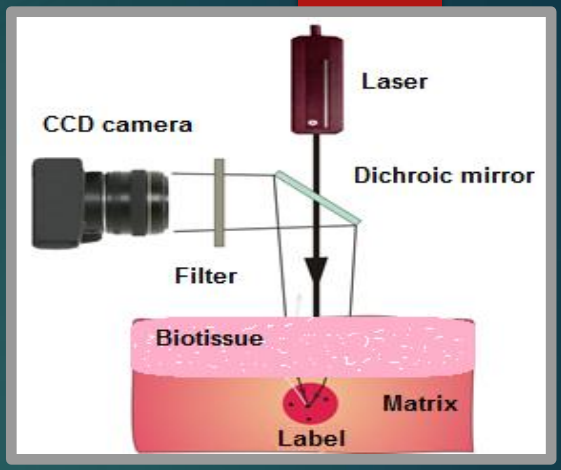

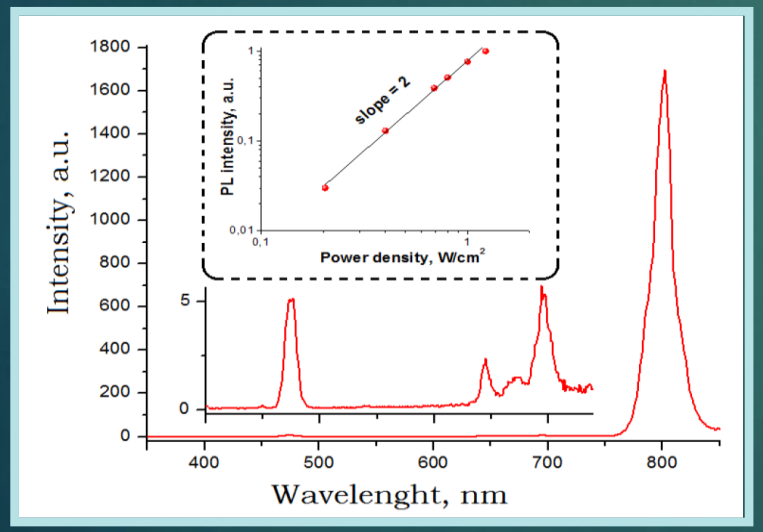

Spectra of luminescent radiation at pumping on **975 nm**

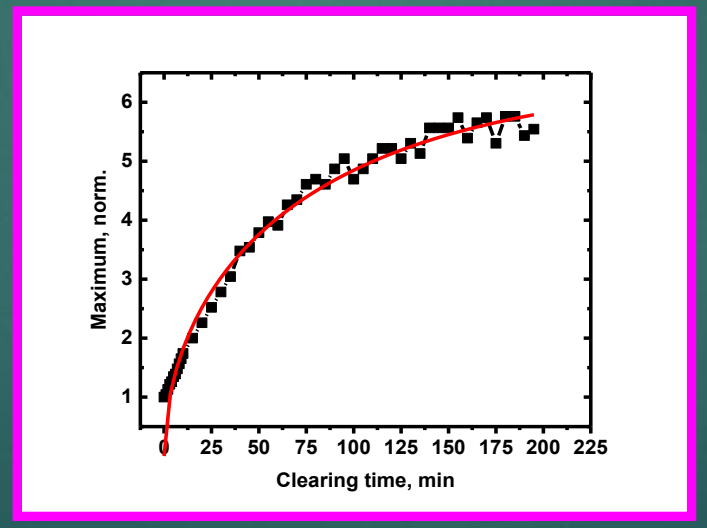

Upconversion luminescence of a star-shaped label at **800 nm**, glycerol clearing of 6-mm-thick porcine muscle tissue

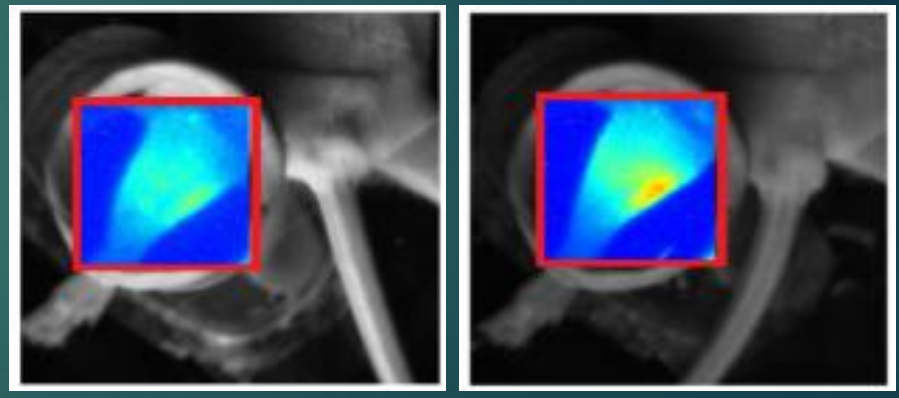

Before and after **255 min** of **glycerol** clearing mouse leg ***in vivo***

Generation of OCAs in the body

Local fat cell lipolysis is the breakdown of lipids and involves hydrolysis of triglycerides into **glycerol (OCA)** and **free fatty acids (enhancers)**

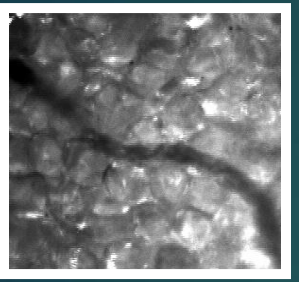

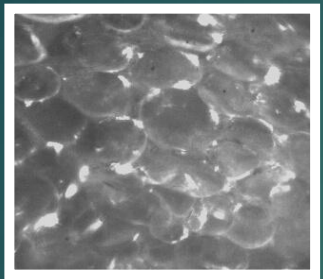

In vivo images through a few mm rat fat layer (heating)

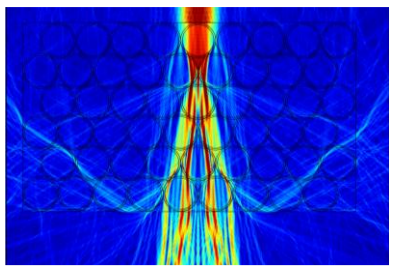

Modeling of light beam propagation through 6 layers of cells

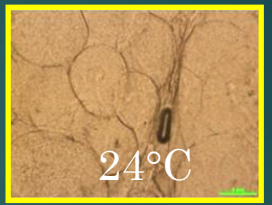

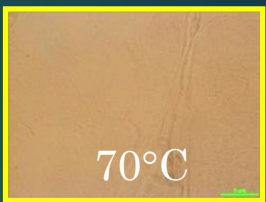

Transillumination images

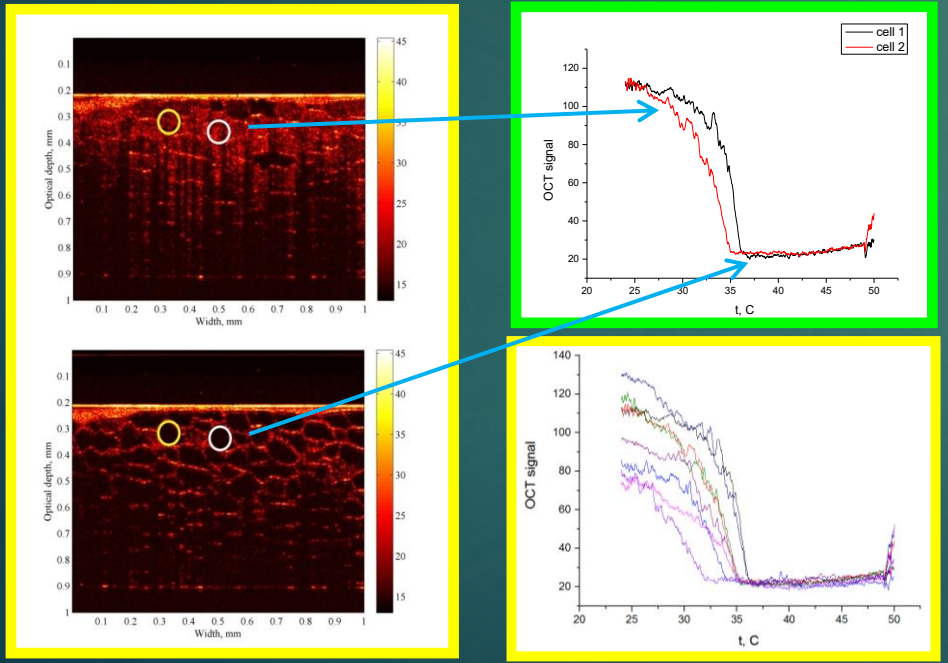

In vitro OCT images of porcine fat tissue

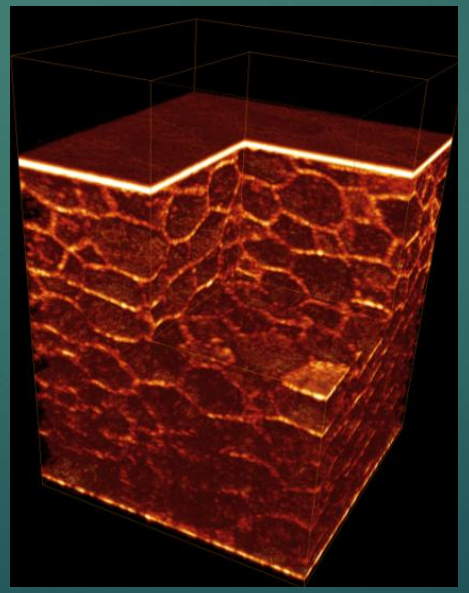

Proteins are also good OCAs

Local RBC hemolysis – Hemoglobin

Popescu et al. and Zhernovaya et al. have proved this experimentally

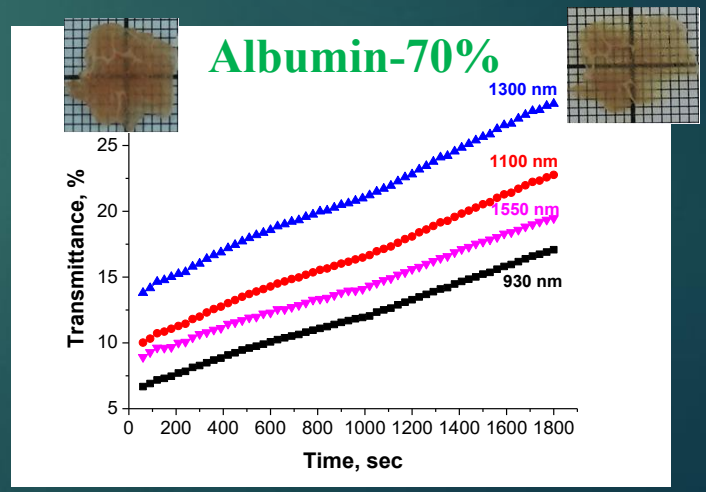

Bashkatov et al., J. Biomed. Opt. **23**(9), 091416 (2018)

Silicone-glycerol mixture tissue phantoms

M.S. Wróbel et al., Nanoparticle-free tissue-mimicking phantoms with intrinsic scattering *Biomed. Opt. Express* **7**(6), 2088-2094 (2016)

Phantom

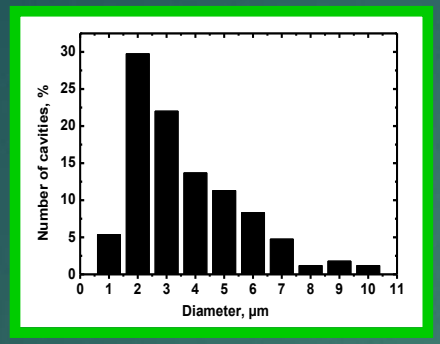

Size distribution of microcavities

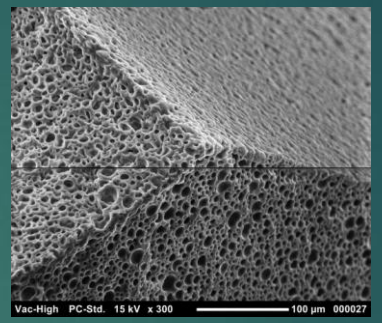

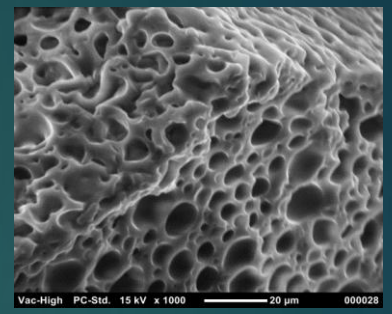

Electronic micrographs of phantom

P. Listewnik, M. Ronowska, M. Wasowicz, V.V. Tuchin, M. Szczerska, Porous phantoms mimicking tissues—investigation of optical parameters stability over time. Materials **2021**, 14, 423-1-11

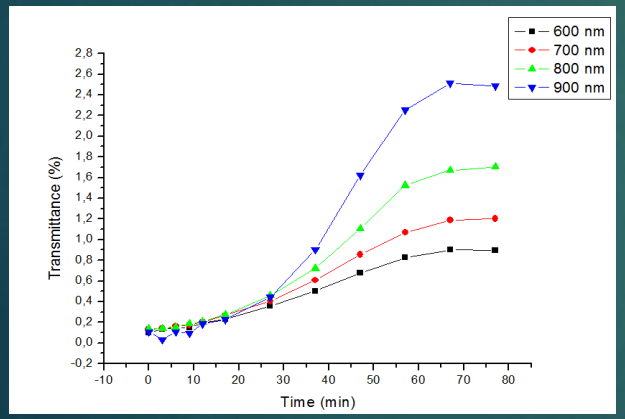

Transmittance kinetics (glucose solution, 40%)

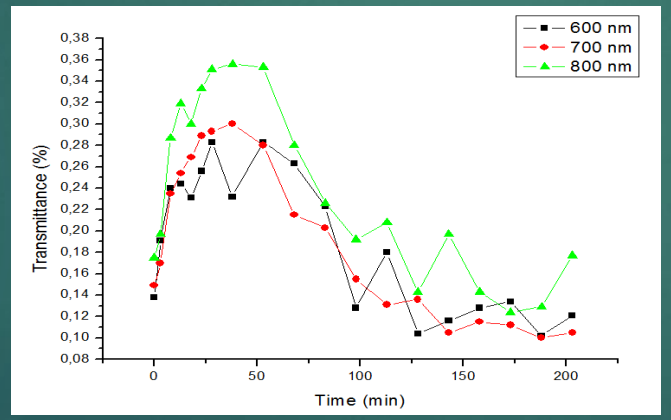

Transmittance kinetics (water)

Quirk et al. OPTICS LETTERS **39**(10):2888-2891, 2014

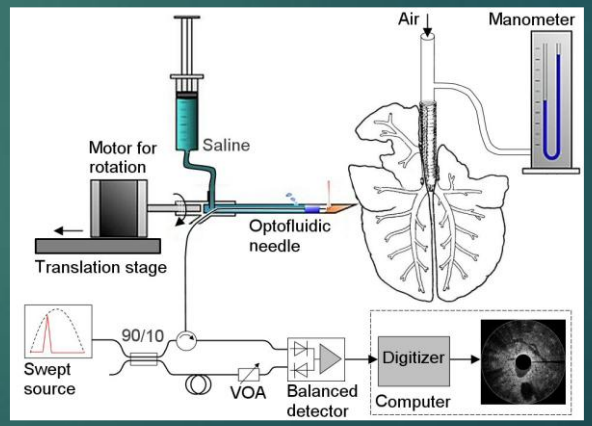

Schematic of the OCT optofluidic needle probe

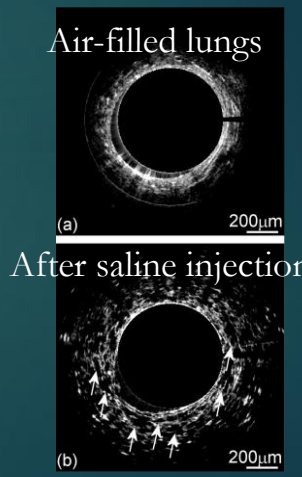

Arrows indicate representative alveoli

Additional benefit: sound and light propagate in phantom with properties close to the actual tissue

materials

Materials 2025, 18, 1035

MDPI

Article

Molecular Diffusion and Optical Properties of Implantable Collagen Materials

Sofya V. Atsigeida [1,*], Daria K. Tuchina [1,2], Peter S. Timashev [3] and Valery V. Tuchin [1,2,4]

Glucose diffusion in implantable collagen materials

"SPILAK", "PER uncrosslinked", "PER crosslinked"
(Institute of Regenerative Medicine, Sechenov Univ.)

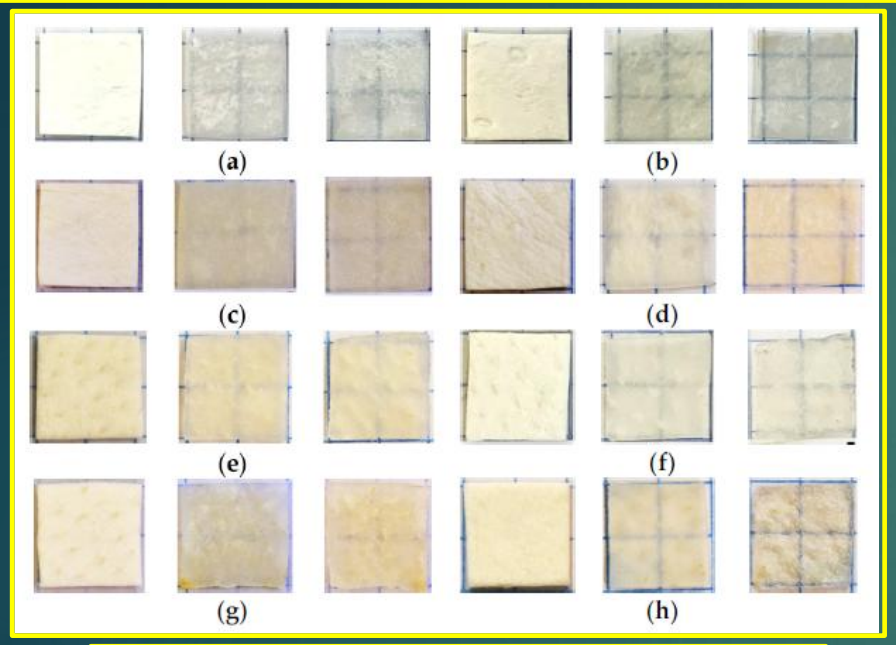

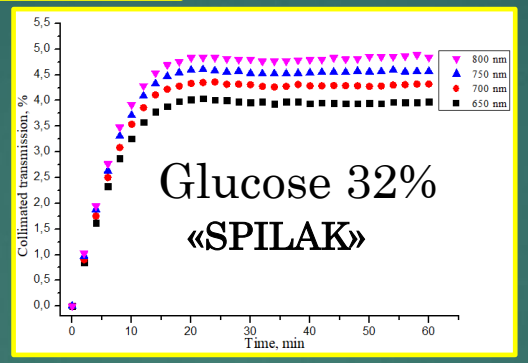

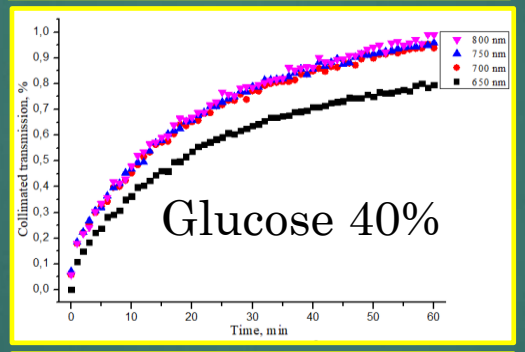

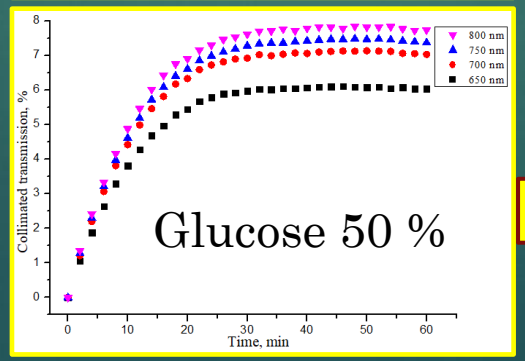

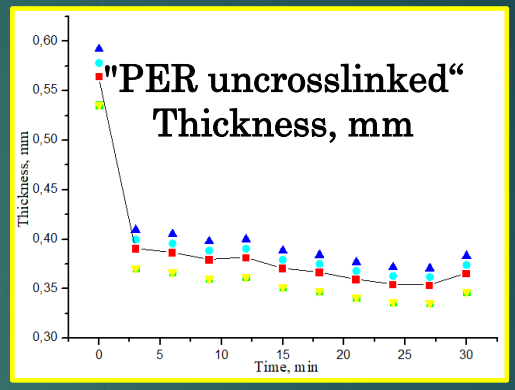

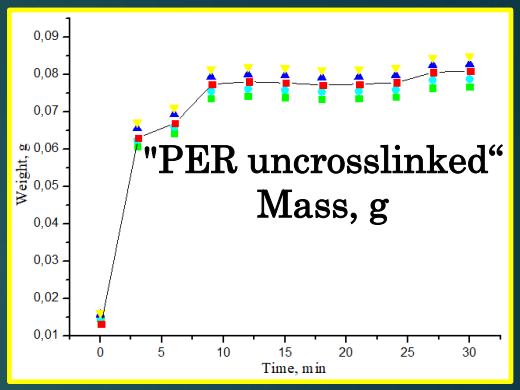

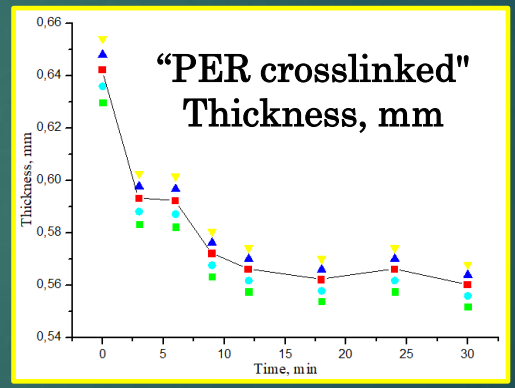

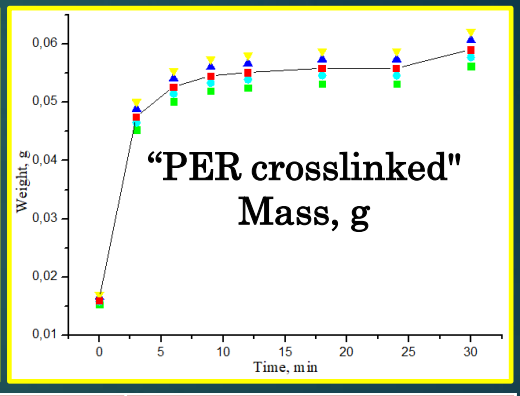

Glucose	τ, min	D, cm²/c
32%	6.9±1.1	(1.52±0.32)x10^{-6}
40%	11.8±2.2	(0.82±0.12)x10^{-6}
50%	8.8±1.3	(1.58±0.41)x10^{-6}

OCT images (930 nm) of light and dark skin

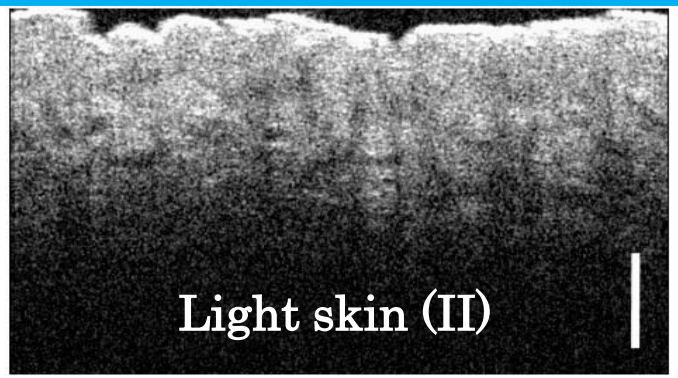

a

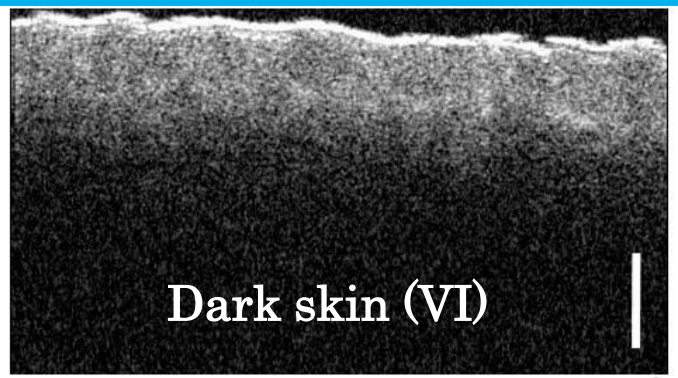

b

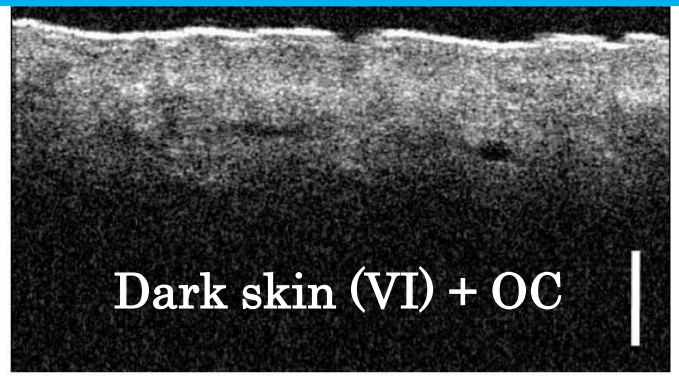

c

MDA
OA
SP

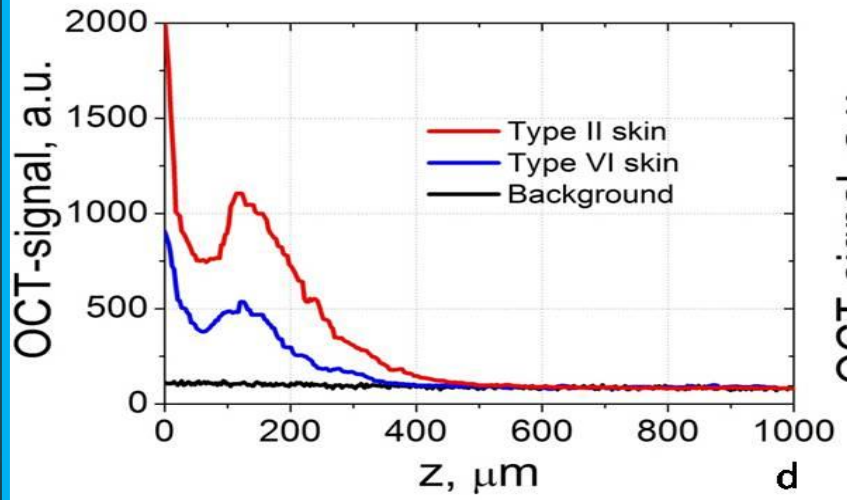

d

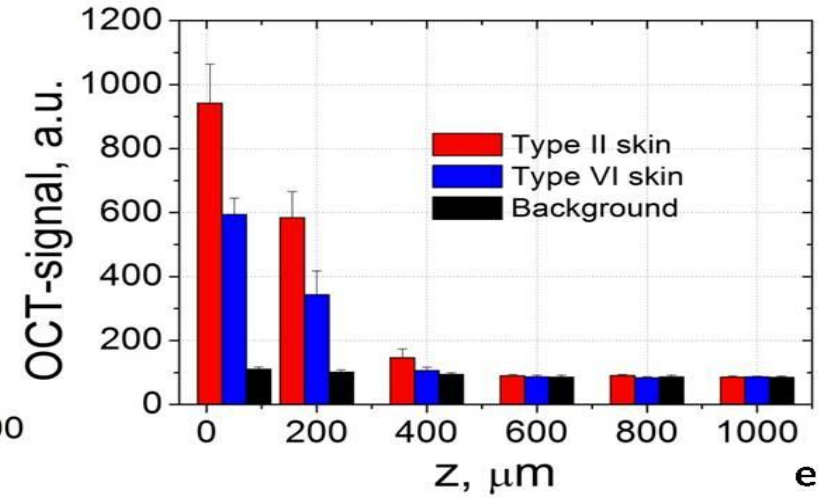

e

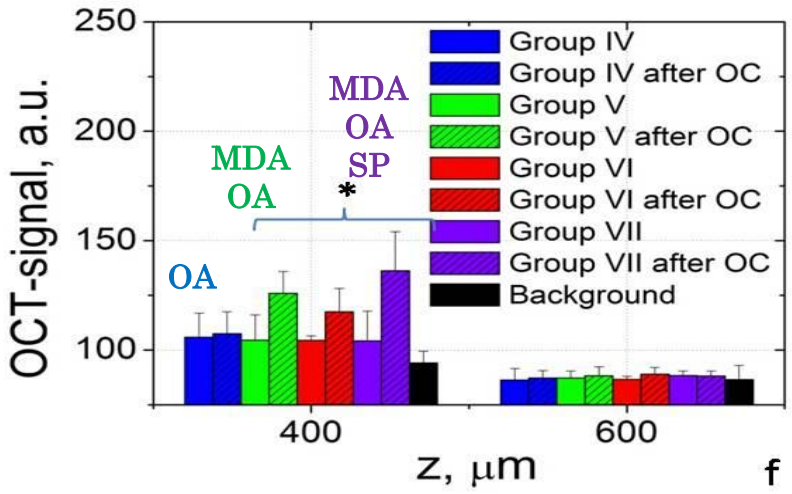

f

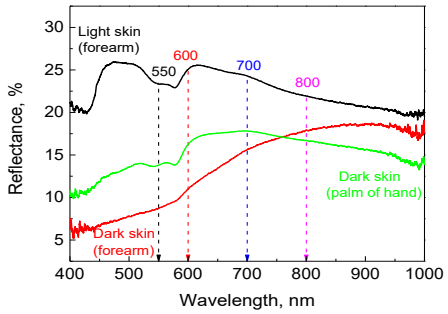

OCT B-scans of intact human skin of type II (a) and VI (b); type VI skin 30 min after the combined action of microdermabrasion (MDA), oleic acid (OA), and sonophoresis (SP) (c). A-scans averaged over the entire scan area of intact skin (d). Histograms of OCT signal at different depths of intact skin averaged over six measurements (e) and mean OCT signals at different depths of type VI skin. Asterisks indicate a group with statistically significant differences between the OCT signals before and after OC (p<0.01). Bars correspond to 200 μm.

Anti-inflammatory drug delivery in dermatology with no side effects

We suggested a novel topical particulate formulation for the glucocorticoid clobetasol propionate (CP) using porous calcium carbonate ($CaCO_3$) carriers in the vaterite crystalline form

M.S. Saveleva et al. Biodegradable calcium carbonate carriers for the topical delivery of clobetasol propionate, *J. Mater. Chem. B* 12, 4867–4881 (2024)

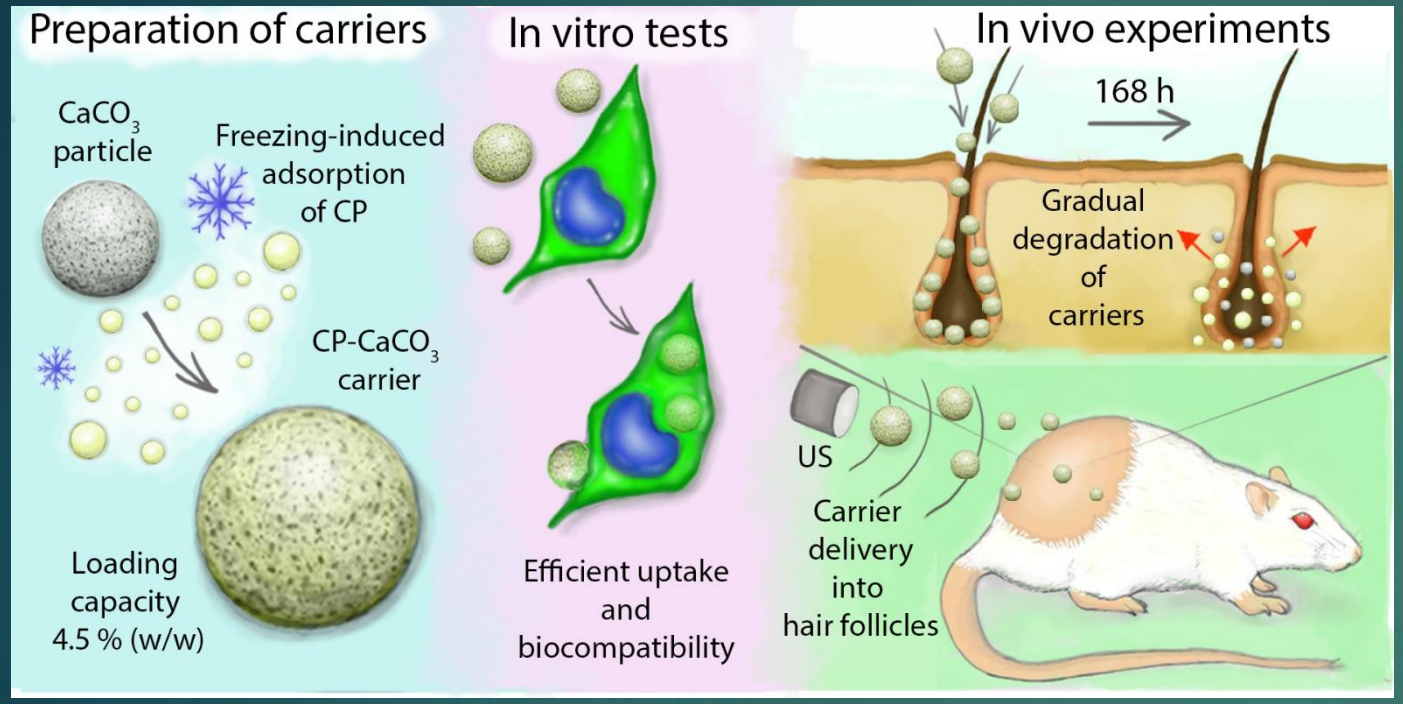

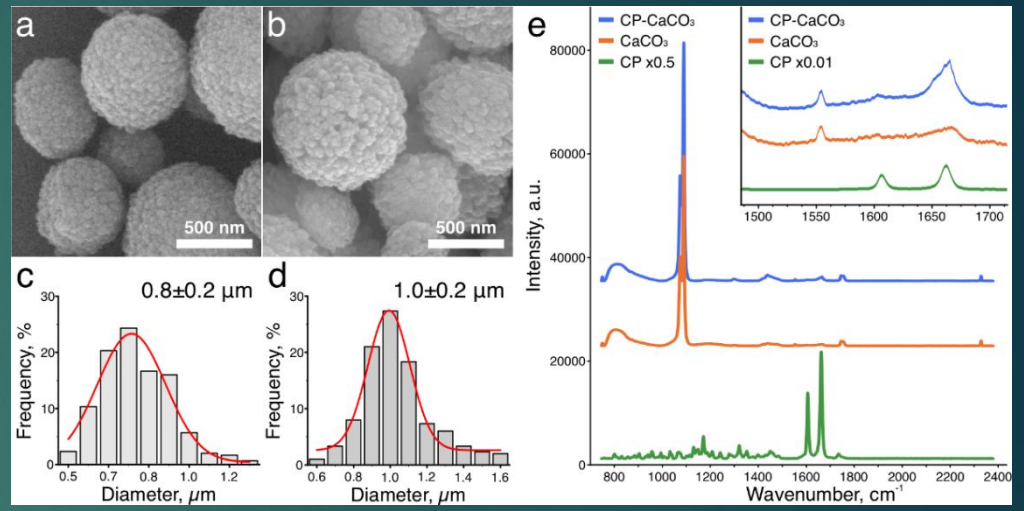

SEM (**a, b**) and size distributions (**c, d**) of the pure $CaCO_3$ (**a, c**) and $CP\text{-}CaCO_3$ carriers (**b, d**). Raman spectra of the $CP\text{-}CaCO_3$ (**e**).

OCT images of rat skin hair follicles performed *in vivo* before and after the application of the $CP\text{-}CaCO_3$ + OCA)

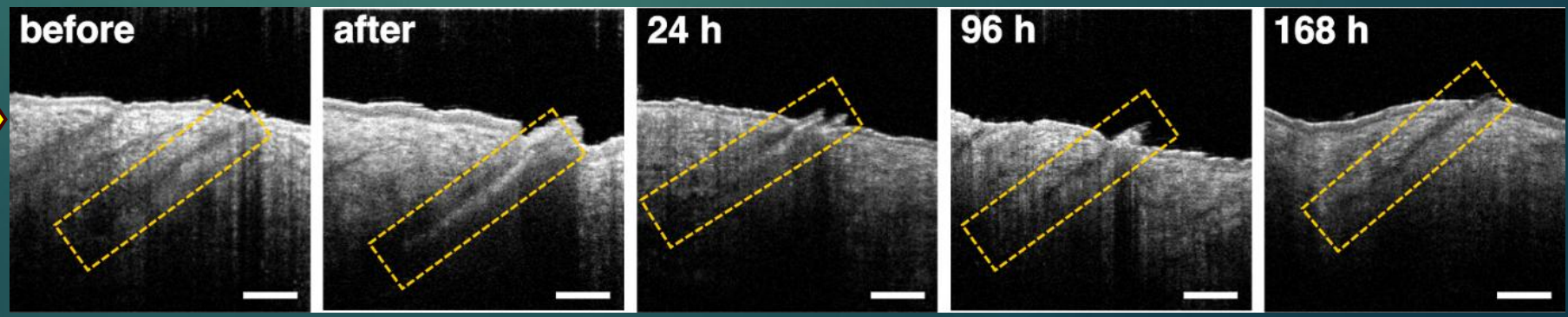

Deep photoinactivation of pathogens using an optical clearing agent (OCA)

V.V. Tuchin et al., Optical clearing of tissues: issues of antimicrobial phototherapy and drug delivery, *Advanced Drug Delivery Reviews*, 2022, 114037

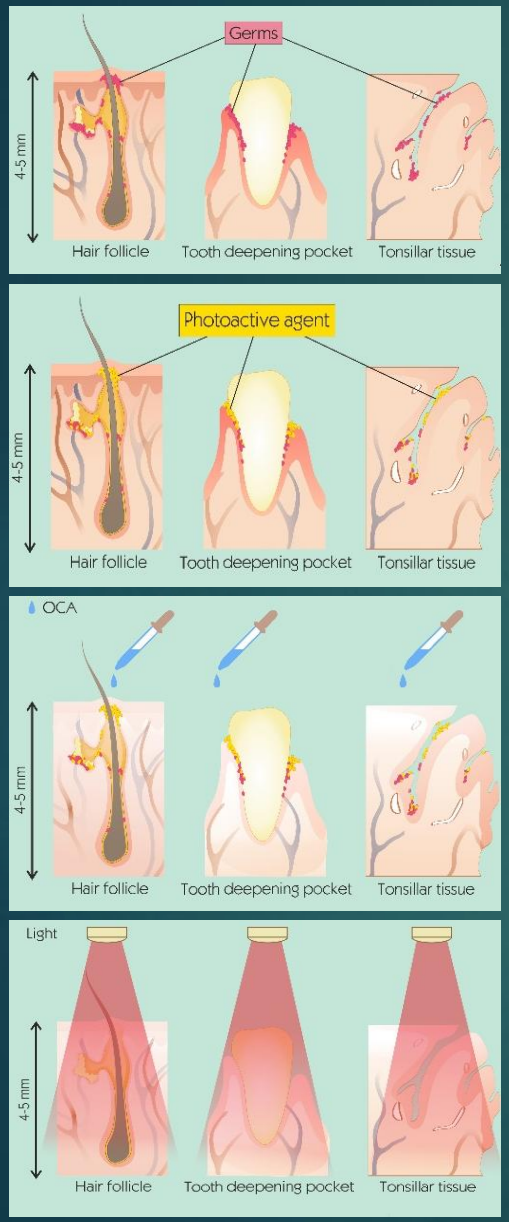

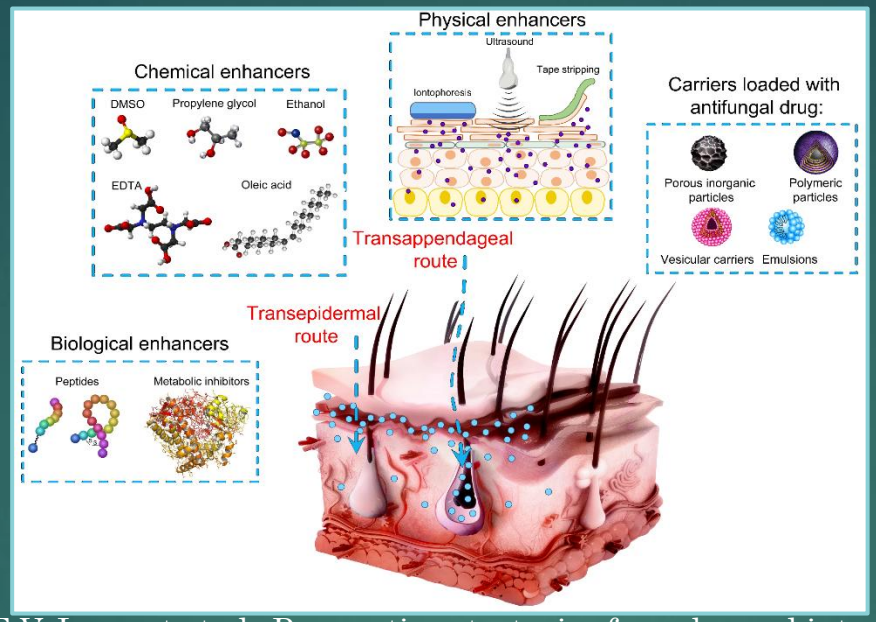

E.V. Lengert et al., Prospective strategies for enhanced intra- and transdermal delivery of antifungal drugs, *Skin Pharmacology and Physiology* **33**, 261–269 (2020)

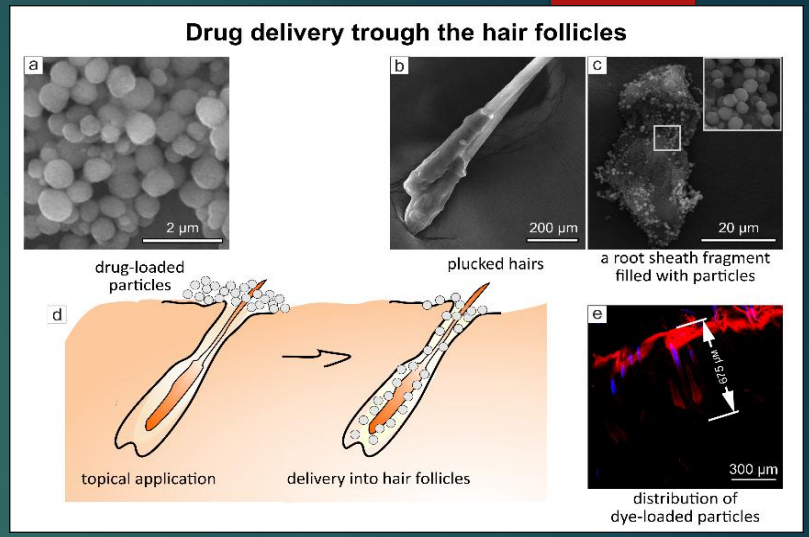

Y.I. Svenskaya et al., Enhanced topical psoralen–ultraviolet A therapy via targeting to hair follicles, *British Journal of Dermatology* **182**,1479–1481 (2020)

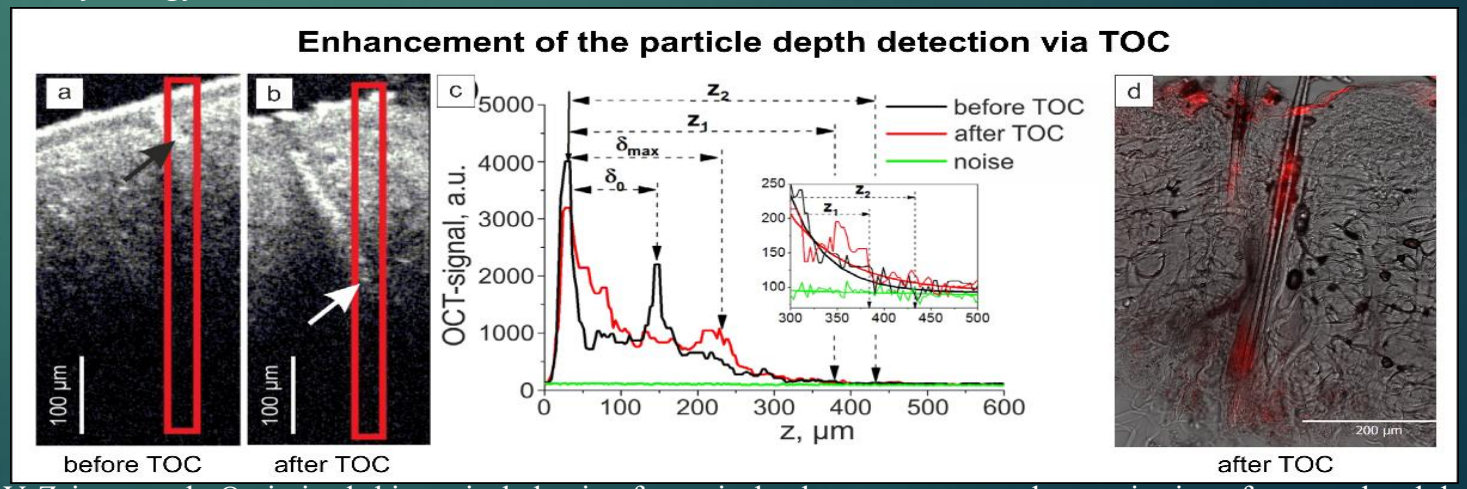

S.V. Zaitsev et al., Optimized skin optical clearing for optical coherence tomography monitoring of encapsulated drug delivery through the hair follicles, J. Biophotonics 13, e201960020 (2020)

diagnostics Diagnostics 2024, 14, 202 MDPI

Article

Multimodal Method for Differentiating Various Clinical Forms of Basal Cell Carcinoma and Benign Neoplasms In Vivo

Yuriy I. Surkov [1,2,3,*], Isabella A. Serebryakova [1,2], Yana K. Kuzinova [4], Olga M. Konopatskova [3,4], Dmitriy V. Safronov [4], Sergey V. Kapralov [4], Elina A. Genina [1,2] and Valery V. Tuchin [1,2,3,5,*]

OCA: 40% glycerol
Exposure time: 10 min

Pathological skin demonstrates enhanced optical clearing efficiency compared to healthy skin, likely due to the disrupted barrier function within the lesion area

Multimodal method

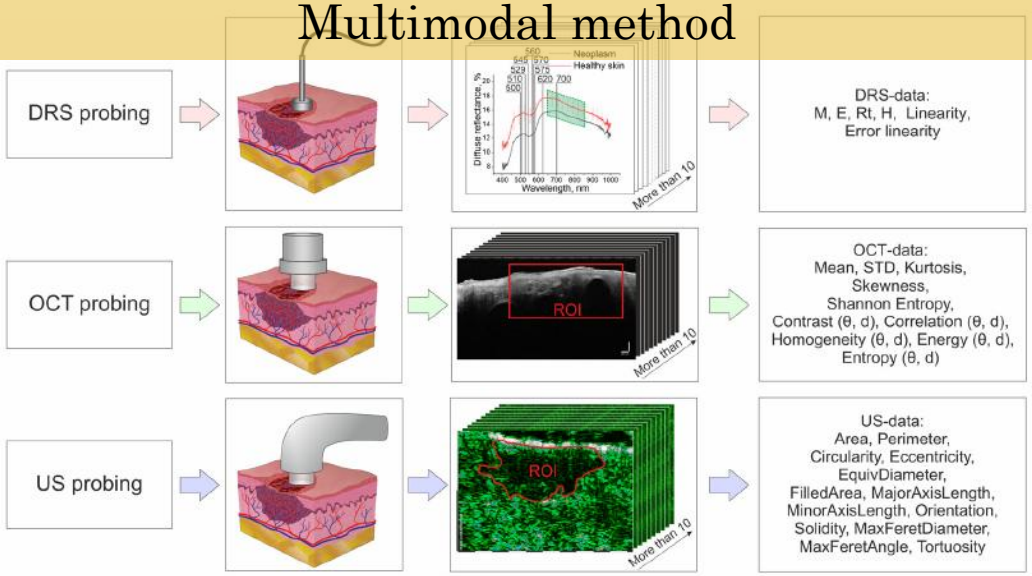

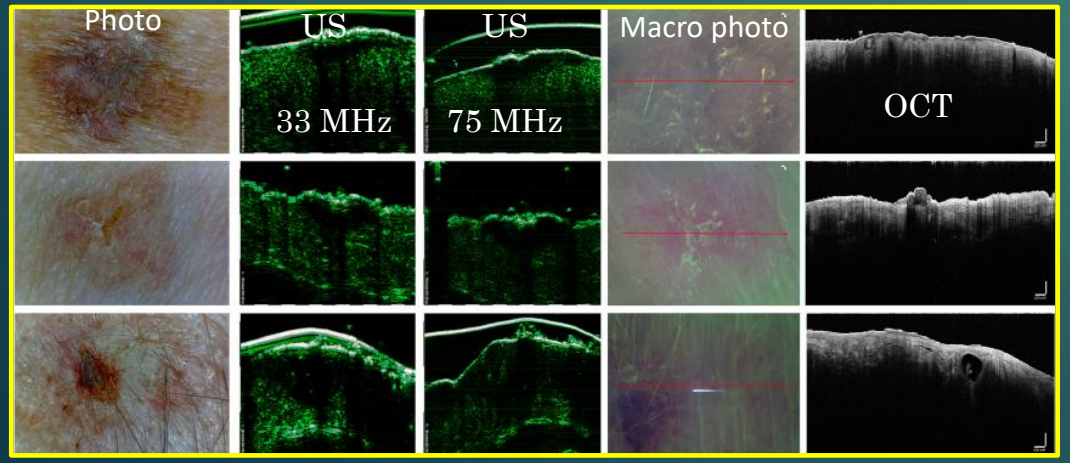

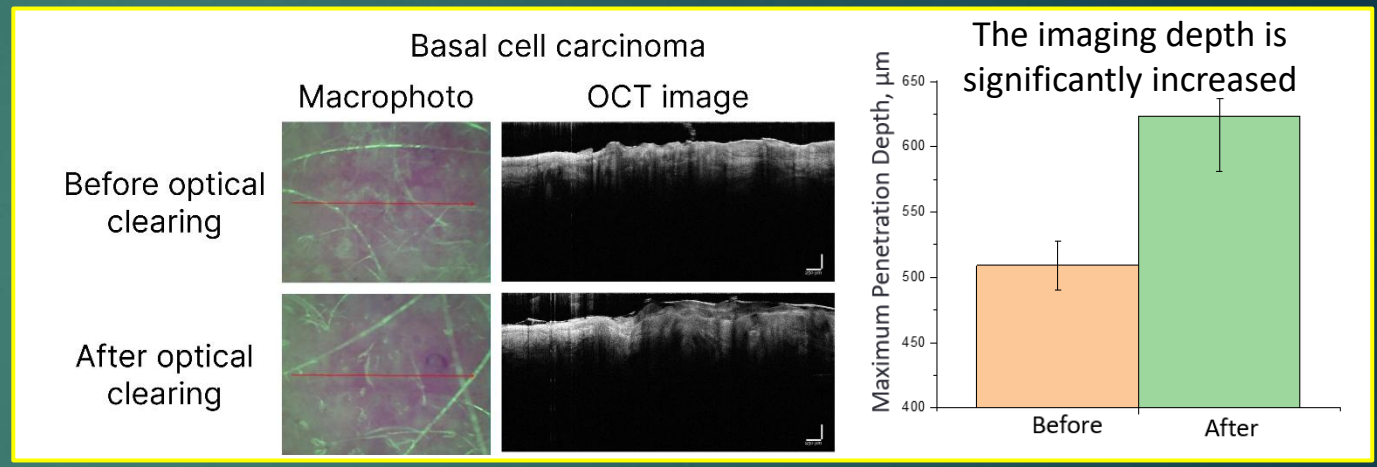

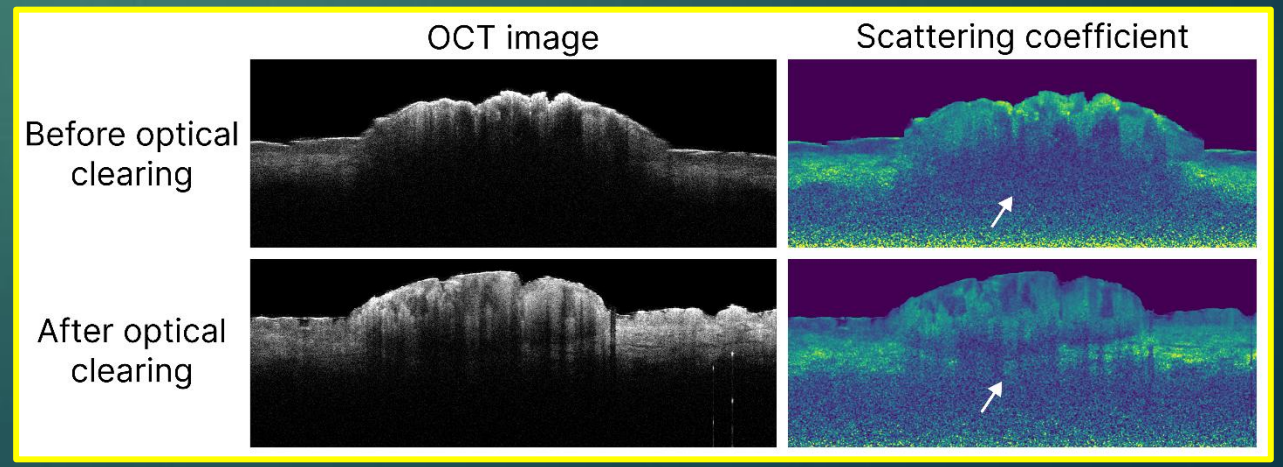

Prospects for *in vivo* OC

iScience
iScience 24, 101888, January 22, 2021
Article

Optical clearing of living brains with MAGICAL to extend *in vivo* imaging

Kouichirou Iijima,[1] Takuto Oshima,[2] Ryosuke Kawakami,[1,2] and Tomomi Nemoto

MAGICAL : Magical Glycerol additive improves light brightness from living object

Increased speed, depth and contrast of multiphoton and CM imaging

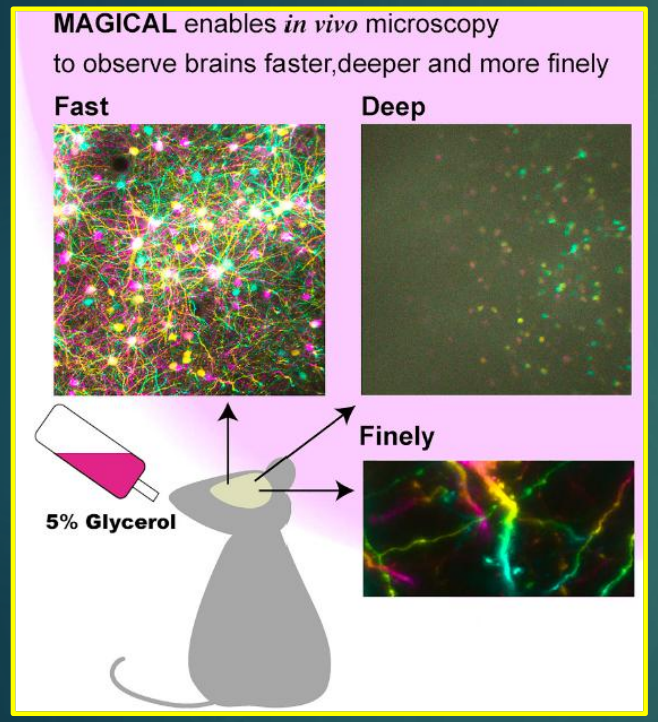

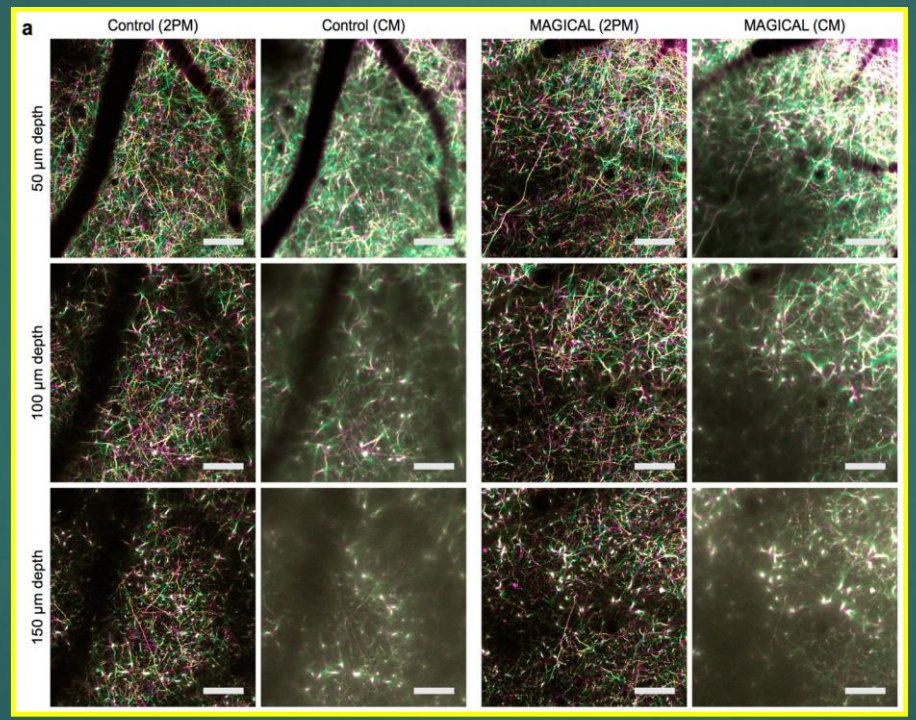

MAGICAL : 5% (w/v) glycerol was administered orally with drinking water, *ad libitum*, 2 weeks before open skull surgery and until the end of the experiment

REVIEW ARTICLE
Sports Med 2010; 40 (2): 113-139
0112-1642/10/0002-0113/$49.95/0

Guidelines for Glycerol Use in Hyperhydration and Rehydration Associated with Exercise

Simon Piet van Rosendal,[1] *Mark Andrew Osborne*,[2] *Robert Gordon Fassett*[1,3] and *Jeff Scott Coombes*[1]

1 School of Human Movement Studies, The University of Queensland, Brisbane, Queensland, Australia
2 Queensland Academy of Sport, Brisbane, Queensland, Australia
3 Royal Brisbane and Women's Hospital, Brisbane, Queensland, Australia

Wald, S.L. et al. Oral glycerol for the treatment of traumatic intracranial hypertension. J. Neurosurg. 56, 323–331 (1982)

An oral *glucose tolerance test*

Glucose is given orally and blood samples are taken to determine how quickly it is removed from the blood

Recent examples of the use of our results

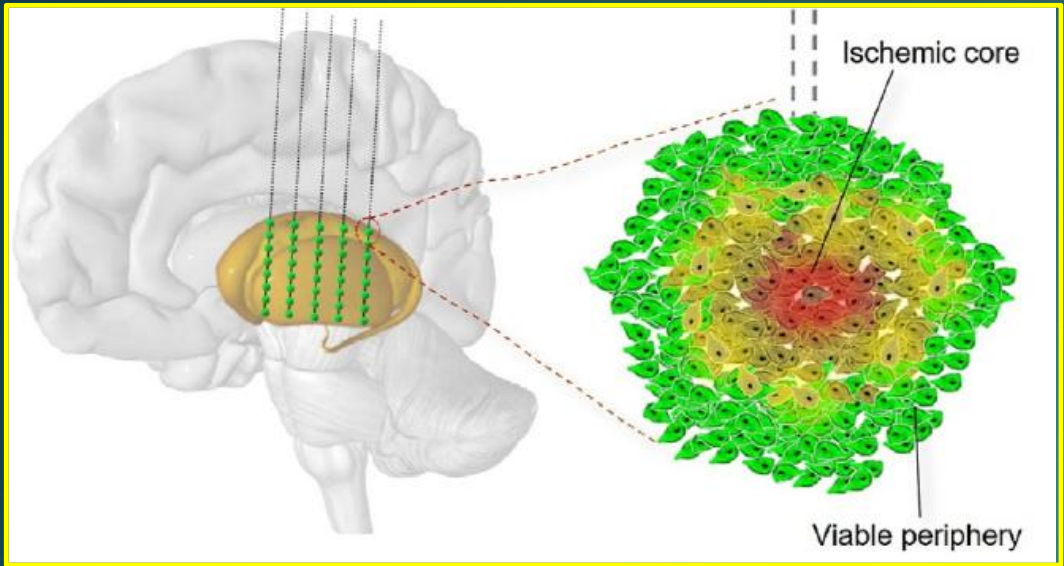

Graft ischemia after cell transplantation into the brain: glucose deficiency as a major factor in rapid cell death

Hakami A et al., Graft ischemia post cell transplantation to the brain: Glucose deprivation as the primary driver of rapid cell death, Neurotherapeutics, e00518 (2024)

The values of the diffusion coefficients of glucose in human tissues were used (Bashkatov AN, Genina EA, Tuchin VV. Measurement of glucose diffusion coefficients in human tissues. Chap 19:587–621 (2009))

Nutrient starvation limits antibiotic effectiveness in structured bacterial populations

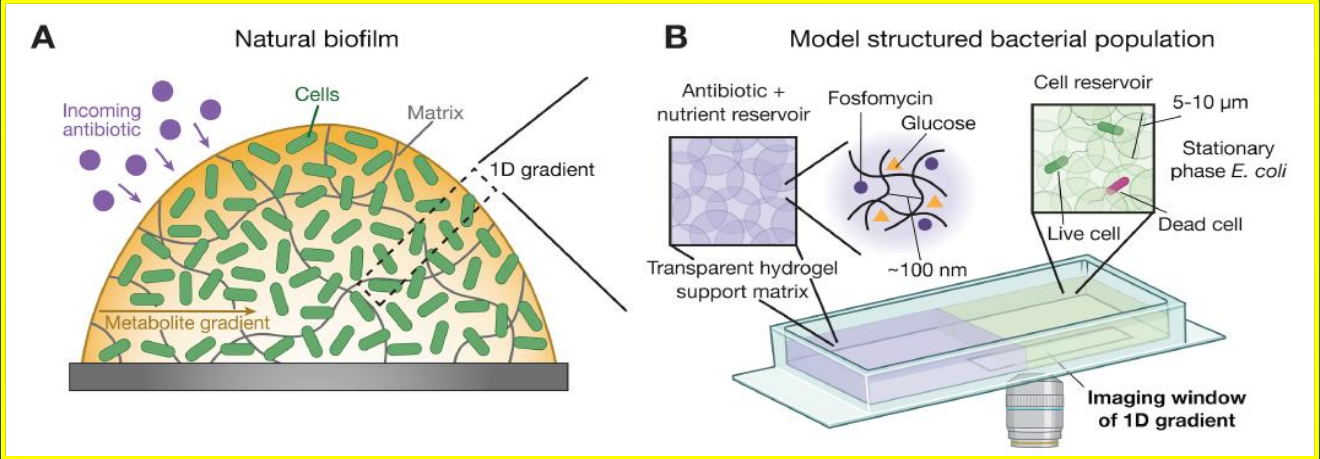

A.M. Hancock, et al. A nutrient bottleneck limits antibiotic efficacy in structured bacterial populations, Princeton Univ., Caltech, USA, bioRxiv https://doi.org/10.1101/2025.03.12.642894

A. N. Bashkatov, E. A. Genina, Y. P. Sinichkin, V. I. Kochubey, N. A. Lakodina, and V. V. Tuchin, Biophysical Journal 85, 3310 (2003), 226 цит.

Summary

Polarization

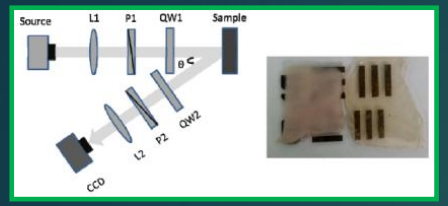

Adaptive OCT

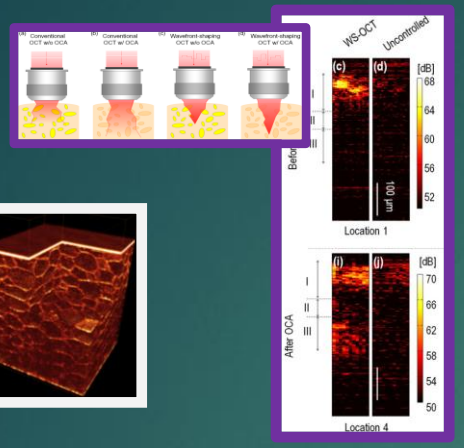

Skull, tooth, bone, cartilage

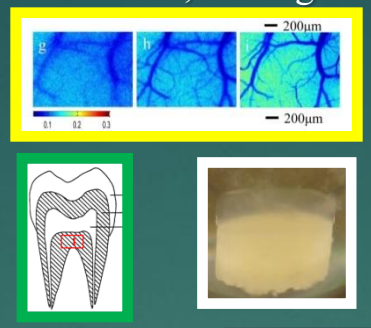

OCT

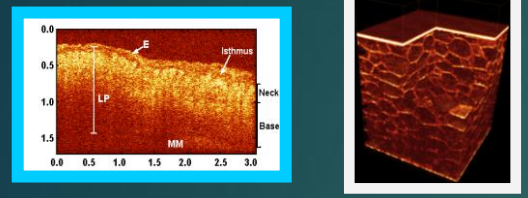

Confocal microscopy

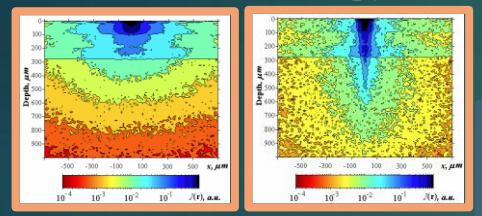

Speckles

Raman spectroscopy

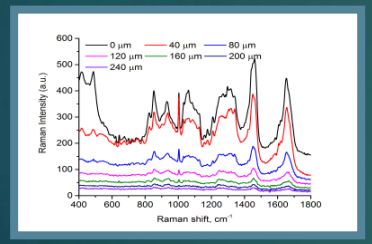

Two-photon and SHG microscopy

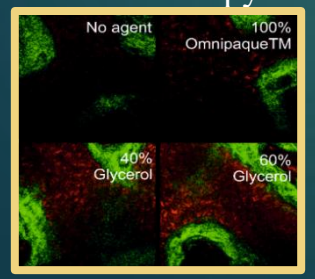

THz clearing

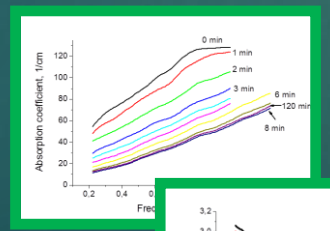

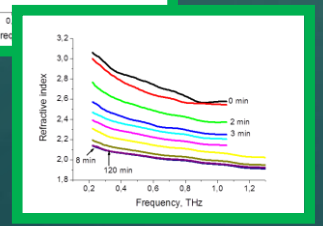

Optical Clearing of Tissues and Blood

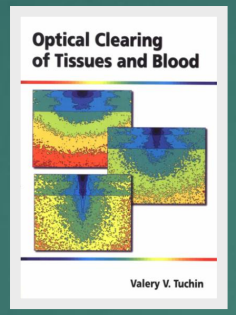

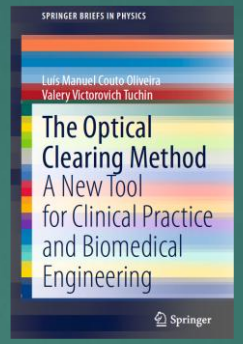

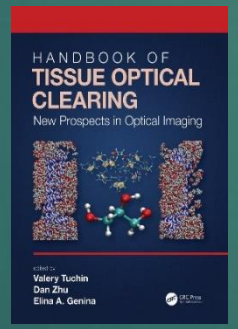

Cancerous tissue differentiation

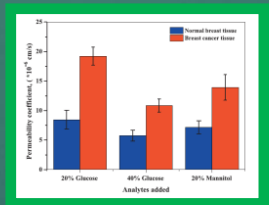

Cell imaging in lymph nodes

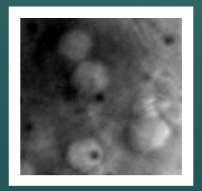

Blood vessel imaging

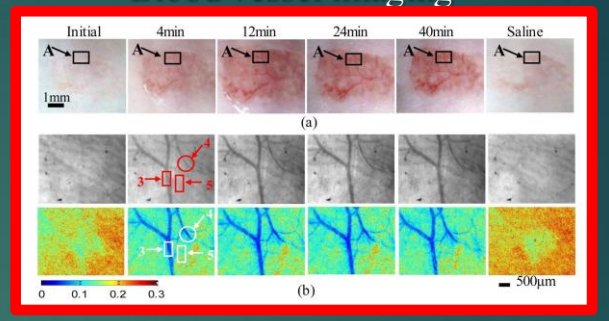

Glycated tissue differentiation

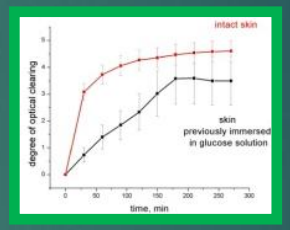

Rheumatoid arthritis

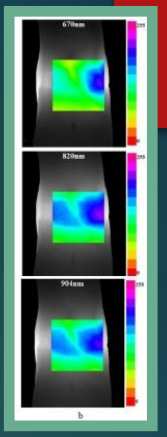

Glucose sensing

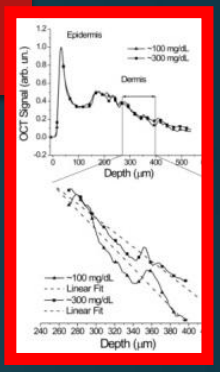

Nanophotonics

Upconversion nanoparticles

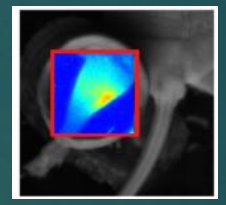

Gold nanoparticles

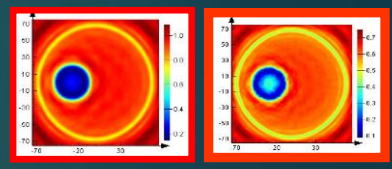

Precise laser surgery

PWS patients and the *en face* OCTA

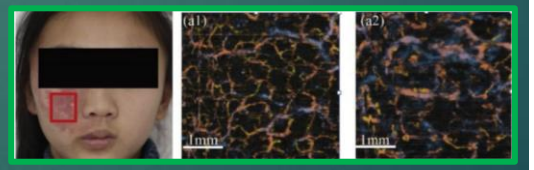

Scarred vocal fold

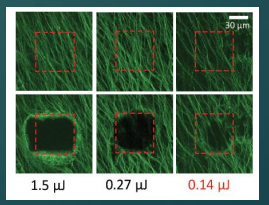

Laser tattoo removal

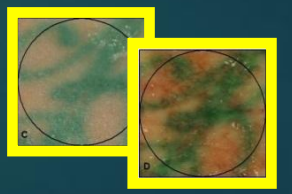

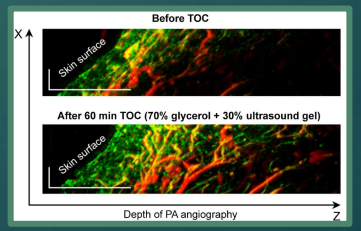

PA microscopy, angiography, lymphography & flow cytometry

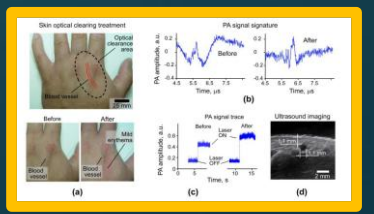

Monographs

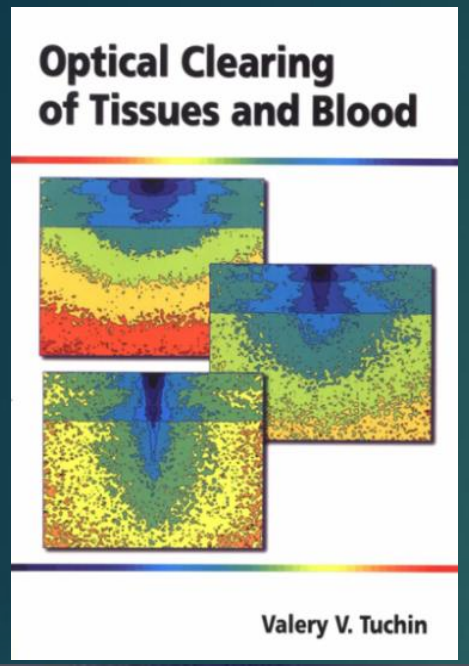
Optical Clearing
of Tissues and Blood
Valery V. Tuchin

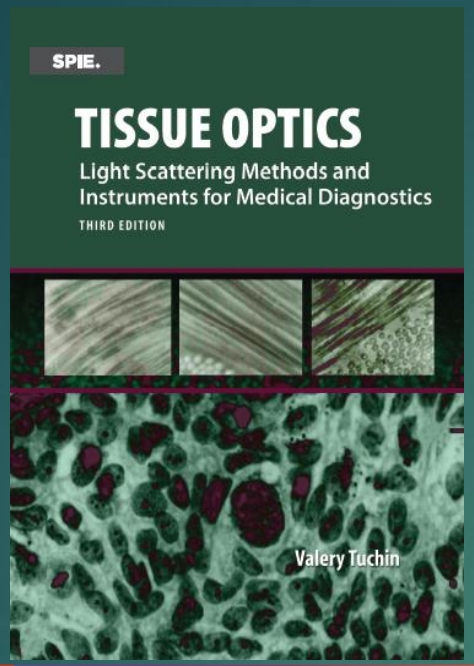
SPIE.
TISSUE OPTICS
Light Scattering Methods and
Instruments for Medical Diagnostics
THIRD EDITION
Valery Tuchin

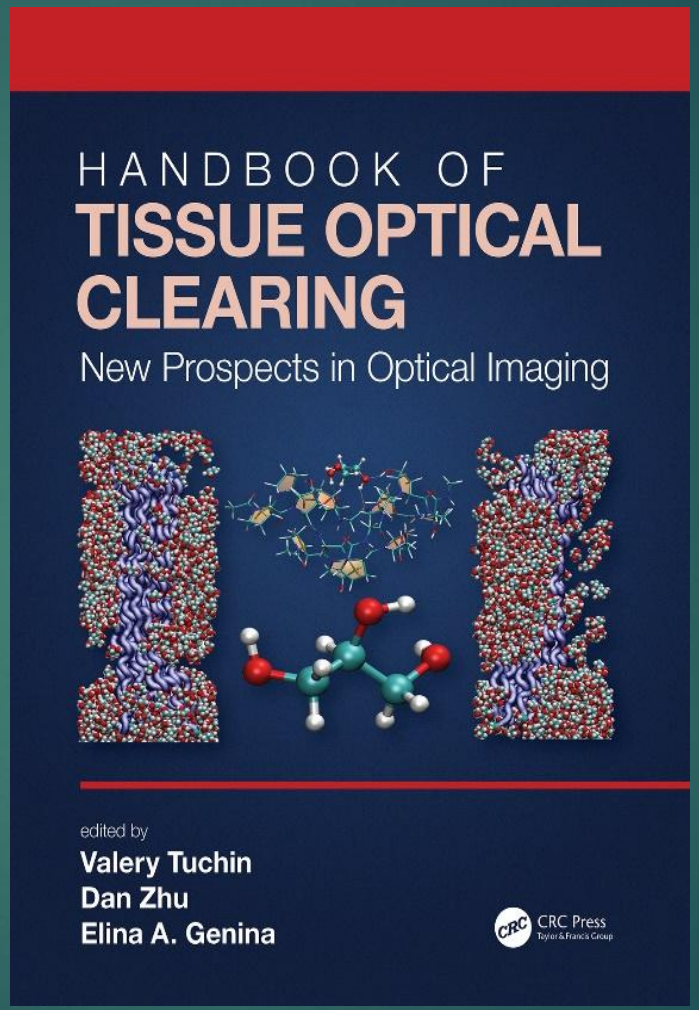
HANDBOOK OF
TISSUE OPTICAL
CLEARING
New Prospects in Optical Imaging
edited by
Valery Tuchin
Dan Zhu
Elina A. Genina
CRC Press

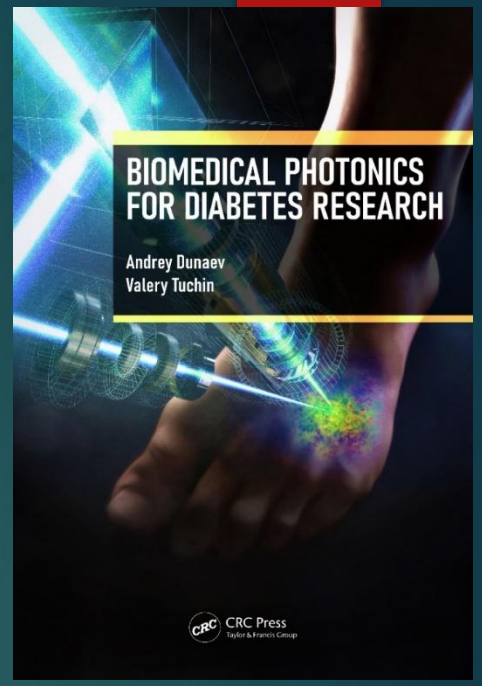
BIOMEDICAL PHOTONICS
FOR DIABETES RESEARCH
Andrey Dunaev
Valery Tuchin
CRC Press

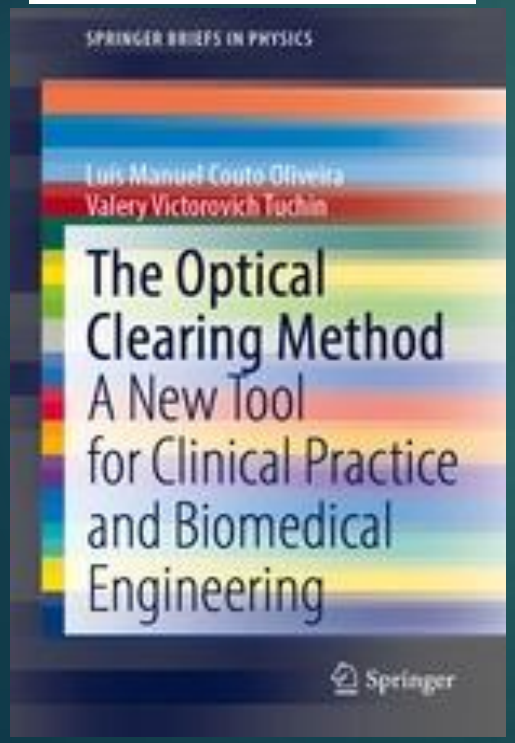
SPRINGER BRIEFS IN PHYSICS
Luis Manuel Couto Oliveira
Valery Victorovich Tuchin
The Optical
Clearing Method
A New Tool
for Clinical Practice
and Biomedical
Engineering
Springer

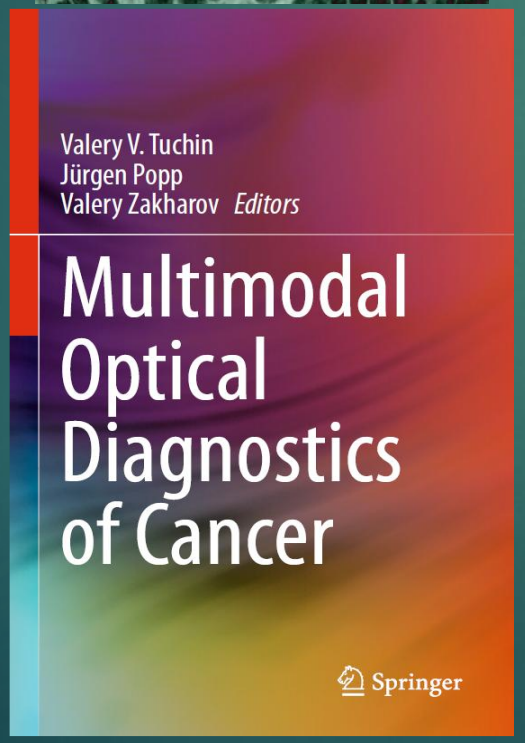
Valery V. Tuchin
Jürgen Popp
Valery Zakharov Editors
Multimodal
Optical
Diagnostics
of Cancer
Springer

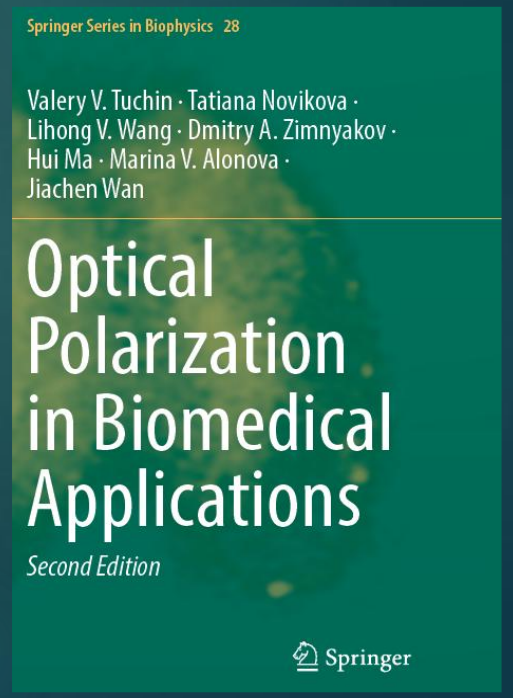
Springer Series in Biophysics 28
Valery V. Tuchin · Tatiana Novikova ·
Lihong V. Wang · Dmitry A. Zimnyakov ·
Hui Ma · Marina V. Alonova ·
Jiachen Wan
Optical
Polarization
in Biomedical
Applications
Second Edition
Springer

Выводы

Технология оптического просветления:

- Существенно повышает эффективность оптической спектроскопии, визуализации и терапии
- Расширяет возможности применения лазеров и других источников света, работающих в диапазоне длин волн от глубокого УФ до ТГц, в биомедицине
- Благодаря использованию инновационных оптических просветляющих агентов позволяет комбинировать оптические методы, такие как КР, ГКР, РКР, конфокальная микроскопия, ОКТ, флуоресцентная микроскопия, FLIM, нелинейная микроскопия (МФ, вторая и третья гармоника), ОА метод, диффузная спектроскопия, ТГц-спектроскопия, с широко используемыми в клиниках КТ, МРТ и УЗИ
- Позволяет вводить маркеры для мониторинга осложнений при сахарном диабете и дифференциации опухолей
- Перспективна для мониторинга криоконсервации органов

Благодарности

SSU, SSMU

Elina Genina, Irina Yanina, Polina Timoshina, Daria Tuchina, Alexey Selifonov, Vadim Genin, Ekaterina Lazareva, Olga Zhernovaya, Alla Bucharskya et al.

National and international collaborators

Yulia Alexandrovskaya et al. Inst. Photon Technologies RAS
Yury Kistenev, et al. Tomsk State University
Dan Zhu, Qingming Luo et al. HUST Univ., Hainan Univ. China
Hui Ma, Shenzhen University, China
Luis Oliveira et al. ISEP-IPP, Porto, Portugal
Alexander P. Savitsky, et al., FRC of Biotechnology, RAS
Alexei A. Bogdanov Jr, UMass, USA
Viacheslav Artyushenko, artphotonics gmbH, Germany
Vladimir L. Kuzmin, PTG St. Petersburg Polytechnic Univ., Russia
Martin Leahy, University of Galway, Ireland
Kirill Larin, University of Houston, USA
Irina Larina, Baylor College of Medicine, USA
Maxim Darvin, Charité - Universitätsmedizin Berlin
Andrey Dunaev et al., Orel State Univ., Russia
Dmitry Gorin et al., SkolTech
Alexander Priezzhev, Andrey Lugovtsov et al., Moscow State Univ.
Qinyu Lin, Sichuan University, China
Kirill Zaytsev, Irina Dolganova, et al., GPI RAS, ISSP RAS, Moscow










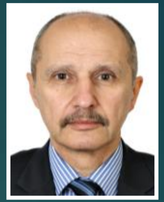


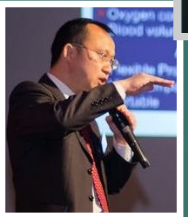














Russian Science Foundation grant 24-44-00082 https://www.rscf.ru/project/24-44-00082/

САМАРСКИЙ УНИВЕРСИТЕТ
SAMARA UNIVERSITY

Journal of Biomedical Photonics & Engineering

Top reasons to submit your research to JBPE

- **Platform** for cross disciplinary research in the fields of optics, chemistry, engineering and life sciences
- **Rapid publication** from acceptance to online publication.
- **Professional** copyediting and typesetting
- **Open Access online ready** allows your article to be published online ahead of an issue

JPBE Metrics 2024

- **CiteScope™ (Scopus)** 1.6, Q2-Q4
- Total articles published 54
- Acceptance rate 53%
- Submission to first decision 5 days
- After peer review 44 days
- Acceptance to Online Ready 3 weeks
- New Registered readers 24349

Special Issue. Call for papers

Light for Life Sciences

Editors: Oleg Vasyutinskii, Valery Tuchin, Junle Qu, Dongping Zhong

This special section is intended as a collection of selected papers presented at the International Russian-Chinese Workshop “Light for Life Sciences,” (October 17 – 20, 2025, St. Petersburg, Russia). We invite papers covering the latest scientific advances and innovations in the application of optics in the life sciences: optical and laser technologies for medicine and biology, the dynamics of ground and excited states of biomolecules under laser excitation, precision mechanics and control of tissues and cells, related materials and environmental issues, optical imaging, spectroscopy, and molecular modeling

https://jbpe.ssau.ru/index.php/JBPE/pages/view/ircw

Advanced Photonic Technologies in Biomedicine

Editors: Ivan A. Bratchenko and Elina A. Genina

This special section is planned as a collection of selected papers presented at Saratov Fall Meeting 2025 – International Symposium on Optics and Biophotonics (Sept 30 – Oct 3, 2025, Saratov, Russia). Papers focused on optical and laser technologies for medicine and biology, morphology, precision mechanics and control of tissues and cells, related material and environmental problems, optical imaging, spectroscopy and molecular modeling are invited

https://jbpe.ssau.ru/index.php/JBPE/pages/view/sfm2025

OPEN ACCESS
Journal of Innovative Optical Health Sciences
(2023) 2302001 (4 pages)
© The Author(s)
DOI: 10.1142/S1793545823020017

World Scientific
www.worldscientific.com

Introduction to the special issue on celebrating the 15th anniversary of JIOHS and the 70th anniversary of HUST

OPEN ACCESS
Journal of Innovative Optical Health Sciences
Vol. 14, No. 5 (2021) 2102003 (2 pages)
© The Author(s)
DOI: 10.1142/S179354582102003X

World Scientific
www.worldscientific.com

Editorial

Introduction to the Special Issue on Advances in Biophotonics and Biomedical Optics

Polina Dyachenko (Timoshina)*, Tingting Yu†,‡, Dan Zhu†,‡ and Valery V. Tuchin*
*Research-Educational Institute of Optics and Biophotonics
Saratov State University, Saratov 410012, Russia
†Britton Chance Center for Biomedical Photonics
Wuhan National Laboratory for Optoelectronics
Huazhong University of Science and Technology
Wuhan 430074, P. R. China
‡MoE Key Laboratory for Biomedical Photonics
School of Engineering Sciences
Huazhong University of Science and Technology
Wuhan 430074, P. R. China

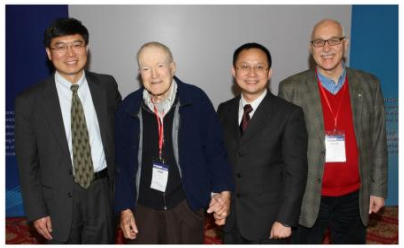

Organizers of PIBM: Lihong Wang, Britton Chance, Qingming Luo and Valery Tuchin, HUST 2008

Valery Tuchin discusses tissue optics with CBMP students, HUST, September 7, 2005

Valery Tuchin and his colleagues visiting the Dan Zhu group, HUST, October 23, 2011

Best Student Paper Award Ceremonies at PIBM, HUST, 2008, 2009, 2010, 2011, and 2013

First Chinese-Russian Workshop on Biophotonics and Biomedical Optics, HUST, 2006

Chinese-Russian Workshop on Biophotonics and Biomedical Optics, Saratov, Russia, 2012

Frontiers of Optoelectronics

Index by ESCI, EI, Scopus, DOAJ, PMC, CSCD, ...

IF 2024/25: 5.2 **CiteScore 2024/25: 4.7** **Q1**

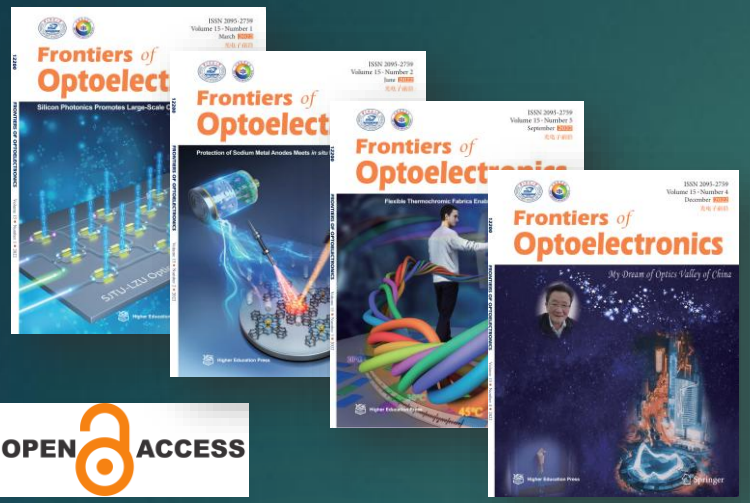

OPEN ACCESS

Frontiers of Optoelectronics (FOE) ***emphasizes to reflect the scientific discovery and technology innovation in the fields of photonics or optoelectronics, including biophotonics***

Editors-in-Chief

Prof. Qihuang Gong (龚旗煌)
Peking Univ.

Prof. Xinliang Zhang (张新亮)
Xidian Univ. & Huazhong Univ. Sci. & Tech.

Features:

- Indexed by: ESCI, EI, Scopus, DOAJ, PMC, CSCD, etc.
- Impact factor (IF) 2024/25: 5.2
- Full open access (OA) publication
- No article-processing charges, no page limitation
- Continuous article publication

Hosted by

- Higher Education Press
- Huazhong University of Science and Technology
- The Chinese Optical Society

Published by: Higher Education Press | Springer

journal.hep.com.cn/foe

springer.com/journal/12200

Phone Number: (027)87793063 Email: foc@hust.edu.cn Online submission: https://mc.manuscriptcentral.com/foe

Frontiers Journals HIGHER EDUCATION PRESS | Springer

LAM Introduction

new, highly selective, open access

Sister journal of the Nature Journal
Light: Science and Applications (IF 20.6)

1st IF 10.6

- Scopus, WoS, DOAJ
- Q1 in four categories
- Top 7% of Optics journals

Topics:

(Interdisciplinary: Optics & Manufacturing Engineering)

- Laser manufacturing
- Extreme manufacturing
- AI assisted photonic
- Photonic integration
- Green Photonics
- Micro and nano fabrication
- AR/VR/MR
- Terahertz technologies
- Flexible electronics
- Characterization and on-line measurements
- Optical surface finishing
- Space optical technologies
- Manufacturing in extreme environments
- Super-resolution and extra-wide field imaging…

For only the finest works in light-based manufacturing

www.light-am.com
light_am@jihualab.ac.cn

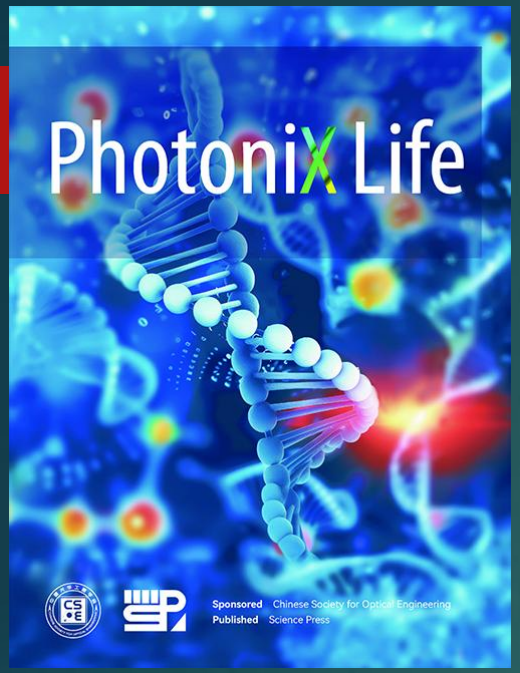

PhotoniX Life is a new international open access journal, sponsored by the Chinese Society for Optical Engineering. The journal aims to promote interdisciplinary research by publishing cutting-edge research and high-quality research across all scientific disciplines, such as *biology, materials, physics, chemistry, nanotechnology, and life science.*

EDITORS-IN-CHIEF

Topics including but not limited to:

- *Photothermal therapy*
- *Imaging in NIR-II window*
- *Photodynamic therapy*
- *Photoacoustic imaging*
- *Quantum dots*
- *Optical immunotherapy*
- *Live cell imaging*
- *Afterglow luminescence in bio-applications*
- *Chirality in light-matter interaction*
- *Super-resolution microscopy*
- *Optogenetics*
- *Phosphorescence bioimaging or biosensing*
- *X-ray bio-imaging*
- *Förster resonance energy transfer*
- *Molecular imaging*


Welcome to SFM-26
September 21 – 25, 2026
https://sfmconference.org/
XXX International School for Junior Scientists and Students on Optics, Laser Physics & Biophotonics and XIV Symposium Optics & Biophotonics
SARATOV FALL MEETING SFM '26
September 21 - 25, 2026